

1 Dear Editor:

2 Thank you very much for providing the opportunity for us to revise our paper.

3 Thank you very much for your contributions to this paper. And we are all
4 extremely grateful for having a chance to make further improvements. Reading and
5 considering all comments of two reviewers carefully, we have made major revisions
6 on our paper. The major three suggestions of reviewer1 and detail comments on the 4
7 points of reviewer2 are very helpful for us. Following the two reviewers' suggestions,
8 we have made major revisions on our paper.

9 Finally, we write the point-by-point response to answer the two reviewers'
10 questions for better communication. If there are still any problems on the method,
11 diction, phrasing, grammar, and spelling, please do not hesitate to tell us and we'll try
12 our best to improve them.

13 Thank you again for your comments to improve our paper. Wish your journal
14 better and better.

15
16 Yours,

17
18
19 Mei Hong

20 2018-02-06

24 **Responses to reviewer#1:**

25 All the authors are extremely grateful to you for providing your excellent
26 comments and valuable advices for this paper. Your major suggestions that the
27 reliability of this datasets is not mentioned and the authors did not verify their results
28 in spring season are very helpful for us. Based on your suggestions, we have made
29 some revisions to on our paper. We have added the discussion of reliability of this
30 datasets and the new results in spring season based on your specific comments.

31 Thank you again for your valuable comments to improve our submission. If there
32 are still any problems on the method, diction, phrasing, grammar, and spelling, please
33 do not hesitate to tell us and we'll try our best to improve them.

34 In the following, kind comments you suggested before are in black text with
35 corresponding actions taken by us following in blue.

36

37 Specific comments:

38 1. The method used in this study is based on the statistic regression, which basically
39 depends on the quality of observations. In section 2.1, although the authors claimed
40 that the monthly average SST data from the UK Met Office Hadley Centre is adopted
41 in this study, the reliability of this datasets is not mentioned. Besides, the verification
42 of this datasets with in-situ observation is also strongly recommended by this
43 reviewer.

44 Responses: Good suggestions. In the previous paper, we have neglected the
45 discussion of reliability of this datasets. Now there are three main categories of SST

46 data. The gridded 2 °×2 NOAA Extended Reconstructed SST dataset (ERSST.v3b;
47 Smith et al. 2008) includes in situ data (ships and buoys), but does not include
48 satellite data. The gridded 1 °×1 Met Office Hadley Sea Ice and SST dataset
49 (HadISST1; Rayner et al. 2003) includes both in situ and available satellite data. The
50 gridded 1 °×1 NOAA Optimal Interpolation SST (OISST.v2; Reynolds et al. 2002)
51 incorporates in situ and satellite data, but unlike the other two SST datasets, it is only
52 available in the recent period from November 1981 to the present. Both HadISST1
53 and ERSST.v3b are available from the mid-to-late 1800s, but only monthly data from
54 1951 to 2010 was considered in this study.

55 Considering comprehensively, the gridded 1 °×1 Met Office Hadley Sea Ice and
56 SST dataset data, no matter from data quality or data length, is the most appropriate to
57 used.

58 The specific revision can be seen from line118 to line120 in page6.

59 We sincerely hope for your satisfaction with our revision. Thank you again for
60 your kind suggestion.

61 References:

62 Smith TM, Reynolds RW, Peterson TC, Lawrimore J (2008) Improvements to
63 NOAA's historical merged land–ocean surface temperature analysis (1880–2006). *J*
64 *Clim* 21:2283–2296.

65 Rayner NA, Parker DE, Horton EB, Folland CK, Alexander LV, Rowell DP, Kent EC,
66 Kaplan A (2003) Global analyses of sea surface temperature, sea ice, and night marine
67 air temperature since the late nineteenth century. *J Geophys Res* 108(D14):4407.

68 [doi:10.1029/2002JD002670](https://doi.org/10.1029/2002JD002670)

69 Reynolds RW, Rayner NA, Smith TM, Stokes DC, Wang W (2002) An improved in
70 situ and satellite SST analysis for climate. *J Clim* 15:1609–1625

71 2. One important conclusion of this study is “The difference between forecast results
72 in summer and those in winter is not high, indicating that the improved model can
73 overcome the spring predictability barrier to some extent”. This conclusion is vague
74 and lack of rigorous verification because the authors did not verify their results in
75 spring season.

76 Responses: Good suggestions. The skill of forecasts that start in February or May
77 drops faster than that of forecasts that start in August or November. This behavior,
78 often termed the spring predictability barrier, is in part because predictions starting
79 from February or May contain more events in the decaying phase of ENSO (Jin et al.,
80 2008). Based on the reviewer’s suggestion, we have added the experiments in the
81 spring and in the autumn in Table4. From the table, we can see the forecast result in
82 spring of our model is also good, indicating that the improved model can overcome
83 the spring predictability barrier to some extent. The specific revision can be seen in
84 from page66.

85 We sincerely hope for your satisfaction with our revision. Thank you again for
86 your kind suggestion.

87

88 **Table. 4.** Temporal correlation(TC) and the mean absolute percentage error (MAPE) between
89 model forecasts and observations within 12 months for Nov.–Jan., Dec.–Feb., and Jan.–Mar. as
90 lead time of winter, for Feb.–Apr. , Mar.–May and Apr.–June as lead time of spring, for May-July,
91 June-August and July-Sep. as lead time of summer and for August-Oct., Sep.-Nov. and Oct.-Dec.

92 as lead time of autumn.

Forecast events	Lead time of all seasons combined		Lead time of summer (MJJ-JJA-JAS)		Lead time of autumn (ASO-SON-OND)		Lead time of winter (NDJ-DJF-JFM)		Lead time of spring (FMA-MAM-AMJ)	
	TC	MAPE	TC	MAPE	TC	MAPE	TC	MAPE	TC	MAPE
The average of 18 El Niño examples	0.604	9.70%	0.569	10.33%	0.632	8.85%	0.677	8.02%	0.538	11.6%
The average of 22 La Niña examples	0.625	8.97%	0.581	9.82%	0.645	8.41%	0.695	7.83%	0.579	9.82%
The average of 20 Neutral examples	0.798	5.96%	0.752	6.86%	0.831	5.31%	0.844	4.60%	0.765	7.07%
The average of total 60 examples	0.712	7.62%	0.633	8.51%	0.786	6.88%	0.776	6.52%	0.653	8.03%

93

94 3. Lines 42-44, Compared with six mature models published previously,

95 the present model has an advantage in prediction precision and length, and is a

96 novel exploration of the ENSO forecast method”. The major concerns of this reviewer

97 are: what is the sample size in comparing the forecast results? Are those samples

98 really representative?

99 Responses: Good suggestions. As shown in Table 4, our ENSO forecast is a total of 60

100 experiments, including 18 El Niño examples, 22 La Niña examples, and 20 Neutral

101 examples, and each experiment contains lead time of four seasons. Finally, it is the

102 equivalent of 240 experiments. Figure 11 and Figure 12 is the average TC and RMSE

103 of the 240 experiments of compared with six mature models, covers a variety of

104 different types of ENSO and different lead time. So those samples should be really

105 representative . We haven't explained it in previous paper, and now we explain it from
106 line564 to 567 on page27.

107 We sincerely hope for your satisfaction with our revision. Thank you again for
108 your kind suggestion.

109

110 Minor comments:

111 1.Line 122, give the full name of “SOI”.

112 Responses: Good suggestions. Now we have given the full name of “SOI” as the
113 Southern Oscillation Index (SOI) in line128 in page6.

114 We sincerely hope for your satisfaction with our revision. Thank you again for
115 your kind suggestion.

116 2. Line 549, “mode” should be “model”.

117 Responses: Good suggestions. Now we have revised “mode” as“model” in
118 line545 in page26.

119 We sincerely hope for your satisfaction with our revision. Thank you again for
120 your kind suggestion.

121

122

123 **Responses to reviewer#2:**

124 All the authors are extremely grateful to you for providing your excellent
125 comments and valuable advices for this paper. Your major four suggestions that
126 Construction of the first two predictors ieT1 and T2; Selection of the other predictors;
127 Structure of the model and Model validation are very helpful for us. Based on your

128 suggestions, we have made major revisions to on our paper. We have added the
129 discussion of the selection of the predictors, the structure of the model and the model
130 validation based on your specific comments.

131 Thank you again for your valuable comments to improve our submission. If there
132 are still any problems on the method, diction, phrasing, grammar, and spelling, please
133 do not hesitate to tell us and we'll try our best to improve them.

134 In the following, kind comments you suggested before are in black text with
135 corresponding actions taken by us following in blue.

136 1 . Section 2.2 EOF deconstruction. This section requires some more detail. While
137 the given reference describes the EOF method, we need to know how it is applied
138 here. Is the correlation or covariance matrix used? How are the anomalies constructed
139 – simple removal of the monthly means? How are the anomalies smoothed - how
140 strong is the smoothing and is it applied spatially or over time? More importantly,
141 why are only the first 2 EOFs considered? A similar analysis has recently been
142 reported by L'Heureux et al (Clim Dyn 2013, DOI 10.1007/s00382-012-1331-2).
143 Their first two EOFs are similar to those described here (but with no smoothing and
144 hence lower explained variance). Using different data sets and time periods, they
145 show that the 2nd EOF is not stable, being entirely due to the strong trend (also
146 evident in Figure 1d). The pattern does not appear if the data is detrended, and also
147 becomes less important if different time periods and/or domains are used. Most
148 importantly, they do not interpret it as indicating "the ENSO signal beginning to
149 decay".

150 Responses: Good suggestions. We have used covariance matrix, because the
 151 covariance matrix was selected to diagnose the primary patterns of co-variability in
 152 the basin-wide SSTs, rather than the patterns of normalized covariance (or correlation
 153 matrix). We have used the smooths function with MATLAB, which is five points two
 154 times moving, mainly filtering out some noise points and outliers.

155 Because the variance contribution of the first EOF mode is 61.33% and the
 156 variance contribution of the second EOF mode is 14.52%, so the first two EOF modes
 157 account for 75.85% of the total variance contribution, which has occupied most of the
 158 variance contribution and also contains most of the information of the field
 159 decomposition. So the first 2 EOFs are considered.

160 Based on the reference of L'Heureux et al. (Clim Dyn 2013, DOI
 161 10.1007/s00382-012-1331-2), we need to do more experiments to prove that we
 162 choose the second mode of EOF to be appropriate, and whether different time periods
 163 will make us forecast unstable or not. Our original data is the monthly average SST
 164 data from January 1951 to Dec. 2010, which are 60 years. We will increase the length
 165 of the data for 20 years (Jan.1931 –Dec.2010), for 10 years (Jan.1941- Dec.2010) and
 166 decrease the length of the data for 10 years (Jan.1961- Dec.2010), for 20 years
 167 (Jan.1971- Dec.2010). And then we use the same method to reconstruct a model and
 168 forecast the ENSO index as section5.4. The prediction results are shown in the
 169 following table:

170 Table5. The forecast results of the different data periods

Forecast events	The data periods (Jan.	The data periods (Jan.	The data periods (Jan.	The data periods (Jan.	The data periods(Jan.
-----------------	------------------------	------------------------	------------------------	------------------------	-----------------------

	1951-Dec.2010) Lead time of all seasons combined	1931-Dec.2010) Lead time of all seasons combined	1941-Dec.2010) Lead time of all seasons combined	1961-Dec.2010) Lead time of all seasons combined	1971- Dec.2010) Lead time of all seasons combined					
	TC	MAPE	TC	MAPE	TC	MAPE	TC	MAPE	TC	MAPE
The average of 18 El Niño examples	0.604	9.70%	0.683	9.02%	0.642	9.35%	0.572	10.15%	0.551	10.44%
The average of 22 La Niña examples	0.625	8.97%	0.701	8.33%	0.675	8.55%	0.589	9.42%	0.567	9.82%
The average of 20 Neutral examples	0.798	5.96%	0.845	5.12%	0.821	5.56%	0.746	6.21%	0.721	6.58%
The average of total 60 examples	0.712	7.62%	0.771	7.14%	0.740	7.38%	0.680	7.96%	0.652	8.15%

171 From the table, we can see that in the 60 experiments, the prediction results of
172 the data period increased by 20 years are the best, and the prediction results of the
173 data period decreased by 20 years is the worst. This is because the more data we use,
174 the more information it contain. But from the table we can also see the difference
175 among forecast results of both TC and MAPE of five different sample data are less,
176 and no abnormal change suddenly worse or better appear. All these indicate that using
177 different data sets and time periods, even though may have a certain impact on the
178 pattern of the 2nd EOF, but the impact on our forecast is not great and it will not make
179 our forecast unstable.

180 The "indicating the ENSO signal beginning to decay" in our previous paper is a
181 mistake of writing, which is not seen from the space mode of Figure 1 (c), but from

182 the time mode of Figure 1 (d). From Figure1 (d) we can see the time coefficient has a
183 significant upward trend over time, indicating "the ENSO signal beginning to
184 enhanced".

185 We have added the discussion about the stability of our forecast in page6-7 and
186 page28-29 and revised as "the ENSO signal beginning to enhanced " in page7.

187 We sincerely hope for your satisfaction with our revision. Thank you again for
188 your kind suggestion.

189

190 2. Section 2.3 Predictor selection The selection of other potential predictors is
191 confusing. Apart from T1 and T2, the other potential predictors come from a fairly
192 limited set, and are not well supported by the referenced works. In lines 157-160,
193 zonal winds in the western and eastern equatorial Pacific are mentioned, and it is well
194 known that westerly wind anomalies in the western equatorial Pacific can (and do)
195 trigger equatorially trapped oceanic Kelvin waves. There is an extensive amount of
196 literature on the relationship between western equatorial Pacific zonal wind and
197 ENSO, but here no references are given and only the eastern equatorial winds is
198 considered. Trenberth et al. discuss a link between ENSO and the PNA pattern
199 (amongst other modes of extratropical variability), but this is the context of ENSO
200 forcing of the PNA, ie ENSO leads to PNA teleconnections, but PNA does not predict
201 ENSO. Yang et al introduce the EAWM index, but they note that "the relationship
202 between ENSO and the east Asian winter monsoon is relatively weak". Nowhere do

203 they suggest that the EAWMI is closely related to any ENSO indices. It is not
204 surprising that the east Pacific wind and PNA do not feature in the final model.

205 Responses: Good suggestions. Your opinion is very good. In pervious paper
206 the factors that we may consider are relatively few. But we are a complex coupled
207 model of four factor differential equations and are not the similar with a simple
208 statistical model (such as stepwise regression). So in our pervious paper using the
209 stepwise regression method to select factors also has a problem. According to your
210 opinion, we have read more literatures. We have expanded the scope of factor
211 selection and revised the criterion of selecting factors, and the paragraph has revised
212 as follows:

213 Considering the complexity of computation, the amount of variables in the
214 equations of our model can't be too large, usually 3 or 4 for the best. This has been
215 explained in our previous studies (Zhang et al., 2006; Zhang et al., 2008). If there are
216 more than 4 variables in the modeling equation, it will cause the amount of
217 parameters such as $a_1, a_2, \dots, a_n, b_1, b_2, \dots, b_n, \dots$ too large. The huge computation makes it
218 difficult to be precisely modeled. Thus, the total number of parameters in the model of
219 five variables was 102, which may cause an overfitting problem. Hence, when we
220 selected the model of five or six variables which entailed large amounts of
221 computation that made precision difficult, and too many parameters might cause an
222 overfitting phenomenon. If we choose only two or even fewer variables, the forecast
223 performance is poor too. Too few variables cause too small reconstructed parameters,
224 resulting in amounts of important information missing out in the model. Thus, four

225 variables are best for dynamically and accurately modeling. Because we have chosen
226 two time series in section 2.2 as the modeling objects, now we should select the other
227 two ENSO intensity impact factors.

228 The ENSO intensity impact factor is an important issue in ENSO prediction.
229 Previous studies have been completed in this area, which found that teleconnection
230 patterns, temperature, precipitation, wind and SSH may affect ENSO strength. For
231 example, Trenberth et al. (1998) noted that PNA, SOI and OLR in the Pacific
232 Intertropical Convergence Zone (ITCZ) are all closely related to ENSO.
233 Webster (1999) pointed out after the 1970, Indian Ocean dipole (IOD) is not only
234 affected by ENSO, but also affected the strength of ENSO (Ashok et al., 2001). Yoon
235 and Yeh (2010) reported that the Pacific Decadal Oscillation (PDO) disrupts the
236 linkage between El Niño and the following Northeast Asian summer monsoon
237 (NEASM) through inducing the Eurasian pattern in the mid-high latitudes. The vast
238 majority of studies (Tomita and Yasunari, 1996; Zhou and Wu, 2010; Kim et al.,
239 2017) have concentrated on the impacts of ENSO on the East Asian winter
240 monsoon (EAWM). During the EAWM season, ENSO generally reaches its mature
241 phase and has the most prominent impact on the climate. Wang et al. (1999a) and
242 Wang et al. (1999b) suggested that the zonal wind factors in the eastern and western
243 equatorial Pacific play a critical role in the phase of transition of the ENSO cycle,
244 which could excite eastward propagating Kelvin waves and affect the SSTA in the
245 equatorial Pacific. Zhao et al. (2012) analyzed the characteristics of the tropical
246 Pacific SSH field and its impact on ENSO events.

247 Based on the above analysis, we have selected nine factors, which may be
248 closely related with the ENSO index (Niño3.4).

249 (1)The zonal wind in the eastern equatorial Pacific factor (u1) was calculated
250 as the grid-point average of zonal wind in the area [5 °S ~ 5 °N, 150 °W ~ 90 °W].

251 (2) The zonal wind in the western equatorial Pacific factor (u2) was calculated
252 as the grid-point average of zonal wind in the area [0 °~ 10 °N; 135 °E ~ 180 °E].

253 (3) The PNA teleconnection factor was obtained from the CPC.

254 (4) the dipole mode index factor (DMI) was obtained from SSTA for
255 June-July-August (JJA) based on Saji(1999) method.

256 (5) The SOI factor was obtained from the CPC.

257 (6) The PDOI factor was obtained from department of Atmospheric Sciences
258 in the university of Washington. The web is
259 <http://tao.atmos.washington.edu/pdo/RDO.latest>.

260 (7) The EAWM index (EAWMI) factor was proposed by Yang et al. (2002),
261 which is defined by the meridional 850-hPa winds averaged over the region (20 °
262 ~40 °N, 100 °~140 °E).

263 (8) The OLR in the ITCZ factor was calculated as the grid-point average of
264 OLR in the area [10 °N~20 °N, 120 °E~150 °E].

265 (9) The SSH factor was calculated as the grid-point average of the SSH data in
266 the area [10 °S ~ 10 °N; 120 °E ~ 60 °W].

267 A correlation analysis of the above factors was carried out and the results are
268 shown in Table 2.

269 Table 2 shows that SOI and EAWMI have the stronger correlation with the
 270 front two time series T_1, T_2 than the other 7 factors. The results are also consistent with
 271 previous research (Clarke and Van Gorder, 2003; Drosdowsky, 2006; Zhang et al.,
 272 1996; Wang et al., 2008; Yang and Lu, 2014). Therefore, the first time series T_1 , the
 273 second time series T_2 , SOI and EAWMI will be selected as prediction model factors.

274 Table 2. The correlation analysis between the front two time series T_1, T_2 and nine impact factors

factors	u_1	u_2	PNA	DMI	SOI	PDOJ	EAWMI	OLR	SSH
T_1	0.3161	0.5684	0.4386	-0.3457	0.7734	0.4081	0.6284	0.3287	0.3363
T_2	0.2118	0.4181	0.2560	-0.2345	0.5232	0.3065	0.4825	0.1816	0.2169

275

276 Actually, how many variables and which variables are used in our model
 277 become a key issue to be resolved. We are a complex four factor differential
 278 equations coupling model. We are a complex coupled model of four factor differential
 279 equations, so we are more concerned with the correlation between each other. The
 280 correlation must be considered as an important criterion to select the factors, but in
 281 order to further verify the correctness of the selection criterion, we have carried out
 282 the prediction experiments (the 60 cross-validated retroactive hindcasts experiments
 283 of the ENSO index for all seasons combined at lead times of 8 months) of different
 284 variables. The forecast results of the models of different variables are as following:

285 Table3. The forecast results (The temporal correlation (TC) and the root mean square
 286 error (RMSE))of the models of different variables

The forecast	Three variables of the model
--------------	------------------------------

results						
	T_1, T_2, u_1	T_1, T_2, u_2	T_1, T_2, PNA	T_1, T_2, DMI	T_1, T_2, SOI	$T_1, T_2, PDOI$
TC	0.4423	0.5628	0.3852	0.3226	0.6027	0.3809
RMSE	0.9025	0.7855	0.9244	1.0041	0.7275	1.0642
	$T_1, T_2, EAWMI$	T_1, T_2, OLR	T_1, T_2, SSH			
TC	0.5829	0.3205	0.4288			
RMSE	0.7516	0.9814	0.9090			
	four variables of the model					
	T_1, T_2, u_1, u_2	T_1, T_2, u_1, PNA	T_1, T_2, u_1, DMI	T_1, T_2, u_1, SOI	$T_1, T_2, u_1, PDOI$	$T_1, T_2, u_1, EAWMI$
TC	0.4672	0.3628	0.5617	0.5201	0.5028	0.5822
RMSE	0.8824	0.9902	0.7617	0.8233	0.8092	0.7132
	T_1, T_2, u_1, OLR	T_1, T_2, u_1, SSH	T_1, T_2, u_2, PNA	T_1, T_2, u_2, DMI	T_1, T_2, u_2, SOI	$T_1, T_2, u_2, PDOI$
TC	0.3815	0.4128	0.3107	0.4125	0.5910	0.5504
RMSE	0.9702	0.9017	1.0255	0.9392	0.7128	0.7503
	$T_1, T_2, u_2, EAWMI$	T_1, T_2, u_2, OLR	T_1, T_2, u_2, SSH	T_1, T_2, PNA, DMI	T_1, T_2, PNA, SOI	$T_1, T_2, PNA, PDOI$
TC	0.6048	0.4528	0.5308	0.3022	0.3875	0.2876
RMSE	0.6910	0.9028	0.8344	1.0578	0.9706	1.1305
	$T_1, T_2, PNA, EAWMI$	T_1, T_2, PNA, OLR	T_1, T_2, PNA, SSH	T_1, T_2, DMI, SOI	$T_1, T_2, DMI, PDOI$	$T_1, T_2, DMI, EAWMI$
TC	0.3527	0.2556	0.2175	0.5688	0.2028	0.5807
RMSE	0.9518	1.2024	1.3244	0.7425	1.2905	0.7015
	T_1, T_2, DMI, OLR	T_1, T_2, DMI, SSH	$T_1, T_2, SOI, PDOI$	$T_1, T_2, SOI, EAWMI$	T_1, T_2, SOI, OLR	T_1, T_2, SOI, SSH
TC	0.3504	0.4833	0.6022	0.6344	0.5876	0.5476

RMSE	1.1624	0.8530	0.7054	0.6728	0.7408	0.7895
	$T_1, T_2, \text{PDOI}, \text{EAWMI}$	$T_1, T_2, \text{PDOI}, \text{OLR}$	$T_1, T_2, \text{PDOI}, \text{SSH}$	$T_1, T_2, \text{EAWMI}, \text{OLR}$	$T_1, T_2, \text{EAWMI}, \text{SSH}$	$T_1, T_2, \text{OLR}, \text{SSH}$
TC	0.4217	0.2017	0.2044	0.5872	0.4607	0.2028
RMSE	0.9147	1.2085	1.2542	0.7233	0.8925	1.3524

287 From the table, we can see that for all the forecast results of the models of
288 different variables, the prediction results of T_1, T_2, SOI is the best among those of the
289 three factors and the prediction result of $T_1, T_2, \text{SOI}, \text{EAWMI}$ is the best among those of
290 the four factors. But the prediction result of $T_1, T_2, \text{SOI}, \text{EAWMI}$ is best among all, which
291 proves that our selection factors are correct. In our previous study (Hong et al., 2015),
292 the model of the Western Pacific subtropical high was established by using the
293 correlations as a criterion to select factors and their forecast results are also good.
294 Now we use the correlations as a criterion to select factors is also in line with our
295 previous research.

296 With the deepening of the research, there are still a lot of new literatures that
297 reveal the relationship between ENSO and the East Asian winter monsoon. For
298 example:

299 [1] Kim Ji-Won ,Soon-Il An,Sang-Yoon Jun,Hey-Jin Park,Sang-Wook Yeh. 2017. ENSO and East
300 Asian winter monsoon relationship modulation associated with the anomalous northwest Pacific
301 anticyclone, *Climate Dynamics*, Volume 49, Issue 4, pp 1157–1179.

302 [2] Yang Se-Hwan and Lu Riyu . 2014. Predictability of the East Asian winter monsoon indices
303 by the coupled models of ENSEMBLES, *Advances in Atmospheric Sciences*, Volume
304 31, Issue 6, pp 1279–1292.

305 [3] Wang L., Chen W. and Huang R. H., 2008. Interdecadal modulation of PDO on the impact of
306 ENSO on the east Asian winter monsoon, Geophysical Research Letter, DOI:
307 10.1029/2008GL035287.

308 So there is a good correlation between ENSO and the East Asian winter
309 monsoon.

310 The specific revision can be seen in section2.3 in page7-10 and line616 to632 in
311 page29-30.We sincerely hope for your satisfaction with our revision. Thank you again
312 for your kind suggestion.

313 References:

314 [1] Mei Hong, Ren Zhang, et al., Reconstruction and forecast experiments of a statistical-dynamical
315 model of the Western Pacific subtropical high and Eastern Asian summer monsoon factors, Weather
316 and Forecasting, 2015,30:206-216.

317 [2]Zhang R. and Hong M., et al.: Non-linear Dynamic Model Retrieval of Subtropical High Based on
318 Empirical Orthogonal Function and Genetic Algorithm,Applied Mathematics and
319 Mechanics,27(12),1645-1654, 2006.

320 [3]Zhang R. and Hong M.,et al.: Retrieval of the non-linear dynamic forecast model of El Nino/La
321 Nina index based on the genetic algorithm optimization. Chinese Journal of
322 Geophysics,51(5),1354-1362, 2008.

323 [4]Trenberth, E. K., et al.: Progress during TOGA in understanding and modeling global
324 teleconnections associated with tropical sea surface temperatures,J. Geophys. Res., 107, C7,
325 14291-14324,1998.

326 [5]Webster P. J., Moore A. M., Loschnigg J. P., et al.: Coupled ocean-atmosphere dynamics in the

327 Indian Ocean during 1997- 98, *Nature*, 401(6751),356-360, 1999.

328 [6]Ashok K, Guan Z, Yamagata T : Impact of the Indian Ocean Dipole on the decadal relationship
329 between the Indian monsoon rainfall and ENSO, *Geophys Res Lett*,28(23), 4499-4502, 2001.

330 [7]Yoon, J., and S. W. Yeh: Influence of the Pacific Decadal Oscillation on the relationship between El
331 Niño and the northeast Asian summer monsoon, *J. Climate*,23, 4525–4537, 2010.

332 [8]Tomita, T., and T. Yasunari: Role of the northeast winter monsoon on the biennial oscillation of the
333 ENSO/monsoon system,*J. Meteor. Soc. Japan*, 74,399–413 , 1996.

334 [9]Zhou, L.-T., and R. G. Wu: Respective impacts of the East Asian winter monsoon and ENSO on
335 winter rainfall in China,*J. Geophys. Res.*,115, doi: 10.1029/2009JD012502, 2010.

336 [10]Wang B., Wu R., Lukas R.: Roles of western North Pacific wind variation in thermocline
337 adjustment and ENSO phase transition,*J Meteor Soc Japan*,77,1-16,1999a.

338 [11]Wang C., Weisberg R. H. and Virmani J. I.: Western Pacific interannual variability associated with
339 the El Niño-Southern Oscillation,*J Geophys Res.*,104,5131-5149, 1999b.

340 [12]Zhao J. H., Liu X. Y. and Jiang H. Y., et al.: Characteristics of Sea Surface Height in Tropical
341 Pacific and its relationship with ENSO events,*Meteorological and Environmental Sciences*,
342 35(2),33-39, 2012.

343 [13]Yang, S., K. M. Lau, and K. M. Kim: Variations of the East Asian jet stream and
344 Asian-Pacific-American winter climate anomalies, *J. Climate*, 15,306–325 , 2002.

345 [14]Saji N. H., Goswami B. N., Vinayachandran P. N., et al.: A dipole mode in the tropical Indian
346 Ocean,*Nature*, 401(6751),360-363, 1999.

347 [15]Clarke A. J. and S. Van Gorder: Improving El Niño prediction using a space-time integration of
348 Indo-Pacific winds and equatorial Pacific upper ocean heat content, *Geophys. Res. Lett.*,30,1399.

349 doi:10.1029/2002GL016673, 2003.

350 [16]Drosowsky W.: Statistical prediction of ENSO (Niño 3) using sub-surface temperature
351 data, Geophys. Res. Lett., 33, L03710. doi:10.1029/2005GL024866, 2006.

352 [17]Zhang, R. H., A. Sumi, and M. Kimoto: Impact of El Niño on the East Asian monsoon: A
353 diagnostic study of the '86/87 and '91/92 events, J. Meteor. Soc. Japan, 74, 49–62, 1996.

354 [18]Wang, L., W. Chen, and R. H. Huang: Interdecadal modulation of PDO on the impact of ENSO on
355 the east Asian winter monsoon, Geophys. Res. Lett., 35, L20702, doi:10.1029/2008GL035287, 2008.

356

357 3-1. The remainder of section 2.3, concerned with determining the number of
358 predictors is difficult to follow. It is not until section 3 (page 11) that it is revealed that
359 the model is a dynamical system of four second order coupled equations, involving
360 the products of the various predictors as well as the predictors themselves. Nowhere is
361 the inclusion of these terms discussed or justified. What physical processes do these
362 terms represent? What do the predictors squared represent?, and the cross products ie
363 what do $T1 * SOI$ or $T2 * EAWMI$ mean? Since the model is not a linear regression
364 model, is stepwise regression a valid procedure for determining the significance of the
365 predictors?

366 Responses: Good suggestions. Your opinion is very good. Based on your
367 suggestion of question 2, we have revised the discussion of how to determine the
368 number of predictors. Our model is not a linear regression model, the stepwise
369 regression may be a valid procedure for determining the significance of the predictors,

370 so we also have revised the method for determining the significance of the predictors,
371 the specific revision can be seen our answer of the question2.

372 The inclusion of these terms and the physical processes do these terms represent
373 are important, especially for the discussion of dynamical characteristics of the
374 dynamical model. But now we are difficult to give a clear meaning. Now the main
375 work of our paper is the prediction experiments of the model. For the reason of time
376 and length, this paper mainly discusses the prediction results of the model. The
377 physical processes do these terms represent and the discussion of the dynamical
378 characteristics of the model will be the focus of our next work. Before this, we have
379 also used the Takens' delay embedding theorem to reconstruct the dynamical model of
380 the Western Pacific subtropical high(WPSH). And Based on the reconstructed
381 dynamical model, dynamical characteristics of WPSH are analyzed and an aberrance
382 mechanism is developed, in which the external forcings resulting in the WPSH
383 anomalies are explored, which have been published(Hong et al., 2016). We also study
384 the bifurcation and catastrophe of the West Pacific subtropical high ridge index of a
385 nonlinear model (Hong et al., 2017). Based on our previous method and work, our
386 next work is to analyze the physical processes and the dynamical characteristics of the
387 SST field.

388 The specific revision can be seen from line689 to704 in page33.We sincerely
389 hope for your satisfaction with our revision. Thank you again for your kind
390 suggestion.

391 References:

392 [1] Mei Hong*, Ren Zhang, et al., Catastrophe and Mechanism Analyses of Multiple
393 Equilibria in the Western Pacific Subtropical High System Based on Objective Fitting
394 of Spatial Basis Functions. *Monthly Weather Review*, 2016,144:997-1015.

395 [2] Mei Hong*, Ren Zhang, et al., Bifurcations and catastrophes in a nonlinear
396 dynamical model of the western Pacific subtropical high ridge line index and its
397 evolution mechanism, *Theor. Appl. Climatol.*, 129, 363-384, 2017.

398

399 3-2. line 195. The idea that a model with the number of predictors less than 10% of
400 the sample size can avoid overfitting is new to me. The reference given (Tetko et al) is
401 about neural networks. Is this applicable to the system of coupled equations used here?
402 (I could only see the first page) Also I am not sure if the discussion in 198-203 is
403 incorrect. Even if only 34 parameters are accepted, the full set of 56 parameters must
404 be estimated to know which to accept or reject. This may be more a problem of
405 introducing artificial skill, which has long been recognised as a problem in statistical
406 forecasting. It generally arises when you try enough predictors, and retain those that
407 "work" and discard the others.

408 This question of the number of parameters / predictors is exacerbated in Section 4 and
409 5 where the number of predictors is increased again by including lagged values. On
410 first inspection Equations 3 and 7 involve 112 parameters. There are 28 alphas, 28
411 thetas, as given in lines 395 and 396. (In line 202, it is stated that there are 28 self
412 memorization parameters beta; but there are no betas in Eqs 3 and 5, but there are in
413 Appendix B) In addition each of the four F "dynamical cores" involve 14 parameters

414 as shown in Equation 1, assuming that the same F is used at each lagged time. Given
415 that the input data (the x_i) are different at each lag, is the same F a valid assumption?
416 Even with the authors 34 accepted values in the F s, there is still a total of 90
417 parameters. This is well over 10%, and on the authors own criterion, this would
418 suggest that the system is perhaps overfit. Additionally, all the 720 observations are
419 not statistically independent. Both T1 and the SOI (and probably T2 with its strong
420 trend) are strongly auto-correlated, and the effective sample size is probably
421 significantly less than 720. All in all, this discussion is very confusing!

422 Responses: Good suggestions. Our final number of 90 parameters is still a little
423 large for a sample size of 720. In the previous paper, this discussion of overfitting is a
424 little confusing. So it is still necessary to further discuss whether our model has the
425 overfitting problem or not. Thank reviewers to remind us this problem.

426 The definition of overfitting: The learned hypothesis may fit the training set very
427 well, but fail to predict to new examples (fail to fit additional data or predict future
428 observations reliably).

429 The potential for overfitting depends not only on the number of parameters and
430 data but also the conformability of the model structure with the data shape, and the
431 magnitude of model error compared to the expected level of noise or error in the
432 data(Burnham and Anderson, 2002). So there are many reasons causing the overfitting
433 phenomenon. But this does not mean having many parameters relative to the number
434 of observations inevitably causes the overfitting problem (Golbraikh et al., 2003).
435 There is no evidence that more parameters will be certain to result in overfitting.

436 Based on the definition of overfitting and the previous studies(Golbraikh et al., 2003;
437 Everitt and Skron dal,2010), we can judge whether a model is overfitting or not by the
438 accuracy of prediction results of independent samples (Golbraikh and Tropsha, 2002;
439 Qi and Li, 2006).

440 In the sample training, our model does not purposely pursue the high degree of
441 the training samples fitting and improve the effectiveness of the independent
442 generalization. In fact in our paper the forecast results of the Cross-validated
443 retroactive hindcasts (section 5.2) and the independent samples validation (table3 and
444 table4) are both good. Especially, the independent samples validation of the ENSO
445 index as the table4, we have carried out the 240 independent sample validation
446 prediction of four seasons of different ENSO events and the coverage of independent
447 samples test is very wide. Moreover, compared with 6 mature prediction models, the
448 forecast results of our model are also good, which prove the overfitting problem does
449 not exist in our model. According to the previous literature (Islam and Sivakumar,
450 2002; Sivakumar et al.,2001), we can see that prediction principle and structure of the
451 phase space reconstruction (PSR) of dynamical system is not the same with the
452 traditional neural network and in the small sample situation the forecasting results of
453 PSR model are better than those of the traditional neural network (Sivakumar et
454 al. ,2002), which can be verified in the independent sample test (table3 and table4). So
455 according to the definition of overfitting, we can say the over fitting phenomenon
456 does not exist in our model.

457 Now we have added the new discussion of the overfitting problem from line633
458 to663in page30-31.

459 We sincerely hope for your satisfaction with our revision. Thank you again for
460 your kind suggestion.

461

462 References:

463 [1]Burnham, K. P.; Anderson, D. R. (2002), Model Selection and Multimodel Inference (2nd ed.),
464 Springer-Verlag.

465 [2] Everitt B.S., Skrondal A. (2010), Cambridge Dictionary of Statistics, Cambridge University
466 Press.

467 [3] Golbraikh A.,Shen M., Xiao Z. Y., Xiao Y. D., Lee Kuo-Hsiung, Tropsha A., 2003: Rational
468 selection of training and test sets for the development of validated QSAR models. Journal of
469 Computer-Aided Molecular Design, 17(2), 241-253.

470 [4] Golbraikh A. and Tropsha A., 2002: Beware of q^2 ! Journal of Molecular Graphics and
471 Modelling, 20 , 269–276.

472 [5] Qin G. H. and Li Z. H., 2006: Over-fitting of BP NN research and its application, Engineering
473 Journal of Wuhan University,39(6),1671-1679

474 [6] Leinweber, D. J., 2007: Stupid Data Miner Tricks. The Journal of Investing, 16, 15–22.

475 [7] Islam M.N. Sivakumar B., 2002. Characterization and prediction of runoff dynamics:a
476 nonlinear dynamical view. Advances in Water Resources, 25, 179-190.

477 [8]Sivakumar B, Berndtsson R, Persson M. 2001. Monthly Runoff Prediction Using Phase -space
478 Reconstruction. Hydrological Sciences Journal, 46(3), 377 -388.

479 [9]Sivakumar B., Jayawardena A.W., Fernando T.M.K.G., 2002. River flow forecasting: use
480 of phase-space reconstruction and artificial neural networks approaches. Journal of Hydrology,
481 265, 225-245.

482

483 4. Model Validation

484 4-1.line 281-288. This paragraph took me a long time to understand, especially how
485 one could obtain correlations and MAPE values based on a single forecast. As I
486 understand it, "at this time" refers to the forecast at five months, and the correlation
487 and MAPE are calculated over the first five months forecasts, and in general the
488 values at the Nth month are based on the first N months forecast. (I assume that this is
489 the "n" in the equation for MAPE on line 283)

490 Responses: Good suggestions. Your understanding is right. "at this time" refers to
491 the forecast at five months, and the correlation and MAPE are calculated over the first
492 five months forecasts, and in general the values at the Nth month are based on the first
493 N months forecast. Now we revise the sentence "Using T_1 as an example, at this time,
494 the temporal correlation between model predictions and corresponding observations
495 was 0.8966 and the mean absolute percentage error (MAPE) (Hu et al.,

496 2001), $MAPE = \frac{1}{n} \sum_{i=1}^n \left| \frac{D_e(i) - D_0(i)}{D_0(i)} \right| \times 100$, was 8.32%." as "Using as an example,

497 the CC between model predictions and corresponding observations over the first five
498 months forecasts was 0.8966 and MAPE was 8.32%." for readers' better
499 understanding.

500 The specific revision can be seen from line275 to276 in page13. We sincerely
501 hope for your satisfaction with our revision. Thank you again for your kind
502 suggestion.

503

504 4-2. This method would suggest that the correlation at one month is undefined, and
505 1.0 (perfectly accurate) at two months? This same type of calculation appears to be
506 used in Tables 3 and 4.

507 Responses: Good suggestions. In previous paper, we have not explained the concept
508 of correlation. There two different correlations in our paper. The first correlation in
509 our paper is the pearson correlation coefficient (CC), which also can be called
510 the linear correlation coefficient. It measures the strength and direction of a linear
511 relationship between two variables (for example model output and observed values).

512 The mathematical formula for computing r is:

513

$$r = \frac{\sum_{i=1}^n (D_e(i) - \bar{D}_e) \cdot (D_0(i) - \bar{D}_0)}{\sqrt{\sum_{i=1}^n (D_e(i) - \bar{D}_e)^2 \cdot \sum_{i=1}^n (D_0(i) - \bar{D}_0)^2}}$$

514 Where n is the number of pairs of data, D_e, D_0 is a series of n observations and n
515 forecast values.

516 The CC (Wang et al. 2009) and the mean absolute percentage error (MAPE)(Hu
517 et al. 2001) are employed as objective functions to calibrate the model. The CC
518 evaluates the linear relationship between the observed and predicting values and
519 MAPE measures the difference between the observed and predicting values. The
520 forecast results of T_1, T_2 in Section3, table2 and table3 have used the above two
521 evaluation criteria (r and MAPE).

522 While the evaluation criteria of the ENSO index in table4 is the temporal
523 correlation (TC), its definition and specific calculation steps can be seen in these
524 literatures (Kathrin et al.,2016; Nicosia et al. 2013); The TC is often used to measure
525 the prediction effect of the ENSO index. For example, in 1995,Chen et al. used TC as
526 the evaluation criteria to test the improved Predictability of El Nino Forecasting of
527 their model and Barnston et al.in 2012 also used the TC to compare the forecast skill
528 of 21 real-time seasonal ENSO models.

529 In the previous paper, we didn't explain two different correlations clearly, which
530 will be easy for readers to misunderstand. Now we have explained two different
531 correlations and the specific revision can be seen in all my paper.

532 We sincerely hope for your satisfaction with our revision. Thank you again for
533 your kind suggestion.

534

535 **References:**

536 [1] Wang, W. C., K. W. Chau, C. T. Cheng, and L. Qiu, 2009: A comparison of performance of
537 several artificial intelligence methods for forecasting monthly discharge time series. *J. Hydrol.*,
538 374, 294–306, doi:10.1016/j.jhydrol.2009.06.019.

539 [2] Hu, T. S., K. C. Lam, and S. T. Ng, 2001: River flow time series prediction with a
540 range-dependent neural network. *Hydrol. Sci. J.*, 46, 729–745, doi:10.1080/02626660109492867.

541 [3] Kathrin B üttner, Jennifer Salau, and Joachim Krieter,2016: Temporal correlation coefficient for
542 directed networks. *Springerplus*, 5(1): 1198-1203.

543 [4] Nicosia V, Tang J, Mascolo C, Musolesi M, Russo G, Latora V. Graph metrics for temporal
544 networks. In: Holme P, Saram äki J, editors. *Temporal networks*. Berlin: Springer; 2013. pp. 15–40.

545 [5] Chen D., S. E. Zebiak, A. J. Busalacchi and M. A. Cane: An Improved Procedure for El Niño
546 Forecasting: Implications for Predictability, *Science*, 269, 1699-1702, 1995

547 [6] Barnston A. G., et al.: Skill of real-time seasonal ENSO model predictions during
548 2002-2011, *Bull. Amer. Meteor. Soc.*, 93, 631-651, 2012.

549

550

551 4-3.line 289-298. Another confusing paragraph. January 1951 to January 1952

552 inclusive? is 13, not 12 months. How was the omitted section forecast, ie was it

553 simply a 12 (or 13) month forecast starting at the last point before the omitted data?

554 Responses: Good suggestions. This is a mistake in writing and thanks the reviewers'

555 comments. The omitted forecast section is 12 months, Jan. 1951 to Dec.1951, and the

556 training sample time is Jan.1952 to December 2010. Then in the next prediction

557 experiment, the omitted segment is Jan.1952 to Dec. 1952 and the training samples

558 are Jan. 1951 to Dec.1951 and Jan.1953 to Dec.2010. So the forecast time series is

559 Jan.1952 to Dec. 1952. We then repeated this procedure the by moving the omitted

560 segment along the entirety of the available time series. The similar process of the

561 cross-validated retroactive hindcasts has also been used in the previous literatures (Hu

562 et al., 2017).

563 The specific revision can be seen from line 284 to 293 in page14.

564 We sincerely hope for your satisfaction with our revision. Thank you again for

565 your kind suggestion.

566

567 References:

568 [1] Hu Y. J., Zhong Z., Zhu Y. M. et al., A statistical forecast model using the
569 time-scale decomposition technique to predict rainfall during flood period over the
570 middle and lower reaches of the Yangtze River Valley, Theoretical and Applied
571 Climatology, doi: 10.1007/s00704-017-2094-9.

572 4-4.it is difficult to judge how "good" the forecast was based on Figure 3.

573 Responses: Good suggestions. From Fig3, the prediction values (blue line) and the
574 actual values (red line) are relatively close in some places, but in many places,
575 especially in the peaks, the error is large, which in accordance with the analysis of
576 Figure 2. The forecast results within 5 months of the simple dynamical reconstruction
577 model in section3 are good, but the long term prediction results after 5 months
578 become bad and the error increases quickly. So this is why we have to introduce the
579 self -memorization principle to improve the long term prediction results.

580 We sincerely hope for your satisfaction with our revision. Thank you again for
581 your kind suggestion.

582

583 4-5.Again it is not clear how the correlation and MAPE statistics were calculated -
584 only one value is given, so presumably it is taken over all (720 months) forecast?

585 Responses: Good suggestions. In pervious paper we haven't explained clearly
586 how the correlation and MAPE statistics in Fig.3 were calculated. It isn't taken over
587 all (720 months) forecast when only one value is given (The forecast for such a long
588 time is not possible). The figure 3 merges the 60 experiments (each experiment is the
589 prediction of the 12 month similar as Fig.2) on one picture. The Fig.3 is equivalent to

590 60 experiments instead of the results of only one experiment, because the results of
591 one experiment are not entirely representative. And through multiple cross
592 experiments can more objectively reflect the forecast capability of our model. So the
593 forecast results of 60 cross experiment (each experiment is the prediction of the 12
594 month as Fig.2) according to the time sequence can merger into a new time series
595 (from Jan.1951-Dec.2010), and then the pearson correlation coefficient (CC) and the
596 mean absolute percentage error (MAPE) can be calculated by the new prediction time
597 series and the time series of the actual value based on the formula in the above answer
598 of 4-2 problems. Actually, the CC and MAPE are the average of the prediction values
599 of the 60 cross experiments. That's how the correlation and MAPE statistics were
600 calculated in Fig. 3.

601 Now we have added the above explanation from line 294 to 300 in page14 for
602 readers' better understanding.

603 We sincerely hope for your satisfaction with our revision. Thank you again for
604 your kind suggestion.

605

606 4-6. However the discussion in lines 310-312 suggest that individual 12 month
607 forecasts were also evaluated. Overall the discussion of the forecast process and its
608 validation in not clear.

609 Responses: Good suggestions. The CC and MAPE in Fig.3 are the average of the
610 prediction values of the 60 cross experiments. But each MAPE value of the above 60
611 experiments is not the same and the difference between the maximum and the
612 minimum MAPE value is quite large, which means that the prediction results of the

613 simple dynamical reconstruction model in section3 is not stable. So that is another
614 reason why we need to introduce self -memorization principle to improve our model.

615 We sincerely hope for your satisfaction with our revision. Thank you again for
616 your kind suggestion.

617

618 Some minor points

619 1. In line 170, all 4 data sets range from Jan 1951 to Jan 2010, yet in at least 4 places,

620 Responses: Good suggestions. Now we have deleted the other 3 places about the
621 description of the length of the data. And in pervious paper, “ all 4 data sets from Jan.
622 1951 to Jan. 2010” is mistake in writing. Now we revised as “The time series of all
623 data were from Jan. 1951 to Dec. 2010, 720 months in total” from line129 to line130
624 in page6.

625 We sincerely hope for your satisfaction with our revision. Thank you again for
626 your kind suggestion.

627

628 2. lines 292, 373, 402 and 416 forecasts are evaluated up to December 2010?

629 Responses: Good suggestions. In previous paper, “ all 4 data sets from Jan. 1951
630 to Jan. 2010” is mistake in writing. Now we revised as “The time series of all data
631 were from Jan. 1951 to Dec. 2010, 720 months in total.” So the lines 292, 373, 402
632 and 416 forecasts are surely evaluated up to December 2010.

633 We sincerely hope for your satisfaction with our revision. Thank you again for
634 your kind suggestion.

635 3. lines 249-253. Why does normalising the raw values avoid the overfitting
636 problem?

637 Responses: Good suggestions. Now we have revised the sentences” To avoid the
638 overfitting problem, we used $x_{nor} = \frac{x - x_{min}}{x_{max} - x_{min}}$ to normalize the raw value of each of
639 the four predictors, then we used the normalized value to model and forecast.” as “In
640 order to eliminate the dimensionless relationship between variables, data
641 standardization is to transform data from different orders of magnitude to the same
642 order of magnitude, thus making the data comparable. So we used $x_{nor} = \frac{x - x_{min}}{x_{max} - x_{min}}$
643 to normalize the raw value of each of the four predictors, then we used the normalized
644 value to model and forecast.” from line243 to line248 in page12.

645 We sincerely hope for your satisfaction with our revision. Thank you again for
646 your kind suggestion.

647

648 4. line 254. What criterion is used to determine what are "weak items" with "small
649 dimension coefficient".

650 Responses: Good suggestions. In the previous paper, we have neglected to
651 explain the criterion is used to determine what are "weak items" with "small
652 dimension coefficient".

653 In order to quantitatively compare the relative contribution of each item of our
654 model to the evolution of the system, we calculated the relative variance contribution.

655 The formula is as follows: $R_i = \frac{1}{n} \sum_{j=1}^n \left[\frac{T_i^2}{\sum_{i=1}^{14} T_i^2} \right], i = 1, 2, \dots, 14$, Where n is the length of
656 the data, $T_i = a_1x_1, a_2x_2, \dots, a_{14}x_3x_4$ is the item in the equation. According to our
657 previous research (Hong et al., 2007), the variance contribution of the real item
658 reflecting the performance of the model has a large proportion, while the variance
659 contribution of the false term is almost zero, so we delete the weak items of
660 $R_i < 0.01$.

661 Now we have added the above explanation about the criterion is used to
662 determine what are "weak items" from line250-257 in page12.

663 We sincerely hope for your satisfaction with our revision. Thank you again for
664 your kind suggestion.

665 References:

666 [1] Hong Mei, Zhang Ren, Wu Guoxiong, et al., 2007. A Nonlinear Dynamic System
667 Reconstruction of the Subtropical High Characteristic Index based on Genetic
668 Algorithm. Chinese Journal of Atmospheric Sciences,31(2):346-352.

669

670 5. line 280 "forecast performance ... was better" than what??

671 Responses: Good suggestions. Now we have revised the sentence "From Fig. 2,
672 forecast performance of T_1 and T_2 within 5 months was better." as "From Fig. 2,
673 forecast performance of T_1 and T_2 within 5 months was good."

674 We sincerely hope for your satisfaction with our revision. Thank you again for
675 your kind suggestion.

676

677 6.Section 6.2 - Table 5 The values reported here do not make sense. By construction,
678 EOFs (the spatial patterns) are orthogonal, and the PCs (the time series) are uncor-related.
679 L'Heureax et al report that the correlation between PC1 and PC2 (using the
680 same HADISST data set) is 0.4 when the time series are detrended. This is the same
681 value quoted in Table 5. Has T2 been detrended here also?

682 Responses: Good suggestions. In table 5, the values reported here do not make
683 sense. Now we have deleted the Table5. In previous paper, we don't have detrended
684 T_2 . We have just smoothed the SSTA field before EOF. But due to a careless mistake,
685 we use the data of a prediction experiment of 12 months to calculate the correlation
686 coefficient in table5 and this is a mistake. We should use the all data from Jan.1951 to
687 Dec.2010, a total of 720 months to calculate the correlation coefficient, so the
688 correlation coefficients in the table5 are not correct in our pervious paper. Now we
689 have recalculated with the right data. And after the time series are detrended, we have
690 recalculated that the correlation between PC1 and PC2 is 0.4024, which is the similar
691 as L'Heureax et al.

692 We sincerely hope for your satisfaction with our revision. Thank you again for
693 your kind suggestion.

694

695 7.EOF1 is the canonical ENSO pattern, and its time series is stronly correlated with the
696 standard Nino indices (l'Heureaux et al give a value of 0.94 between their first EOF and
697 the Nino3.4 index). In turn the Nino3.4 index is strongly correlated to the SOI, so that

698 is difficult to see the correlation between T_1 and the SOI being as small as the 0.4 given
699 in Table 5. (This correlation is where the term ENSO i.e. El Niño - Southern Oscillation
700 arises)

701 Responses: Good suggestions. In the answer of the previous question, we
702 mentioned that because of a careless mistake, correlation coefficient in the table5
703 formula is not correct. Now we have recalculated with the right data. In the answer to
704 question 2, the correlation coefficient of T_1 and SOI in table2 is 0.773, which is
705 consistent with the fact that the Niño3.4 index is strongly correlated to the SOI.

706 We sincerely hope for your satisfaction with our revision. Thank you again for
707 your kind suggestion.

708

709 8. Acronyms need to be defined the first time they are used, eg EOF on lines 128-130

710 Responses: Good suggestions. Now we have defined Acronyms in the first time
711 they are used.

712 We sincerely hope for your satisfaction with our revision. Thank you again for
713 your kind suggestion.

714

715 9. Figure caption (line 912) for figure 1 in List of figures is incorrect, and different to that
716 given with the figure itself (line 959).

717 Responses: Good suggestions. Now we have revised the figure caption (line
718 1027) for figure 1 in List of figures.

719 We sincerely hope for your satisfaction with our revision. Thank you again for

720 your kind suggestion.

721

722 10. References are incomplete; there are at least 15 references that are not cited in the
723 text, and a number that are cited but referenced.

724 Responses: Good suggestions. Now we have revised the list of references
725 carefully and make all the references complete.

726 We sincerely hope for your satisfaction with our revision. Thank you again for
727 your kind suggestion.

728

729

730

731

732

733

734

735

736

737

738

739

740

741

742 **Forecasting experiments of a dynamical-statistical model**
743 **of the sea surface temperature anomaly field based on the**
744 **improved self-memorization principle**

745 Mei Hong^{1,2}, [Ren Zhang^{1,2}](#), [Xi Chen⁴](#), ~~Ren Zhang^{1,2}~~, Dong Wang³, Shuanghe
746 Shen², [Xi Chen¹](#), and Vijay P. Singh⁴

747 *[¹Collaborative Innovation Center on Forecast and Evaluation of Meteorological Disaster, Nanjing University of](#)*
748 *[Information Science & Technology, Nanjing 210044, China](#)*

749 ~~*[¹Institute](#)*~~ *[²Institute of Meteorology and Oceanography, National University of Defense Technology, Nanjing](#)*
750 *[211101, China](#)*

751 ~~*[²Collaborative Innovation Center on Forecast and Evaluation of Meteorological Disaster, Nanjing University of](#)*~~
752 *[Information Science & Technology, Nanjing 210044, China](#)*

753 *[³Key Laboratory of Surficial Geochemistry, Ministry of Education; Department of Hydrosciences, School of Earth](#)*
754 *[Sciences and Engineering, Collaborative Innovation Center of South China Sea Studies, State Key Laboratory of](#)*
755 *[Pollution Control and Resource Reuse, Nanjing University, Nanjing 210093, China](#)*

756 *[⁴Department of Biological and Agricultural Engineering, Zachry Department of Civil Engineering, Texas A & M](#)*
757 *[University, College Station, TX 77843, USA](#)*

758
759
760 Corresponding authors address:

761 [1. Ren Zhang, Research Centre of Ocean Environment Numerical Simulation,](#)
762 [Institute of Meteorology and Oceanography, National University of Defense](#)
763 [Technology, Nanjing 211101, China](#)

764 [E-mail: 254247175@qq.com](mailto:254247175@qq.com)

765 ~~1.~~ [2. Xi Chen, Research Centre of Ocean Environment Numerical Simulation, Institute](#)
766 [of Meteorology and Oceanography, National University of Defense Technology,](#)
767 [Nanjing 211101, China](#)

768 E-mail: chenxigkd@163.com

769 ~~2. Ren Zhang, Research Centre of Ocean Environment Numerical Simulation,~~
770 ~~Institute of Meteorology and Oceanography, National University of Defense~~
771 ~~Technology, Nanjing 211101, China~~

772 E-mail: 254247175@qq.com

773

774 **Abstract:** With the objective of tackling the problem of inaccurate long-term El Niño
775 Southern Oscillation (ENSO) forecasts, this paper develops a new
776 dynamical-statistical forecast model of sea surface temperature anomaly (SSTA) field.
777 To avoid single initial prediction values, a self-memorization principle is introduced
778 to improve the dynamic reconstruction model, thus making the model more
779 appropriate for describing such chaotic systems as ENSO events. The improved
780 dynamical-statistical model of the SSTA field is used to predict SSTA in the
781 equatorial eastern Pacific and during El Niño and La Niña events. The long-term
782 step-by-step forecast results and cross-validated retroactive hindcast results of time
783 series T_1 and T_2 are found to be satisfactory, with a [pearson](#) correlation coefficient of
784 approximately 0.80 and a mean absolute percentage error ([MAPE](#)) of less than 15%.
785 The corresponding forecast SSTA field is accurate in that not only is the forecast
786 shape similar to the actual field, but the contour lines are essentially the same. This
787 model can also be used to forecast the ENSO index. The [temporal](#) correlation
788 coefficient is 0.8062, and the MAPE value of 19.55% is small. The difference
789 between forecast results in [summer-spring](#) and those in [winter-autumn](#) is not high,

790 indicating that the improved model can overcome the spring predictability barrier to
791 some extent. Compared with six mature models published previously, the present
792 model has an advantage in prediction precision and length, and is a novel exploration
793 of the ENSO forecast method.

794

795 **Keywords:** Dynamical-statistical forecast model; self-memorization principle; sea
796 surface temperature field; long-term forecast of ENSO

797 **1. Introduction**

798 The El Niño Southern Oscillation (ENSO), the well-known coupled atmosphere
799 –ocean phenomenon, was firstly proposed by Bjerknes (1969). The ENSO
800 phenomenon can influences regional and global climates, so the prediction of ENSO
801 has received considerable public interest (Rasmusson and Carpenter, 1982; Glantz et
802 al., 1991).

803 Over the past two to three decades, one might reasonably expect the ability to
804 predict warm and cold episodes of ENSO at short and intermediate lead times to have
805 gradually improved (Barnston et al., 2012). Many countries have been focusing on
806 ENSO forecasts since the 1990s, and the ENSO forecast has become one of the
807 important research topics in the International Climate Change and Predictability
808 Research plan. The U.S. International Research Institute for Climate and Society, the
809 U.S. Climate Prediction Centre, Japan Meteorological Agency, and European Centre
810 for Medium-Range Weather Forecasting have developed different coupled
811 atmosphere–ocean models to forecast ENSO (Saha et al., 2006; Molteni et al., 2007) .

812 The forecast models can generally be divided into two types (Palmer et al., 2004).
813 The first type is typified by a dynamic model, which mathematically expresses
814 physical laws that govern how the ocean and the atmosphere interact. The second type
815 is typified by a statistical model, which requires large a amount of historical data and
816 analyses the data to do forecasting (Chen et al., 1995; Moore et al., 2006).

817 Over the past three decades, ENSO predictions have made remarkable progress,
818 reaching a stage where reasonable statistical and numerical forecasts (Jin et al.,
819 2008) can be made 6–12 months in advance (Wang et al., 2009a). . However, there are
820 three problems remaining to be resolved (Zhang et al., 2003a): (1) The current
821 ENSO predictions are mainly limited to the short term, such as annual and seasonal
822 predictions; (2) Although the representation of ENSO in coupled models has
823 advanced considerably during the last decade, several aspects of the simulated
824 climatology and ENSO are not well reproduced by the current generation of coupled
825 models. The systematic errors in SST are often very large in the equatorial Pacific,
826 and model representations of ENSO variability are often weak and/or incorrectly
827 located (Neelin et al. 1992; Mechoso et al. 1995; Delecluse et al. 1998; Davey et al.
828 2002). (3) Coupled models of ENSO predictions initialized from observed initial
829 states tend to adjust towards their own climatological mean and variability, leading to
830 forecast errors. The errors associated with such adjustments tend to be more
831 pronounced during boreal spring, which is often called the “spring predictability
832 barrier” (Webster et al., 1999). More efficient models are therefore desired (Belkin
833 and Niyogi, 2003; Weinberger and Saul, 2006). Therefore, the idea of combining

834 dynamical and statistical methods to improve weather and climate prediction has been
835 developed in many studies (~~Chou, 1974;~~ Huang et al., 1993; Yu et al., 2014a; Yu et
836 al., 2014b). By introducing genetic algorithms (GAs), Zhang et al. (2006) inverted and
837 reconstructed a new dynamical-statistical forecast model of the tropical Pacific sea
838 surface temperature (SST) field using historic statistical data (Zhang et al., 2008).
839 However, there is one flaw in the forecast model: the time-delayed SST field. This is
840 because ENSO is a complicated system with many influencing factors. To overcome
841 information insufficiency in the forecast model, Hong et al. (2014) selected the
842 tropical Pacific SST, SSW and SLP fields as three modelling factors and utilized the
843 GA to optimize model parameters.

844 However, the above dynamical prediction equations which were proposed by
845 Hong et al. (2014), greatly depend on a single initial value, creating long-term
846 forecasts over 8 months that diverged significantly. These unsatisfactory results
847 indicate that this model needs to be improved. Cao (1993) first proposed the
848 self-memorization principle, which transforms the dynamical equations with the
849 self-memorization equations, wherein the observation data can determine the memory
850 coefficients. This method has been widely used in forecast problems in environmental,
851 hydrological and meteorological fields (Feng et al., 2001; Gu, 1998; Chen et al.,
852 2009). The method can avoid the question of initial conditions for the differential
853 equations, so it can be introduced here to improve the proposed dynamical forecast
854 model.

855 Therefore, an improved dynamical-statistical forecast model of the SST field

856 and its impact factors with a self-memorization function was developed. The
857 improved model can absorb the information from past observations.

858 This paper is organized as follows: Research data and forecast factors are
859 introduced in section 2. In Section 3 the reconstruction of the dynamical model of
860 SSTA field is described. To improve the reconstruction model, the self-memorization
861 principle is introduced in Section 4. Model forecast experiments are described in
862 Section 5, and conclusions are given in Section 6.

863 **2. Research data and forecast factors**

864 **2.1 Data**

865 The monthly average SST data ~~from January 1951 to January 2010, 720~~
866 ~~months in total,~~ were obtained from the UK Met Office Hadley Centre for the region
867 (30 °S-30 °N; 120 °E -90 °W). The gridded 1° ×1° Met Office Hadley Sea Ice and
868 SST dataset (HadISST1; Rayner et al. 2003) includes both in situ and available
869 satellite data. The sea areas provide important information on ocean-atmosphere
870 coupling in the East and West Pacific Ocean and the El Niño /La Niña events. The
871 reanalysis data, zonal winds and sea level pressures were obtained from the National
872 Center for Environmental Forecast of America and the National Center for
873 Atmospheric Research (Kalnay et al., 1996). The sea surface height (SSH) field was
874 obtained from Simple Ocean Data Assimilation (SODA) data (James and Benjamin,
875 2008). Outgoing longwave radiation (OLR) was obtained from the National Oceanic
876 and Atmospheric Administration (NOAA) satellites, at a resolution of 0.5° ×
877 0.5° (Liebmann and Smith, 1996).~~The sea areas provide important information on~~

878 ~~ocean-atmosphere coupling in the East and West Pacific Ocean and the El Niño and~~
879 ~~La Niña events. The reanalysis data and zonal winds were obtained from the National~~
880 ~~Center for Environmental Forecast (NECP) of America and the National Center for~~
881 ~~Atmospheric Research (NCAR) (Kalnay et al., 1996). The Southern Oscillation Index~~
882 ~~(SOI) data were obtained from the Climate Prediction Center (CPC). The time series~~
883 ~~of all data were from Jan. 1951 to JanDec. 2010, 720 months in total.~~

884 **2.2 EOF deconstruction**

885 The sea surface temperature anomaly (SSTA) field can be calculated from the
886 SSTA field and can be deconstructed into time (coefficients)-space (structure) using the
887 empirical orthogonal function (EOF) method. Detailed information on the EOF
888 method can be seen in the related references (Dommenget & Latif, 2002). We have
889 used covariance matrix, because the covariance matrix was selected to diagnose the
890 primary patterns of co-variability in the basin-wide SSTs, rather than the patterns of
891 normalized covariance (or correlation matrix).

893 We used the smooths function with MATLAB to smooth the SSTA field before
894 the EOF deconstruction, which is five points two times moving, mainly filtering out
895 some noise points and outliers. Then a~~An empirical orthogonal function (EOF)~~
896 analysis of smoothed anomalies was performed, and the first two SSTA EOFs are
897 shown in Figs. 1a and 1c. The principal component (PC) time series corresponding to
898 the first and second EOFs are shown in Figs. 1b and 1d. The first EOF pattern, which
899 accounted for 61.33% of the total SSTA variance, represented the mature ENSO phase

900 (El Niño or La Niña), and the corresponding PC time series was highly correlated
901 (with a correlation coefficient of 0.85) with the cold tongue index (SST anomaly
902 averaged over 4°S – 4°N , 180° – 90°W) over the whole period. The second EOF,
903 accounting for 14.52% of the total SSTA variance, indicated [the ENSO signal](#)
904 [beginning to enhance](#)~~the ENSO signal beginning to decay~~. Compared with the first
905 mode, these were slightly attenuated in terms of the scope and intensity. The above
906 analysis is similar to the EOF analysis of the SSTA field in the previous studies
907 (Johnson et al., 2000; Timmermann et al., 2001). This indicates that the front two
908 variance contribution modes can describe the main characteristics of the SSTA field
909 and El Niño/La Niña. Therefore, we can choose the T_1, T_2 time series EOF
910 decomposition modes as the modelling objects.

911 2.3 Selection of other prediction model factors

912 [Considering the complexity of computation, the amount of variables in the](#)
913 [equations of our model can't be too large, usually 3 or 4 for the best. This has been](#)
914 [explained in our previous studies \(Zhang et al., 2006; Zhang et al., 2008\). If there are](#)
915 [more than 4 variables in the modeling equation, it will cause the amount of](#)
916 [parameters such as \$a_1, a_2, \dots, a_n, b_1, b_2, \dots, b_n, \dots\$ too large. The huge computation makes it](#)
917 [difficult to be precisely modeled. Thus, the total number of parameters in the model of](#)
918 [five variables was 102, which may cause an overfitting problem. Hence, when we](#)
919 [selected the model of five or six variables which entailed large amounts of](#)
920 [computation that made precision difficult, and too many parameters might cause an](#)
921 [overfitting phenomenon. If we choose only two or even fewer variables, the forecast](#)

带格式的: 字体: Times New Roman, 字体颜色: 自动设置

带格式的: 字体: Times New Roman, 字体颜色: 自动设置

带格式的: 字体: Times New Roman, 字体颜色: 自动设置

922 performance is poor too. Too few variables cause too small reconstructed parameters,
923 resulting in amounts of important information missing out in the model. Thus, four
924 variables are best for dynamically and accurately modeling. Because we have chosen
925 two time series in section2.2 as the modeling objects, now we should select the other
926 two ENSO intensity impact factors.

927 The ENSO intensity impact factor is an important issue in ENSO prediction.
928 Previous studies have been completed in this area, which found that teleconnection
929 patterns, temperature, precipitation, wind and SSH may affect ENSO strength. For
930 example, Trenberth et al. (1998) noted that PNA, SOI and OLR in the Pacific
931 Intertropical Convergence Zone (ITCZ) are all closely related to ENSO.
932 Webster(1999) pointed out after the 1970, Indian Ocean dipole (IOD) is not only
933 affected by ENSO, but also affected the strength of ENSO (Ashok et al., 2001). Yoon
934 and Yeh (2010) reported that the Pacific Decadal Oscillation (PDO) disrupts the
935 linkage between El Niño and the following Northeast Asian summer monsoon
936 (NEASM) through inducing the Eurasian pattern in the mid-high latitudes. The vast
937 majority of studies (Tomita and Yasunari, 1996; Zhou and Wu, 2010; Kim et al., 2017)
938 have concentrated on the impacts of ENSO on the East Asian winter
939 monsoon(EAWM). During the EAWM season, ENSO generally reaches its mature
940 phase and has the most prominent impact on the climate. Wang et al. (1999a) and
941 Wang et al. (1999b) suggested that the zonal wind factors in the eastern and western
942 equatorial Pacific play a critical role in the phase of transition of the ENSO cycle,
943 which could excite eastward propagating Kelvin waves and affect the SSTA in the

带格式的: 字体: (默认) Times New Roman, 字体颜色: 自动设置

带格式的: 字体: (默认) Times New Roman, 字体颜色: 自动设置

带格式的: 字体: (默认) Times New Roman, 字体颜色: 自动设置

带格式的: 字体: (默认) Times New Roman, 字体颜色: 自动设置

带格式的: 字体: (默认) Times New Roman, 字体颜色: 自动设置

带格式的: 字体: (默认) Times New Roman, 字体颜色: 自动设置

带格式的: 字体: Times New Roman, 字体颜色: 自动设置

944 equatorial Pacific. Zhao et al. (2012) analyzed the characteristics of the tropical
 945 Pacific SSH field and its impact on ENSO events.

946 Based on the above analysis, we have selected nine factors, which may be
 947 closely related with the ENSO index (Niño3.4).

948 (1)The zonal wind in the eastern equatorial Pacific factor (u1) was calculated
 949 as the grid-point average of zonal wind in the area [5 °S ~ 5 °N, 150 °W ~ 90 °W].

950 (2) The zonal wind in the western equatorial Pacific factor (u2) was calculated
 951 as the grid-point average of zonal wind in the area [0 °~ 10 °N; 135 °E ~ 180 °E].

952 (3) The PNA teleconnection factor was obtained from the CPC.

953 (4) the dipole mode index factor (DMI) was obtained from SSTA for
 954 June-July-August (JJA) based on Saji(1999) method.

955 (5) The SOI factor was obtained from the CPC.

956 (6) The PDOI factor was obtained from department of Atmospheric Sciences
 957 in the university of Washington. The web is
 958 <http://tao.atmos.washinton.edu/pdo/RDO.latest>.

959 (7) The EAWM index (EAWMI) factor was proposed by Yang et al. (2002).
 960 which is defined by the meridional 850-hPa winds averaged over the region (20 °
 961 ~40 °N, 100 °~140 °E).

962 (8) The OLR in the ITCZ factor was calculated as the grid-point average of
 963 OLR in the area [10 °N~20 °N, 120 °E~150 °E].

964 (9) The SSH factor was calculated as the grid-point average of the SSH data in
 965 the area [10 °S ~ 10 °N; 120 °E ~ 60 °W].

- 带格式的：字体：Times New Roman, 字体颜色：自动设置
- 带格式的：字体：Times New Roman, 字体颜色：自动设置
- 带格式的：字体：Times New Roman, 字体颜色：自动设置
- 带格式的：字体：Times New Roman, 字体颜色：自动设置
- 带格式的：字体：Times New Roman, 字体颜色：自动设置
- 带格式的：字体：Times New Roman, 字体颜色：自动设置
- 带格式的：字体：Times New Roman, 字体颜色：自动设置
- 带格式的：字体：Times New Roman, 字体颜色：自动设置
- 带格式的：字体：Times New Roman, 字体颜色：自动设置
- 带格式的：字体：Times New Roman, 字体颜色：自动设置
- 带格式的：字体：Times New Roman, 字体颜色：自动设置
- 带格式的：字体：Times New Roman, 字体颜色：自动设置
- 带格式的：字体：Times New Roman, 字体颜色：自动设置
- 带格式的：字体：Times New Roman, 字体颜色：自动设置
- 带格式的：字体：Times New Roman, 字体颜色：自动设置

966 A correlation analysis of the above factors was carried out and the results are
967 shown in Table 1.

968 Table 1 shows that SOI and EAWMI have the stronger correlation with the
969 front two time series T_1, T_2 than the other 7 factors. The results are also consistent with
970 previous research (Clarke and Van Gorder, 2003; Drosdowsky, 2006; Zhang et al.,
971 1996; Wang et al., 2008; Yang and Lu, 2014). Therefore, the first time series T_1 , the
972 second time series T_2 , SOI and EAWMI will be selected as prediction model factors.

973 ~~The ENSO intensity impact factor is an important issue in the ENSO~~
974 ~~prediction. Previous studies have found that teleconnection patterns, temperature,~~
975 ~~precipitation, wind and SSH may affect the ENSO strength (Trenberth et al.,1998;~~
976 ~~Webster,1999; Ashok et al., 2001; Yoon and Yeh, 2010; Tomita and Yasunari, 1996).~~
977 ~~For example, Trenberth et al. (1998) noted that the Pacific North American Oscillation~~
978 ~~Index (PNA) and SOI in the Pacific Intertropical Convergence Zone (ITCZ) were all~~
979 ~~closely related to ENSO. Liao et al. (2007) also noted that the decadal variation~~
980 ~~during ENSO events had a close relationship with the SOI index. The vast majority of~~
981 ~~studies (Tomita and Yasunari, 1996; Zhou and Wu, 2010) have concentrated on the~~
982 ~~impacts of ENSO on the East Asian winter monsoon (EAWM). During the EAWM~~
983 ~~season, ENSO generally reaches its mature phase and has the most prominent impact~~
984 ~~on the climate. Wang et al. (1999a) and Wang et al. (1999b) suggested that the zonal~~
985 ~~wind factors in the eastern and western equatorial Pacific played a critical role in the~~
986 ~~transition phase of the ENSO cycle, which could excite eastward propagating Kelvin~~
987 ~~waves and affect the SSTA in the equatorial Pacific.~~

带格式的: 字体: Times New Roman, 字体颜色: 自动设置

带格式的: 字体: Times New Roman, 字体颜色: 自动设置

带格式的: 字体: Times New Roman, 字体颜色: 自动设置

带格式的: 字体: Times New Roman, 字体颜色: 自动设置

带格式的: 字体: (默认) Times New Roman, 字体颜色: 自动设置

带格式的: 字体: (默认) Times New Roman, 字体颜色: 自动设置

带格式的: 字体: (默认) Times New Roman, 字体颜色: 自动设置

带格式的: 字体: Times New Roman, 字体颜色: 自动设置

带格式的: 字体: Times New Roman, 字体颜色: 自动设置

带格式的: 字体: Times New Roman, 字体颜色: 自动设置

带格式的: 字体: Times New Roman, 字体颜色: 自动设置

带格式的: 字体: Times New Roman, 字体颜色: 自动设置

988 Based on the above analysis, we selected four factors, which may be closely
989 related with the ENSO index (Niño 3.4) and were obtained as follows:

990 (1) The zonal wind in the eastern equatorial Pacific factor (u_1) was calculated
991 as the grid point average of zonal wind in the area [5°S – 5°N , 150°W – 90°W].

992 (2) The PNA teleconnection factor was obtained from the CPC.

993 (3) The SOI factor was obtained from the CPC.

994 (4) The EAWM index (EAWMI) factor was proposed by Yang et al. (2002),
995 which is defined by the meridional 850 hPa winds averaged over the region (20°
996 40°N , 100° – 140°E).

997 All the four data selected ranged from January 1951 to January 2010.

998 Actually, how many variables and which variables are used in our model
999 become a key issue to be resolved. We can introduce a stepwise regression principle
1000 to choose more reasonable predictors (Yim et al., 2015), because the stepwise
1001 procedure can help selecting statistically important predictors at each step. The
1002 significance of each predictor selected was based on its significance in increasing the
1003 regressed variance by the standard F test (Panofsky and Brier, 1968). A 95 %
1004 statistical significance level was used as a criterion to select a new predictor at each
1005 step. Once selected into the model, a predictor can only be removed if its significance
1006 level falls below 95 % by the addition/removal of another variable. For example, for
1007 the model of only one variable, because we forecast the ENSO index, we should
1008 choose T_1 or T_2 as the variable. Considering that T_1 accounts for 61.33% of the total
1009 SSTA variance, so we chose T_1 as the variable. For the model of two variables, there

1010 are five factors (T_2, M_1 , PNA, SOI and EAWMI) which can be chosen for the second
1011 variable. Taking advantage of the stepwise regression ideas and selecting statistically
1012 important predictors by a standard F test, we can find the largest F test value among
1013 the five factors. That is T_2 . Continuing this step, we can also select the reasonable
1014 factors for the model of three variables. Based on this thought, when the number of
1015 variables is determined, we can choose the most statistically important variables to
1016 reconstruct the prediction model. The forecast results of these models can be seen in
1017 table 1.

1018 From table 1, the forecast results of all six models are satisfactory, where the
1019 temporal correlations of the models are all greater than 0.60 and the root mean square
1020 errors are all less than 0.81. Among all six models, the forecast results of four
1021 variables are the best for the following reasons:

1022 (1) In general, the amount of parameters is less than 10% of the sample size,
1023 which can avoid over fitting (Tetko et al., 1995). The number of parameters
1024 $a_1, a_2, \dots, a_{14}, b_1, b_2, \dots, b_{14}, c_1, c_2, \dots, c_{14}, d_1, d_2, \dots, d_{14}$ of the model of four variables $T_1, T_2, SOI, EAWMI$ is 56,
1025 but we deleted the parameters which contributed little to the prediction. That means
1026 that there are 56 parameters in equation (1) in section 3, but there are only 34
1027 parameters in equation (3) in section 3 which is our final prediction equation. In
1028 section 5.1, because p is identified as 6, the number of parameters of the
1029 self-memorization function β_i is 28. Therefore, the total number of parameters in the
1030 model of four variables is 62, which is less than 10% of the sample size (720 months).
1031 The number of parameters $a_1, a_2, \dots, a_{20}, b_1, b_2, \dots, b_{20}, c_1, c_2, \dots, c_{20}, d_1, d_2, \dots, d_{20}, e_1, e_2, \dots, e_{20}$ of the model

1032 of five variables $T_1, T_2, SOI, EAWMI, u_1$ is 100. Although the parameters which contributed a
1033 little were deleted, the number was still 72, and the number of self memorization
1034 parameters was 30 (p determined as 5). Thus, the total number of parameters in the
1035 model of five variables was 102, which was more than 10% of the sample size (720
1036 months). This will cause an overfitting problem. Hence, when we selected the model
1037 of five or six variables which entailed large amounts of computation that made
1038 precision difficult, and too many parameters caused an overfitting phenomenon. That
1039 is why the forecast results of five or six variables were worse than those of four
1040 variables.

1041 (2) The models of one, two and three variables can avoid the overfitting problem,
1042 but too few variables will result in too few reconstruction parameters, causing
1043 important information missing from the model. Especially, when the model of one or
1044 two variables was considered, we only studied the self memorization of the ENSO
1045 system but did not consider the mutual memorization between factors. Thus,
1046 equations of our model only contained a self-memory term, not an exogenous effect
1047 term. That is why the forecast results of one, two and three variables were worse than
1048 those of four variables.

1049 Based on the above analysis, we finally chose T_1, T_2, SOI and EAWMI as
1050 predictors for the model.

1051 3. Reconstruction of dynamical model based on GA

1052 Takens' delay embedding theorem (Takens, 1981) provides the conditions under
1053 which a smooth attractor can be constructed from observations made with a generic

1054 function. Later results replaced the smooth attractor with a set of arbitrary
 1055 box-counting dimensions and the class of generic functions with other classes of
 1056 functions. Takens had shown that if we measured any single variable with sufficient
 1057 accuracy for a long period of time, it would be possible to construct the underlying
 1058 dynamical structure of the entire system from the behavior of that single variable
 1059 using delay coordinates and the embedding procedure. It was therefore possible to
 1060 construct a dynamical model of system evolution from the observed time series.
 1061 Introducing this idea here, four time series of the T_1 , T_2 , SOI and EAWMI factors
 1062 were chosen to construct the dynamical model.

1063 The basic idea of statistical-dynamical model construction is discussed in
 1064 Appendix A and was introduced in our previous work (Zhang et al., 2006; Hong et al.,
 1065 2014).

1066 A simplified second-order nonlinear dynamical model can be used to depict the
 1067 basic characteristics of atmosphere and ocean interactions (Fraedrich, 1987). Suppose
 1068 that the following nonlinear second-order ordinary differential equations are taken as
 1069 the dynamical model of reconstruction. In the equations, x_1, x_2, x_3, x_4 were used to
 1070 represent the time coefficient series of T_1 , T_2 , SOI and EAWMI.

$$\begin{aligned} \frac{dx_1}{dt} &= a_1x_1 + a_2x_2 + a_3x_3 + a_4x_4 + a_5x_1^2 + a_6x_2^2 + a_7x_3^2 + a_8x_4^2 + a_9x_1x_2 + a_{10}x_1x_3 + a_{11}x_1x_4 + a_{12}x_2x_3 + a_{13}x_2x_4 + a_{14}x_3x_4 \\ \frac{dx_2}{dt} &= b_1x_1 + b_2x_2 + b_3x_3 + b_4x_4 + b_5x_1^2 + b_6x_2^2 + b_7x_3^2 + b_8x_4^2 + b_9x_1x_2 + b_{10}x_1x_3 + b_{11}x_1x_4 + b_{12}x_2x_3 + b_{13}x_2x_4 + b_{14}x_3x_4 \\ \frac{dx_3}{dt} &= c_1x_1 + c_2x_2 + c_3x_3 + c_4x_4 + c_5x_1^2 + c_6x_2^2 + c_7x_3^2 + c_8x_4^2 + c_9x_1x_2 + c_{10}x_1x_3 + c_{11}x_1x_4 + c_{12}x_2x_3 + c_{13}x_2x_4 + c_{14}x_3x_4 \\ \frac{dx_4}{dt} &= d_1x_1 + d_2x_2 + d_3x_3 + d_4x_4 + d_5x_1^2 + d_6x_2^2 + d_7x_3^2 + d_8x_4^2 + d_9x_1x_2 + d_{10}x_1x_3 + d_{11}x_1x_4 + d_{12}x_2x_3 + d_{13}x_2x_4 + d_{14}x_3x_4 \end{aligned}$$

1072

1073

(1)

1074

Based on the parameter optimization search method of GA in Appendix A, the

1075

time coefficient series of T_1 , T_2 , SOI and EAWMI from January 1951 to April 2008

1076

are chosen as the expected data to optimize and retrieve model parameters. In order to

带格式的: 字体: 小四, 字体颜色: 自动设置

1077

eliminate the dimensionless relationship between variables, data standardization is to

1078

transform data from different orders of magnitude to the same order of magnitude,

1079

thus making the data comparable. So we used $x_{nor} = \frac{x - x_{min}}{x_{max} - x_{min}}$ to normalize the raw

带格式的: 字体颜色: 自动设置

1080

value of each of the four predictors, then we used the normalized value to model and

带格式的: 字体: 小四, 字体颜色: 自动设置

1081

forecast. To avoid the overfitting problem, we used $x_{nor} = \frac{x - x_{min}}{x_{max} - x_{min}}$ to normalize

带格式的: 字体颜色: 自动设置

1082

the raw value of each of the four predictors, then we used the normalized value to

带格式的: 字体: Times New Roman, 小四

1083

model and forecast. Finally, we made forecast results revert back to the raw data

带格式的: 缩进: 左侧: 0 厘米, 首行缩进: 2 字符

1084

magnitude by $x = x_{nor}(x_{max} - x_{min}) + x_{min}$.

带格式的: 字体: Times New Roman, 小四

1085

In order to quantitatively compare the relative contribution of each item of our

带格式的: 字体: Times New Roman, 小四

1086

model to the evolution of the system, we calculated the relative variance contribution.

带格式的: 字体: Times New Roman

1087

The formula is as follows: $R_i = \frac{1}{n} \sum_{j=1}^n [\frac{T_i^2}{\sum_{i=1}^{14} T_i^2}]$, $i = 1, 2, \dots, 14$. Where n is the length of

带格式的: 字体: Times New Roman, 字体颜色: 自动设置

1088

the data. $T_i = a_1x_1, a_2x_2, \dots, a_{14}x_3x_4$ is the item in the equation. According to our

带格式的: 字体: Times New Roman, 小四

1089

previous research (Hong et al., 2007), the variance contribution of the real item

带格式的: 字体: Times New Roman

1090

reflecting the performance of the model has a large proportion, while the variance

带格式的: 字体: Times New Roman, 小四

1091

contribution of the false term is almost zero, so we delete the weak items of

带格式的: 字体: Times New Roman, 小四

1092

$R_i < 0.01$.

带格式的: 字体: Times New Roman, 小四

带格式的: 字体: Times New Roman, 小四

带格式的: 字体: Times New Roman, 小四

带格式的: 字体: Times New Roman, 小四

带格式的: 字体: Times New Roman, 小四

带格式的: 字体: Times New Roman, 小四

带格式的: 字体: Times New Roman

带格式的: 字体: Times New Roman, 小四

带格式的: 字体: Times New Roman, 小四

1093 After ~~deleting the weak items~~~~eliminating weak items with small dimension~~
 1094 ~~coefficients~~, the nonlinear dynamical model of the first time series T_1 , the second time
 1095 series T_2 , SOI and EAWMI can be reconstructed as follows:

$$\begin{aligned}
 \frac{dx_1}{dt} = F_1 &= -0.3328x_1 + 1.2574x_2 - 0.3511x_3 - 0.0289x_1^2 + 3.1280x_3^2 + 0.0125x_1x_2 + 2.7805x_1x_3 - 1.5408x_2x_4 \\
 \frac{dx_2}{dt} = F_2 &= 1.0307x_1 - 3.1428x_2 + 0.3095x_4 + 4.2301x_1^2 - 1.2066x_2^2 + 2.5024x_4^2 - 0.2891x_1x_3 + 0.7815x_1x_4 - 0.4266x_3x_4 \\
 \frac{dx_3}{dt} = F_3 &= -2.3155x_1 + 3.2166x_3 + 1.5284x_4 - 1.4527x_2^2 - 0.0034x_3^2 - 4.1206x_4^2 - 0.0025x_1x_4 + 0.0277x_2x_3 + 1.2860x_2x_4 \\
 \frac{dx_4}{dt} = F_4 &= 0.4478x_2 - 0.0268x_4 + 0.8995x_1^2 - 2.3890x_3^2 + 0.2037x_4^2 + 1.3035x_1x_2 + 2.0458x_1x_4 - 2.0015x_2x_4
 \end{aligned}$$

1097 (2)

1098 ~~The appropriate model coefficient estimates determine the robustness of the~~
 1099 ~~model and the accuracy of forecast results. We should now judge whether the model~~
 1100 ~~coefficients are appropriate or not.~~

1101 ~~Frist, the largest Lyapunov exponent (LLE) is one of the indexes that can~~
 1102 ~~represent the characteristics of chaotic systems. The final Lyapunov exponents of Eq.~~
 1103 ~~(2) were [0.0433, -0.0012, -0.1285], containing both a negative Lyapunov exponent~~
 1104 ~~and two positive Lyapunov exponents, which demonstrate that our dynamic system is~~
 1105 ~~indeed a chaotic system.~~

1106 ~~Second, we calculated the equilibrium roots of Eq. (2). Only the third~~
 1107 ~~equilibrium was adjudged to be stable, based upon higher order terms within the~~
 1108 ~~Taylor series, the indices of which were mostly in accordance with the actual weather~~
 1109 ~~system. The indices in the unstable equilibria could not accurately describe the actual~~
 1110 ~~weather. Based on these two aspects, we can see that the model coefficient estimates~~
 1111 ~~were reasonable and reflected the dynamical characteristics of the model.~~

1112 The model required testing. Because the training period was from January 1951

1113 to April 2008, we chose T_1 , T_2 , SOI and EAWMI of May 2008, which were not used
 1114 as initial forecast data in the modeling. Next, the Runge–Kutta method was used to do
 1115 the numerical integration of the above equations, and every step of the integration was
 1116 regarded as 1 month’s worth of forecasting results. As a result, forecast results of four
 1117 time series over a period of 20 months were obtained. Here, the focus was on the
 1118 forecast results of T_1 and T_2 , as shown in Fig.2.

1119 The pearson correlation coefficient (CC) (Wang et al. 2009b) and the mean
 1120 absolute percentage error (MAPE)(Hu et al. 2001) are employed as objective
 1121 functions to calibrate the model. The CC evaluates the linear relationship between the
 1122 observed and predicting values and MAPE measures the difference between the
 1123 observed and predicting values.

1124 From Fig. 2, forecast performance of T_1 and T_2 within 5 months was better.

1125 Using T_1 as an example, ~~the at this time, CC the temporal correlation~~ between model
 1126 predictions and corresponding observations over the first five months forecasts was
 1127 0.8966 and ~~the mean absolute percentage error (MAPE) (Hu et al.,~~

1128 ~~2001), MAPE = $\frac{1}{n} \sum_{i=1}^n \left| \frac{D_e(i) - D_0(i)}{D_0(i)} \right| \times 100, (n=5)$, was 8.32%. However, after 5~~

1129 months, MAPE increased rapidly, and was 31.29% at 10 months. The model forecast
 1130 then significantly diverged from observations, and the forecast became inaccurate.

1131 After 10 months, the forecast results became increasingly worse, which indicated that
 1132 the forecast of the model after 5 months was unacceptable. The forecast results of
 1133 T_2 were similar to those of T_1 .

1134 The model’s skill should be further assessed by cross-validated retroactive

hindcasts of the time series. As in the above example, omitting a portion of the time series (12 months, January-Jan. 1951 to January-Dec. 1951) from observations, we trained the model based on the data from February-Jan. 1952-1951 to December-Dec. 2010, and then predicted the omitted segments (12 months, Jan. 1951 to Dec. 1951). Then in the next prediction experiment, the omitted segment is Jan.1952 to Dec. 1952 and the training samples are Jan. 1951 to Dec.1951 and Jan.1953 to Dec.2010. So the forecast time series is Jan.1952 to Dec. 1952. We then repeated this procedure by moving the omitted segment along the entirety of the available time series. Each experiment ~~have~~has used the different training sample and have established the different model equation (but the method is the same). The similar process of the cross-validated retroactive hindcasts has also been used in the previous literatures (Hu et al., 2017).

带格式的: 字体: Times New Roman, 字体颜色: 自动设置, 英语(英国)

Finally, we obtained cross-validated retroactive hindcast results of T_1 and T_2 , as shown in Fig. 3. So the forecast results of 60 cross experiment (each experiment is the prediction of the 12 month as Fig.2) according to the time sequence can merger into a new time series (from Jan.1951-Dec.2010), and then the pearson correlation coefficient (CC) and the mean absolute percentage error (MAPE) can be calculated by the new prediction time series and the time series of the actual value. Figure 3 is combined results of the 60 forecast experiments.

As Fig. 2, the forecast performance of T_1 and T_2 in Fig. 3 was not satisfactory. The model forecast significantly diverged from observations, and the forecast became inaccurate. The ~~temporal correlations~~CC of T_1 and T_2 between model predictions and corresponding observations were 0.3411 and 0.4176, respectively. Additionally, the

1158 | ~~mean absolute percentage errors~~ (MAPE) of T_1 and T_2 were 65.42% and 57.56%,
1159 | respectively. This indicates that the forecast of the model in the long-term was
1160 | inaccurate and unacceptable.

1161 | The forecast result may be inaccurate when the integral forecasting time is long.
1162 | There will be a significant divergence which will cause an ineffective forecast. To
1163 | improve the forecast accuracy, the forecast not only depends on the integral equation
1164 | but also on a single initial value. Choosing the different initial value will cause
1165 | different forecast accuracy. For example, in a total of 60 cross-validated retroactive
1166 | hindcasts examples, the minimum MAPE was 37.65%, while the maximum MAPE
1167 | was 89.88%. A forecast, depending on a single initial value, will cause instability of
1168 | the forecast results. These two problems are addressed by introducing the
1169 | self-memorization principle in the next section.

1170 |

1171 | **4. Introduction of self-memorization dynamics to improve the** 1172 | **reconstructed model**

1173 | In the above discussion, it was shown that the accuracy of the forecast results of
1174 | equation (2) were unsatisfactory. To improve long-term forecasting results, the
1175 | principle of self-memorization can be introduced into the mature model (Gu, 1998;
1176 | Chen et al., 2009). The principle of self-memorization dynamics (Cao, 1993; Feng et
1177 | al., 2001) can be seen in Appendix B.

1178 | Based on Eq. (B10) in Appendix B, the improved model can be expressed as

1179 follows:
$$\begin{cases} x_{1t} = \sum_{i=-p-1}^{-1} \alpha_{1i} y_{1i} + \sum_{i=-p}^0 \theta_{1i} F_1(x_{1i}, x_{2i}, x_{3i}, x_{4i}) \\ x_{2t} = \sum_{i=-p-1}^{-1} \alpha_{2i} y_{2i} + \sum_{i=-p}^0 \theta_{2i} F_2(x_{1i}, x_{2i}, x_{3i}, x_{4i}) \\ x_{3t} = \sum_{i=-p-1}^{-1} \alpha_{3i} y_{3i} + \sum_{i=-p}^0 \theta_{3i} F_3(x_{1i}, x_{2i}, x_{3i}, x_{4i}) \\ x_{4t} = \sum_{i=-p-1}^{-1} \alpha_{4i} y_{4i} + \sum_{i=-p}^0 \theta_{4i} F_4(x_{1i}, x_{2i}, x_{3i}, x_{4i}) \end{cases} \quad (3)$$

1180 where y_i is replaced by the mean of two values at adjoining times; i.e.,

1181 $y_i \equiv \frac{1}{2}(x_{i+1} + x_i)$; F is the dynamic core of the self-memorization equation, which

1182 can be obtained from Eq. (2); and α and θ are the memory coefficients, the formula

1183 for which can be found in Appendix B.

1184 If the values of α and θ can be obtained, Eq. (3) can be used to obtain the

1185 results of final prediction. The memory coefficients α and θ in Eq. (3) were

1186 calibrated using the least-squares method with the same data (January 1951 to April

1187 2008) as those used in Section 3. Eq. (3) can be deconstructed as follows (M is the

1188 length of the time series):

1189
$$X = \begin{bmatrix} x_{11} \\ x_{12} \\ \cdot \\ \cdot \\ \cdot \\ x_{1M} \end{bmatrix}, \alpha = \begin{bmatrix} \alpha_{-p-1} \\ \alpha_{-p} \\ \cdot \\ \cdot \\ \cdot \\ \alpha_{-1} \end{bmatrix}, Y = \begin{bmatrix} y_{-p-1,1} & y_{-p,1} & \cdots & y_{-1,1} \\ y_{-p-1,2} & y_{-p,2} & \cdots & y_{-1,2} \\ \cdot & \cdot & \cdots & \cdot \\ \cdot & \cdot & \cdots & \cdot \\ \cdot & \cdot & \cdots & \cdot \\ y_{-p-1,M} & y_{-p,M} & \cdots & y_{-1,M} \end{bmatrix}, \Theta = \begin{bmatrix} \theta_{-p} \\ \theta_{-p+1} \\ \cdot \\ \cdot \\ \cdot \\ \theta_0 \end{bmatrix},$$

1190
$$F = \begin{bmatrix} F_{-p,1} & F_{-p+1,1} & \cdots & F_{0,1} \\ F_{-p,2} & F_{-p+1,2} & \cdots & F_{0,2} \\ \cdot & \cdot & \cdots & \cdot \\ \cdot & \cdot & \cdots & \cdot \\ \cdot & \cdot & \cdots & \cdot \\ F_{-p,M} & F_{-p+1,M} & \cdots & F_{0,M} \end{bmatrix}$$

1191 The matrix equation is:

$$1192 \quad X = Y\alpha + F\theta \quad (4)$$

$$1193 \quad \text{where } Z = [Y:F], \quad W = \begin{bmatrix} \alpha \\ \vdots \\ \Theta \end{bmatrix} .$$

1194 Eq. (4) can be written as:

$$1195 \quad X = ZW \quad (5)$$

1196 The memory coefficients vector W can be calibrated using the least squares
1197 method:

$$1198 \quad W = (Z^T Z)^{-1} Z^T X \quad (6)$$

1199 The memory coefficients a, θ can be obtained from Eq. (6). We then made a
1200 prediction using the self- memorization equation (3), which used the p values before
1201 t_0 .

1202 The coefficients in F and W were used with the same training data from January
1203 1951 to April 2008. In the forecast examples, we trained both the coefficients in F and
1204 W at the same time, but in the paper we describe them separately to facilitate the
1205 reader for better understanding.

1206 **5. Model prediction experiments**

1207 **5.1 Forecast of time series T_1 and T_2**

1208 The training sample for the model was from January 1951 to April 2008. Here, from
1209 Eq. (3), the forecast results using T_1, T_2 , SOI and EAWMI factors can be calculated, called
1210 as step-by-step forecast.

1211 When the retrospective order p is confirmed, step-by-step forecasts can be

1212 carried out. For example, when the T_1, T_2 , SOI and EAWMI values of May 2008 were
1213 forecast, y_i was obtained from the previous $p + 1$ time of T_1, T_2 , the SOI and the
1214 EAWMI data, and $F_i(x_{1i}, x_{2i}, x_{3i}, x_{4i})$ was obtained from the previous p times of
1215 T_1, T_2 , the SOI and the EAWMI data. All four equations were integrated simultaneously.
1216 Taking these in Eq. (3), we can get the T_1, T_2 , SOI and EAWMI values of May 2008,
1217 which these can be taken as the initial values for the next prediction step. Then, the
1218 T_1, T_2 , SOI and EAWMI values from June 2008 and so on, can be generated.

1219 5.1.1 Determination of p

1220 Based on the self-memorization principle, the self-memorization of the system
1221 determines the retrospective order p (Cao, 1993). If the system forgets slowly,
1222 parameters a and θ will be small and the p value should be high. The SSTA field
1223 forecasts were on a monthly scale, the change of which was slow in contrast to
1224 large-scale atmospheric motion. So parameters a and θ were small, and generally,
1225 the p value was in the range 5 to 15.

1226 The retrospective order p was obtained by a trial calculation method. We selected
1227 the p values in the range 4 to 16 to construct the model. The ~~correlation~~
1228 ~~coefficients~~ CC (~~CC~~) and MAPE of long-term fitting test (from February 1951 to
1229 December 2010) are shown in Table 2, which can be used as the standard to determine
1230 the retrospective order p .

1231 Table 2 indicates that when $p = 6$, the MAPE values of long-term fitting test
1232 were the smallest and the ~~correlation coefficients~~ CCs were the largest. Also, when p
1233 from 5 to 9, ~~CCs~~ The CCs were all more than 0.58 and the forecast results were all

1234 good, which is consistent with our interpretation of the physical mechanisms in
 1235 section 6.2 below. SOI and EMWMI were 5-12 months lead relationships with SST
 1236 (Xu et al., 1993; Chen et al, 2010; Wang et al., 2003). Using a cumulative period of
 1237 SOI-, EMWMI 5-8 months ahead as initial values can help improve the final forecast
 1238 results. Our results in table 2 are consistent with the actual physical ENSO process.
 1239 Therefore, we selected the retrospective order as $p=6$.

1240 Then, the prediction experiments can be carried out, based on improved
 1241 self-memorization Eq. (3).

1242 The improved self-memorization equation of T_1, T_2 , SOI and EAWMI can then be
 1243 established. After the differential equation was discretely dealt with, the memory
 1244 coefficients were solved by the least-squares method given in section 4 (Training
 1245 period is January 1951 to April 2008). Finally, the improved prediction equation of
 1246 T_1, T_2 , SOI and EAWMI, based on the self-memorization principle, can be expressed
 1247 as:

$$\begin{cases}
 x_{1t} = \sum_{i=-7}^{-1} \alpha_{1i} y_{1i} + \sum_{i=-6}^0 \theta_{1i} F_1(x_{1i}, x_{2i}, x_{3i}, x_{4i}) \\
 x_{2t} = \sum_{i=-7}^{-1} \alpha_{2i} y_{2i} + \sum_{i=-6}^0 \theta_{2i} F_2(x_{1i}, x_{2i}, x_{3i}, x_{4i}) \\
 x_{3t} = \sum_{i=-7}^{-1} \alpha_{3i} y_{3i} + \sum_{i=-6}^0 \theta_{3i} F_3(x_{1i}, x_{2i}, x_{3i}, x_{4i}) \\
 x_{4t} = \sum_{i=-7}^{-1} \alpha_{4i} y_{4i} + \sum_{i=-6}^0 \theta_{4i} F_4(x_{1i}, x_{2i}, x_{3i}, x_{4i})
 \end{cases} \quad (7)$$

1249 where

$$1250 \quad \alpha = [\alpha_{ij}] = \begin{bmatrix} 0.0315 & -2.113 & 0.0284 & 2.1468 & 0.0688 & -0.7014 & 1.3248 \\ 0.4088 & -1.887 & -1.0233 & 1.5485 & 0.9028 & 1.0255 & -0.6443 \\ -0.9088 & -0.2557 & 0.9671 & -0.0054 & 1.0568 & 2.9764 & -0.5234 \\ 0.2088 & -1.0567 & 0.4891 & -0.5066 & -0.4890 & 1.4555 & 1.0966 \end{bmatrix}$$

$(i = 0, 1, \dots, 4; j = -7, -6, \dots, -1)$

$$1251 \quad \theta = [\theta_{ij}] = \begin{bmatrix} 0.0485 & 0.0425 & -1.7688 & 0.8543 & 2.8901 & -0.1788 & -0.9066 \\ 0.07642 & 0.0941 & -1.2466 & -0.2288 & 0.1097 & 2.3221 & -1.4228 \\ -0.5288 & 1.2368 & -0.5568 & -0.0155 & 0.2886 & -0.1560 & 1.2775 \\ 1.5335 & -0.2887 & -0.5336 & -0.6072 & -0.5611 & 1.0225 & -1.0625 \end{bmatrix}$$

$(i = 0, 1, \dots, 4; j = -6, -5, \dots, 0)$

1252 The step-by-step forecast was performed. The retrospective order $p = 6$ means
1253 that earlier seven observation data ($p + 1 = 7$) should be used during the forecasting
1254 process. The forecast results per month were saved for the next period predictions.

1255 5.1.2 Long-term step-by-step forecasts of T_1 and T_2

1256 To test the actual forecast performance of the above improved model, long-term
1257 step-by-step forecasts of T_1 and T_2 from May 2008 to December 2010 for 20 months
1258 were carried out, as shown in Fig. 4. The forecast results of T_1 and T_2 were good.

1259 Within 8 months, the ~~correlation coefficients~~ CCs of T_1 and T_2 were 0.9163 and
1260 0.9187. MAPEs of T_1 and T_2 were small, only 5.86% and 6.78%. The forecast time
1261 series from 8 months to 14 months gradually diverged, but the trend was acceptable.

1262 The ~~CC~~ correlation coefficients of T_1 and T_2 reached 0.8375 and 0.8251, and
1263 MAPEs of T_1 and T_2 were 8.32% and 9.11%. After 14 months, forecast began to

1264 diverge and the error started to increase, but the ~~correlation CC~~ coefficients of T_1 and
1265 T_2 remained about 0.6899 and 0.6782, and MAPEs reached 18.31% and 19.44%,

1266 which can be acceptable.

1267 5.2 Cross-validated retroactive hindcasts of time series T_1 and T_2

1268 As in section 3, the model's skill should be further assessed by cross-validated
1269 retroactive hindcasts of the time series. Because our step-by-step forecasts need the
1270 earlier seven observation data ($p + 1 = 7$), we can obtain cross-validated retroactive
1271 hindcast results of T_1 and T_2 from August 1951 to December 2010, as shown in Fig.
1272 5.

1273 From Fig. 5, the forecast performance of T_1 and T_2 was good. The
1274 ~~CC~~correlation coefficient of T_1 and T_2 were 0.7124 and 0.7036, respectively. The
1275 MAPEs of T_1 and T_2 were small, only 19.57% and 19.79%, respectively. The peaks
1276 and valleys of T_1 and T_2 were also forecasted accurately. The forecast results
1277 indicated that the cross-validated retroactive hindcast results of T_1 and T_2 were close
1278 to the observed values. Compared to Fig. 3, the improved model had better forecast
1279 abilities than the original model.

1280 Many researchers (Zhang et al., 2003b; Smith, 2004) have used Oceanic Niño
1281 Index (ONI) which is used by the U.S. NOAA Climate Prediction Center to determine
1282 the El Niño and La Niña years. It defined that the ONIs of five consecutive months in
1283 winter were all more than 0.5 (less than -0.5) is the ElNiño (La Niña) year. Based on
1284 the above criterion, we can divide the total 60 years (1951-2010) into three categories.
1285 It includes the 18 examples of ElNiño year (such as 1958, 1964, 1966, etc.), 22
1286 examples of LaNiña year (such as 1951, 1955, 1956, etc.) and the remaining 20
1287 experiments of the neutral year. Since the details in Fig.5 is not clear, we list the
1288 forecast results of 60 experiments (including 18 El Niño examples, 22 La Niña
1289 examples and 20 Neutral examples) in table 3.

1290 From table 3, the average of CC of both T_1 and T_2 of 60 experiments
 1291 within 6 months was more than 0.84 and MAPE was less than 8%. The average of CC
 1292 CC within 12 months was more than 0.74 and MAPE was less than 12%. According
 1293 to the literature (Barranel et al., 1999), when MAPE was less than 15%, which means
 1294 the error was not great and the forecast results were good. Obviously, the forecast
 1295 results of El Niño / La Niña experiments were a little worse than those of neutral
 1296 examples, which means the forecast ability of our model for the abnormal situation
 1297 was a little worse than those for the normal situation. But even for El Niño / La Niña
 1298 experiments, the average of CC was still more than 0.7 and MAPE was less than
 1299 15%, which means the error was not too large and was still within an acceptable
 1300 range.

1301 5.3 Forecast of the SSTA field

1302 When we obtained the forecast results of the time coefficient series T_1 and T_2 ,
 1303 we submitted them into the following equation to reconstruct the forecast SSTA field:

$$1304 \hat{x}_t = \sum_{n=1}^2 E_n \bullet T_n, t = 1, 2, \dots, 12 \quad (8)$$

1305 where E_n , T_n are the EOF space fields and forecast time coefficients,
 1306 respectively, and \hat{x}_{ij} is the forecast SSTA field reconstructed by EOF.

1307 After reconstruction of the space mode (treated as constant) and time coefficient
 1308 series (model prediction), the forecast of the SSTA fields was obtained, based on the
 1309 forecast results of T_1 and T_2 in Section 5.2. For economy of space, we cannot draw
 1310 all of the forecasted SSTA fields, so we selected a strong El Niño event (December
 1311 1997), a strong La Niña event (December 1999) and a neutral event (November 2002)
 1312 as examples.

1313 Fig. 6 shows the forecast SSTA field during a strong El Niño event. From the
1314 actual SSTA field in December 1997 (Fig. 6a), an obvious warm tongue structure
1315 occurred in the area of [10°S~5°N, 90°W~150°W] in the Eastern Equatorial Pacific,
1316 and a warm anomalous distribution arose in the west Pacific, which indicated a weak
1317 El Niño event. The forecasted SSTA field of December 1997 is shown in Fig. 6b.
1318 Although the range of warm tongue was a little bigger than the actual situation, the
1319 forecast shape was similar to the actual field and also the contour lines were similar.
1320 The average MAPE between the forecast field and the actual field is 8.56%, which
1321 was controlled within 10%. The forecast results of the improved model event were
1322 quite good for the El Niño event.

1323 Fig.7 shows the forecasted SSTA field of a strong La Niña event. From the actual
1324 SSTA field in December 1999 (Fig. 7a), an obvious cold pool occurred in the area of
1325 [10°S~10°N, 120°W~180°W] in the Equatorial Pacific, which covered the Niño3.4
1326 area. This SSTA field presented a strong strength La Niña event. The forecast SSTA
1327 field from December 1999 is shown as Fig. 7b. Although the strength of the cold pool
1328 was weaker than the actual situation, the forecast shape was similar to that of the
1329 actual field. The average MAPE between the forecast field and the actual field was
1330 9.69%. The errors were larger than that of the El Niño event, but they can be
1331 controlled within 10%, which is acceptable.

1332 Fig. 8 shows the forecasted SSTA field of a neutral event. From the actual SSTA
1333 field in November 2002 (Fig. 8a), a warm pool occurred in the area of [10°S~10°N,
1334 120°W~180°W] in the Equatorial Pacific, which covered the Niño3.4 area. However,

1335 the warm pool was small and weak, which represented a neutral event. The forecasted
1336 SSTA field from November 2002 is shown in Fig. 8b. Comparing Figures 6, 7 and 8,
1337 we can see that the forecasted SSTA field of a neutral event was a little worse than
1338 that of the El Niño and La Niña events. The forecasted shape of the SSTA field
1339 basically described the actual situation, but the warm pool in the Niño3.4 area was
1340 stronger and bigger than that of the actual situation, which indicated a borderline El
1341 Niño event. The average MAPE between the forecasted field and the actual field was
1342 14.50%, which was big but can be accepted.

1343 We obtained the average values of MAPE of 18 El Niño events, 22 La Niña
1344 events and 20 neutral events, which were 9.52%, 9.88% and 14.67%, respectively,
1345 representing a good SSTA field forecasting ability of our model.

1346 **5.4 Forecast of ENSO index**

1347 The ENSO index can be represented as the sea surface temperature anomaly
1348 (SSTA) in the Niño-3.4 region (5°N - 5°S , 120° - 170°W) and the ENSO index
1349 forecast was the 3-month forecast (Barnston et al. 2012). So we also can pick up the
1350 ENSO index from the above forecasted SSTA field. The forecast results of the ENSO
1351 index within 20 months can also be obtained. The definition of lead time can be seen
1352 in the reference (Barnston et al. 2012). Therefore, similar to the forecast experiment in
1353 section 5.1, a succession of running 3-month mean SST anomalies with respect to the
1354 climatological means for the respective prediction periods, averaged over the Niño 3.4
1355 region, can be obtained, as demonstrated in Fig. 9.

1356 [The evaluation criteria of the ENSO index is the temporal correlation \(TC\), its](#)

1357 [definition and specific calculation steps can be seen in these literatures \(Kathrin et](#)
1358 [al.,2016; Nicosia et al. 2013\)](#); The TC is often used to measure the prediction effect of
1359 [the ENSO index. For example, Barnston et al.in 2012 also used the TC to compare the](#)
1360 [forecast skill of 21 real-time seasonal ENSO models.](#)

1361 The forecast results within lead times of 18 months are shown in Fig. 9, which
1362 demonstrate that the forecast results of the ENSO index are good. Within lead time of
1363 12 months, the ~~correlation coefficient~~TC was 0.8985 and the MAPE value was small,
1364 only 8.91%. In addition, the borderline La Niña event in 2008–2009 was predicted
1365 well. After lead times of 12 months, forecasts began to diverge and the errors started
1366 to increase. Although the ~~correlation coefficient~~TC remained approximately 0.61,
1367 MAPE reached 18.58%. Therefore, a moderate strength El Niño event that occurred in
1368 2009/10 was not predicted.

1369 We should give more examples to test the ENSO prediction ability of our model.
1370 As in section 5.3, we can divide 60 examples as three types, which are examples of
1371 ElNiño year, LaNiña year and neutral year. Finally, we can obtain the forecast results
1372 of different types of examples in different lead times, as shown in table 4.

1373 From table 4, the average ~~CC~~TC of 60 experiments was 0.712 and the average
1374 MAPE was 7.62% within 12 months for all seasons of lead time, which indicates that
1375 the overall ENSO forecast ability of our model was good. The forecast results of the
1376 El Niño examples were significantly worse than those of La Niña examples, while the
1377 forecast results of La Niña examples were significantly worse than those of neutral
1378 examples, which show the model forecast ability of the abnormal state was worse than

带格式的： 字体：小四

1379 the normal state of the ENSO index. Even for the forecast results of El Niño examples,
1380 the average ~~CC-TC~~ was still above 0.6 and the average MAPE can be controlled
1381 below 10%, which means the forecast results were still in the acceptable range. Our
1382 model not only accurately predicted the stronger El Niño and La Niña phases but also
1383 the neutral states. ~~But the forecast results in summer were a little worse than those in~~
1384 ~~winter, as shown in Fig.10.~~

1385 The ENSO forecast often had a spring predictability barrier (Webster, 1999),
1386 which was most prominent during decades of relatively poor predictability
1387 (Balmaseda et al., 1995). To test our model, the skill should be computed over the
1388 entire time series and separately for seasonal subsets of the time series. ~~From the~~
1389 ~~table4, we can see that The average cumulative correlation coefficient and MAPE of~~
1390 ~~winter were compared with those of summer, as shown in Fig.10. The average~~
1391 ~~cumulative correlation and average cumulative MAPE values between the forecast~~
1392 ~~values and the actual values changed with time, from which good trends of forecast~~
1393 ~~results can be seen. As long as the forecast time increased, the cumulative MAPE~~
1394 ~~increased and the correlation decayed gradually. The forecast results appeared to~~
1395 ~~diverge. Although the forecast results of the present model in the summer-spring~~
1396 were worse than in the ~~winter-autumn~~, the margin was not high, which means the
1397 model can overcome the “spring predictability barrier,” to some extent.

1398 **5.5 Compared with six mature models**

1399 Barnston et al. (2012) compared many ENSO forecast models. Based on his
1400 research, we selected four high quality dynamical models, including ECMWF, JMA,

1401 the National Aeronautics and Space Administration Global Modelling and
1402 Assimilation Office (NASAGMAO) and the National Centre for Environmental
1403 Prediction Climate Forecast System (NCEP CFS; Version1). Two high quality
1404 statistical models also be selected, including the University of California, Los Angeles
1405 Theoretical Climate Dynamics (UCLA-TCD) multilevel regression model and the
1406 NOAA/NCEP/CPC constructed Analogue (CA) model. The detail of the above
1407 models can be seen in these references ([ReynoldsReynoldset al., 2002](#); Luo et al.,
1408 2005; Barnston et al., 2012).

1409 We then compared the forecast ability of the above six models with that of our
1410 model. All of the experiments of our model and six other models were conducted
1411 under the same conditions using the same historical data for modelling and the same
1412 initial values to forecast. In the CPC website, there are detailed explanations of six
1413 models' training samples and the initial values. So we do not need to install all these
1414 models on their own machines and run them for forecasting. We just made training
1415 samples and initial values of our model were the same with those of selected six
1416 models. At an 8-month lead time, the [correlation-abilityTC](#) of our model for all
1417 seasons combined was 0.613 (Fig. [4-10](#)). In brief, the forecast ability of the ECMWF
1418 model was slightly better than that of our model but the ability of the other 5 models
1419 was worse than that of our model. While, in regard to the forecast length, the [temporal](#)
1420 [correlationTC](#) within 12 months of our model is greater than 0.6, which was superior
1421 to the ECMWF model. In addition, the forecast results of the UCLA-TCD model and
1422 the CPC CA model reduced quickly after 5-month lead times, so the forecast ability of

1423 our model was more stable than them.

1424 The root mean square error (RMSE) was also examined to assess the
1425 performance of discrimination and calibration. Barnston et al. (2012) believed that all
1426 seasonal RMSE values contributed equally to a seasonally combined RMSE. So we
1427 drew figure [12-11](#) to show seasonally combined RMSE.

1428 From Fig. [14-0](#) and Fig. [1211](#), we can see the highest correlation tend to
1429 have lower RMSE. So the RMSE of our model was slightly higher than that of
1430 ECMWF model, but it was much lower than those of the other 5 models. [Figure 11](#)
1431 [and Figure 12 is the average CETS and RMSE of the 240 experiments of compared](#)
1432 [with six mature models, covers a variety of different types of ENSO and different lead](#)
1433 [time. So those samples should be really representative .](#)

带格式的: 缩进: 首行缩进: 2 字符

带格式的: 字体: Times New Roman, 字体颜色: 自动设置, 英语(英国)

带格式的: 字体: Times New Roman, 字体颜色: 自动设置, 英语(英国)

带格式的: 字体: Times New Roman, 字体颜色: 自动设置, 英语(英国)

1434 6. Conclusions and discussion

1435 6.1 Conclusions

1436 A new forecasting model of the SSTA field was proposed based on a dynamic
1437 system reconstruction idea and the principle of self-memorization. The approach of
1438 the present paper consisted of the following steps:

1439 (1) The SST field can be time (coefficients)-space (structure) deconstructed
1440 using the EOF method. Take T_1 , T_2 , SOI and EAWMI and consider them as
1441 trajectories of a set of four coupled quadratic differential equations based on the
1442 dynamic system reconstruction idea. The parameters of this dynamic model were
1443 estimated using a GA.

1444 (2) The forecast results of the dynamic model can be improved by the

1445 self-memorization principle. The memory coefficients in the improved
1446 self-memorization model were obtained using the GA method.

1447 (3) The long-term step-by-step forecast results and cross-validated
1448 retroactive hindcast results of time series T_1 and T_2 are all found to be good, with the
1449 ~~a correlation coefficient~~CC of approximately 0.80 and ~~a mean absolute percentage~~
1450 ~~error~~ the MAPE of less than 15%.

1451 (4) The improved model was used to forecast the SSTA field. The
1452 forecasted SSTA fields of three types of events are accurate. Not only is the forecast
1453 shape similar to the actual field but also the contour lines are similar.

1454 (5) The improved model was also used to forecast the ENSO index. The
1455 average ~~correlation coefficient~~TC of 60 examples within 12 months is 0.712, and the
1456 MAPE value is small, only 7.62%, which proves that the improved model has better
1457 forecasting results of the ENSO index. Although the forecast results of the model in
1458 the summer were worse than in the winter, the margin was not high, which means that
1459 the model can overcome the spring predictability barrier to some extent. Finally,
1460 compared with the six mature models, the new dynamical-statistical forecasting
1461 model has a scientific significance and practical value for the SST in the eastern
1462 equatorial Pacific and El Niño/La Niña event predictions.

1463 6.2 Discussion

1464 L'Heureux et al.(2013) reported that using different data sets and time periods,
1465 the 2nd EOF is not stable, being entirely due to the strong trend. So we need to do
1466 more experiments to prove that we choose the second mode of EOF to be appropriate.

带格式的：缩进：首行缩进： 3 字符

带格式的：字体：(中文) 宋体，小四，非加粗

1467 and whether different time periods will make us forecast unstable or not. Our original
1468 data is the monthly average SST data from January 1951 to Dec, 2010, which are 60
1469 years. We will increase the length of the data for 20 years (Jan.1931 –Dec,2010), for
1470 10 years (Jan.1941- Dec,2010) and decrease the length of the data for 10 years
1471 (Jan.1961- Dec,2010), for 20 years (Jan.1971- Dec,2010). And then we use the same
1472 method to reconstruct a model and forecast the ENSO index as section5.4. The
1473 prediction results are shown in the table5.

带格式的: 字体: (中文) 宋体, 小四, 非加粗

带格式的: 字体: (中文) 宋体, 小四, 非加粗

带格式的: 字体: (中文) 宋体, 小四, 非加粗

带格式的: 字体: (中文) 宋体, 小四, 非加粗

带格式的: 字体: (中文) 宋体, 小四, 非加粗

1474 From the table, we can see that in the 60 experiments, the prediction results of
1475 the data period increased by 20 years are the best, and the prediction results of the
1476 data period decreased by 20 years is the worst. This is because the more data we use,
1477 the more information it contain. But from the table we can also see the difference
1478 among forecast results of both TC and MAPE of five different sample data are less,
1479 and no abnormal change suddenly worse or better appear. All these indicate that using
1480 different data sets and time periods, even though may have a certain impact on the
1481 pattern of the 2nd EOF, but the impact on our forecast is not great and it will not
1482 make our forecast unstable.

1483 Actually, how many variables and which variables are used in our model
1484 become a key issue to be resolved. We are a complex four factor differential
1485 equations coupling model. We are a complex coupled model of four factor differential
1486 equations, so we are more concerned with the correlation between each other. The
1487 correlation must be considered as an important criterion to select the factors, but in
1488 order to further verify the correctness of the selection criterion, we have carried out

1511 data but also the conformability of the model structure with the data shape, and the
1512 magnitude of model error compared to the expected level of noise or error in the
1513 data(Burnham and Anderson, 2002). So there are many reasons causing the overfitting
1514 phenomenon. But this does not mean having many parameters relative to the number
1515 of observations inevitably causes the overfitting problem (Golbraikh et al., 2003).
1516 There is no evidence that more parameters will be certain to result in overfitting.
1517 Based on the definition of overfitting and the previous studies(Golbraikh et al., 2003;
1518 Everitt and Skrondal,2010), we can judge whether a model is overfitting or not by the
1519 accuracy of prediction results of independent samples (Golbraikh and Tropsha, 2002;
1520 Qin and Li, 2006).

带格式的

1521 In the sample training, our model does not purposely pursue the high degree of
1522 the training samples fitting and improve the effectiveness of the independent
1523 generalization. In fact in our paper the forecast results of the Cross-validated
1524 retroactive hindcasts (section 5.2) and the independent samples validation (table3 and
1525 table4) are both good. Especially, the independent samples validation of the ENSO
1526 index as the table4, we have carried out the 240 independent sample validation
1527 prediction of four seasons of different ENSO events and the coverage of independent
1528 samples test is very wide. Moreover, compared with 6 mature prediction models, the
1529 forecast results of our model are also good, which prove the overfitting problem does
1530 not exist in our model. According to the previous literature (Islam and Sivakumar,
1531 2002; Sivakumar et al,2001), we can see that prediction principle and structure of the
1532 phase space reconstruction (PSR) of dynamical system is not the same with the

带格式的

1555 the spring predictability barrier (Zhang et al, 2012; Philander et al., 1992). When the
1556 original model uses the indexes in summer as the initial values to predict, the SOI
1557 factor representing the air-sea interaction is most unstable in the spring and the
1558 EMWMI factor does not have much influence on ENSO in summer, so the forecast
1559 results using the indexes in summer as the initial values are certainly much worse than
1560 those using the indexes in the winter as the initial values. That is why our original
1561 model does not overcome the spring predictability barrier.

1562 However, the introduction of the self-memorization dynamics principle can help
1563 our model overcome the spring predictability barrier to some extent. Although the
1564 lead time is still summer (such as JJA), the information of the initial value actually
1565 contains the previous $p + 1$ month (in this case $p = 6$, which contains the information
1566 of the previous seven months, including the information of T_1, T_2 , SOI, EMWMI
1567 factor in winter (January, February), spring (March, April, May) and summer (June
1568 and July)). From the dynamical analysis, in this situation, the information and
1569 interaction relationship of four factors have been a long period (from winter to
1570 summer) accumulated, containing much air-sea interaction processes and winter
1571 monsoon continued abnormal information, so the forecast results of our improved
1572 model will be much better than the original model which simply uses only one initial
1573 value. That is why the improved model overcomes the spring predictability barrier to
1574 some extent.

1575 The forecast results of our model are good, but it still has some problems:

1576 (1) [The inclusion of these terms and the physical processes do these terms in](#)

1577 equation (2) represent are important, especially for the discussion of dynamical
1578 characteristics of the dynamical model. But now we are difficult to give a clear
1579 meaning. Now the main work of our paper is the prediction experiments of the model.
1580 For the reason of time and length, this paper mainly discusses the prediction results of
1581 the model. The physical processes do these terms represent and the discussion of the
1582 dynamical characteristics of the model will be the focus of our next work. Before this,
1583 we have also used the Takens' delay embedding theorem to reconstruct the dynamical
1584 model of the Western Pacific subtropical high(WPSH). And Based on the
1585 reconstructed dynamical model, dynamical characteristics of WPSH are analyzed and
1586 an aberrance mechanism is developed, in which the external forcings resulting in the
1587 WPSH anomalies are explored, which have been published (Hong et al., 2016). We
1588 also study the bifurcation and catastrophe of the West Pacific subtropical high ridge
1589 index of a nonlinear model (Hong et al., 2017). Based on our previous method and
1590 work, our next work is to analyse the physical processes and the dynamical
1591 characteristics of the SST field.

1592 ~~Although the reason why the improved model has good forecast results has~~
1593 ~~discussed in the section6.2, the deep physical mechanisms that the proposed model~~
1594 ~~has dealt with is not very clear, so its dynamical characteristics should be further~~
1595 ~~analysed.~~

1596 — (2)The experiments in the present study have proven that the forecasting results
1597 of the improved model are good for large-scale systems, such as ENSO events, and
1598 the forecasting period has been extended. However, for small-scale systems, such as

1599 Hurricanes, whether the forecast results could be improved using the present
1600 improved model needs to be further verified.

1601 (3) Our paper focuses primarily on these defined indices with T_1, T_2 to
1602 reconstruct a prediction model. Maybe, we can select variables (predictor) based on
1603 EOF analysis and our model may be a more physically oriented model. Maybe we can
1604 learn from Yim et al. (2013; 2015) to draw correlation maps between these fields and
1605 the SSTA field and select the predictors from physical considerations. All these above
1606 questions require that a lot of experiments to be carried out.

1607 These items will be our future work.

1608

1609 **Acknowledgments** This study was supported by the Chinese National Natural
1610 Science Fund (nos 41375002, 41075045, 41306010, 41571017, 51190091 and
1611 41071018) and the Chinese National Natural Science Fund (BK20161464) of Jiangsu
1612 Province, the Program for New Century Excellent Talents in University
1613 (NCET-12-0262), the China Doctoral Program of Higher Education
1614 (20120091110026), the Qing Lan Project, the Skeleton Young Teachers Program, and
1615 the Excellent Disciplines Leaders in Midlife-Youth Program of Nanjing University.

1616

1617 **APPENDIX A: THE PRINCIPLE OF DYNAMICAL MODEL** 1618 **RECONSTRUCTION**

1619 Suppose that the physical law of a nonlinear system going by over time can be
1620 expressed as the following difference form:

1621
$$\frac{q_i^{(j+1)M} - q_i^{(j-1)M}}{2\Delta t} = f_i(q_1^{jM}, q_2^{jM}, \dots, q_i^{jM}, \dots, q_N^{jM}) \quad j = 2, 3, \dots, M-1 \quad (A1)$$

1622 where f_i is the generalized nonlinear function of $q_1, q_2, \dots, q_i, \dots, q_N$, N is the number
 1623 of variables, and M is the length of observed data. $f_i(q_1^{jM}, q_2^{jM}, \dots, q_i^{jM}, \dots, q_N^{jM})$ can be assumed
 1624 to contain two parts: G_{jk} representing the expanding items which contain variable
 1625 q_i , P_{ik} just representing the corresponding parameters which are real numbers
 1626 ($i = 1, 2, \dots, N, j = 1, 2, \dots, M, k = 1, 2, \dots, K$).

1627 It can be supposed as follows:

1628
$$f_i(q_1, q_2, \dots, q_n) = \sum_{k=1}^K G_{jk} P_{ik} \quad (A2)$$

1629 $D = GP$ is the matrix form of Eq.(A2), in which

1630
$$D = \begin{Bmatrix} d_1 \\ d_2 \\ \dots \\ d_M \end{Bmatrix} = \begin{Bmatrix} \frac{q_i^{3\Delta t} - q_i^{\Delta t}}{2\Delta t} \\ \frac{q_i^{4\Delta t} - q_i^{2\Delta t}}{2\Delta t} \\ \dots \\ \frac{q_i^{M\Delta t} - q_i^{(M-2)\Delta t}}{2\Delta t} \end{Bmatrix}, \quad G = \begin{Bmatrix} G_{11}, G_{12}, \dots, G_{1K} \\ G_{21}, G_{22}, \dots, G_{2,K} \\ \dots \\ G_{M1}, G_{M2}, \dots, G_{M,K} \end{Bmatrix}, \quad P = \begin{Bmatrix} P_{i1} \\ P_{i2} \\ \dots \\ P_{iK} \end{Bmatrix} \quad (A3)$$

1631 Parameters of the above equation can be determined through inverting the
 1632 observed data. Vector P which satisfies the above equation can be solved, based on a
 1633 given vector D . Assuming q is unknown, it is a nonlinear system. However, assuming
 1634 P is unknown, it is a linear system.

1635 With the restriction $S = (D - GP)^T (D - GP)$ as a minimum, GA is introduced as an
 1636 optimization solution search in the model parameters space.

1637 Assuming that the parameters matrix P is the population (solutions), the
 1638 $S = (D - GP)^T (D - GP)$ is an objective function, $l_i = \frac{1}{S}$ is the value of individual
 1639 fitness, and $L = \sum_{i=1}^n l_i$ is the value of total fitness. The operating steps of GA include:

1640 creation and coding of initial population (solutions), fitness calculation, the choice of

1641 male parents, crossover and variation, etc. A detailed theoretical explanation can be
 1642 got from Wang (2001). The step length is 1 month during the calculation. After
 1643 optimization searches and genetic operations, the target value can be rapidly
 1644 converged on and each optimal parameter of the dynamical equations can be obtained.

1645 Through the above approach, we can obtain parameters of a nonlinear
 1646 dynamical system, and reconstruct the nonlinear dynamical equations from observed
 1647 data.

1648

1649 **APPENDIX B: THE MATHEMATICAL PRINCIPLE OF**
 1650 **SELF-MEMORIZATION DYNAMICS OF SYSTEMS**

1651 The dynamical equations of a system can be expressed as:

1652
$$\frac{\partial x_i}{\partial t} = F_i(x, \lambda, t) \quad i = 1, 2, \dots, J \quad (\text{B1})$$

1653 where J is an integer, x_i is the i th variable of the system state, and λ is
 1654 the parameter. Equation (B1) represents the relationship between a source function
 1655 F and a local change of x . Obviously, x is a scalar function with time t and
 1656 space r_0 . A set of time $T = [t_{-p} \dots t_0 \dots t_q]$ can be considered, where t_0 is an initial
 1657 time. A set of space $R = [r_a \dots r_i \dots r_\beta]$ can be considered, where r_i is a spatial point.

1658 An inner product in space $L^2 : T \times R$ is defined by:

1659
$$(f, g) = \int_a^b f(\xi)g(\xi)d\xi, f, g \in L^2 \quad (\text{B2})$$

1660 Accordingly, a norm can be defined as:

1661
$$\|f\| = \left[\int_a^b (f(\xi))^2 d\xi \right]^{1/2}$$

1662 For a completion L^2 , it can become a Hilbert space H . A generalized one
 1663 in H can be regarded as a solution of the multi-time model. By introducing a
 1664 memorization function $\beta(r, t)$, we can obtain:

$$1665 \int_{t_0}^t \beta(\tau) \frac{\partial x}{\partial \tau} d\tau = \int_{t_0}^t \beta(\tau) F(x, \tau) d\tau \quad (B3)$$

1666 where r in $\beta(r, t)$ can be dropped through fixing on the spatial point r_0 . Suppose
 1667 that function $\beta(r, t)$ and variable x etc. are all continuous, differentiable and
 1668 integrable, an integration by the left parts of Eq. (B3) can be made as:

$$1669 \int_{t_0}^t \beta(\tau) \frac{\partial x}{\partial \tau} d\tau = \beta(t)x(t) - \beta(t_0)x(t_0) - \int_{t_0}^t x(\tau)\beta'(\tau)d\tau \quad (B4)$$

1670 where $\beta'(t) = \partial\beta(t) / \partial t$. The mean value theorem can be introduced into the third
 1671 term in Eq. (B4), the following equation can be obtained:

$$1672 -\int_{t_0}^t x(\tau)\beta'(\tau)d\tau = -x^m(t_0)[\beta(t) - \beta(t_0)] \quad (B5)$$

1673 where $x^m(t_0) \equiv x(t_m), t_0 < t_m < t$. Substituting Eq. (B4) and Eq. (B5) in Eq. (B3) and
 1674 carrying out an algebraic operation, the following equation can be obtained:

$$1675 x(t) = \frac{\beta(t_0)}{\beta(t)} x(t_0) + \frac{\beta(t) - \beta(t_0)}{\beta(t)} x^m(t_0) + \frac{1}{\beta(t)} \int_{t_0}^t \beta(\tau) F(x, \tau) d\tau \quad (B6)$$

1676 Because the x value which is at initial time t_0 and middle time t_m , only on
 1677 the fixed point r_0 itself, relates to the first term and the second term in Eq. (B6),
 1678 they are called as a self-memory term. Also, we can call the third term as an
 1679 exogenous effect, i.e., which is contributed by other spatial points.

1680 Similarly as Eq. (B4), for multi-time $t_i, i = -p, -p+1, \dots, t_0, t$, it gives

1681
$$\int_{t-p}^{t-p+1} \beta(\tau) \frac{\partial x}{\partial \tau} d\tau + \int_{t-p+1}^{t-p+2} \beta(\tau) \frac{\partial x}{\partial \tau} d\tau + \dots + \int_{t_0}^t \beta(\tau) \frac{\partial x}{\partial \tau} d\tau = \int_{t-p}^t \beta(\tau) F(x, \tau) d\tau .$$

1682 After the same term $\beta(t_i)x(t_i), i = -p+1, -p+2, \dots, 0$ was eliminated, we

1683 have

1684
$$\beta(t)x(t) - \beta(t_{-p})x(t_{-p}) - \sum_{i=-p}^0 [\beta(t_{i+1}) - \beta(t_i)]x^m(t_i) - \int_{t-p}^t \beta(\tau)F(x, \tau)d\tau = 0 \quad (\text{B7})$$

1685 As a matter of convenience, we set $\beta_t \equiv \beta(t), \beta_0 \equiv \beta(t_0), x_t \equiv x(t), x_0 \equiv x(t_0)$; the

1686 following text uses similar notations. Then, Eq. (B7) can be expressed as:

1687
$$\beta_t x_t - \beta_{-p} x_{-p} - \sum_{i=-p}^0 x_i^m (\beta_{i+1} - \beta_i) - \int_{t-p}^t \beta(\tau)F(x, \tau)d\tau = 0 \quad (\text{B8})$$

1688 Setting $x_{-p} \equiv x_{-p-1}^m, \beta_{-p-1} = 0$, the Eq. (B8) can be written as:

1689
$$x_t = \frac{1}{\beta_t} \sum_{i=-p-1}^0 x_i^m (\beta_{i+1} - \beta_i) + \frac{1}{\beta_t} \int_{t-p}^t \beta(\tau)F(x, \tau)d\tau = S_1 + S_2 \quad (\text{B9})$$

1690 S_1 is called as a self-memory term and S_2 is called as an exogenous effect term.

1691 For the convenience of calculations, the above self-memorization equation can

1692 be discretized. The differential by difference and the summation can replace the

1693 integration in Eq. (B9), and the mean of two values which are at adjoining times; i.e.,

1694
$$x_i^m \approx \frac{1}{2}(x_{i+1} + x_i) \equiv y_i$$
 can simply replace x_i^m .

1695 Taking an equal time interval $\Delta t_i = t_{i+1} - t_i = 1$ and incorporating β_i and β_t ,

1696 we can obtain a discretized self-memorization equation as follows:

1697
$$x_t = \sum_{i=-p-1}^{-1} \alpha_i y_i + \sum_{i=-p}^0 \theta_i F(x, i) \quad (\text{B10})$$

1698 where F is the dynamic kernel of the self-memorization equation, $\alpha_i = \frac{(\beta_{i+1} - \beta_i)}{\beta_t}$;

1699
$$\theta_i = \frac{\beta_i}{\beta_t} .$$

1700 Based on Eq. (B10), the above technique performed computations and the
1701 forecast can be called as a self-memorization principle.

1702

1703

1704 REFERENCES

1705 [Ashok K, Guan Z, Yamagata T : Impact of the Indian Ocean Dipole on the decadal relationship](#)
1706 [between the Indian monsoon rainfall and ENSO, Geophys Res Lett,28\(23\), 4499-4502, 2001.](#)

1707 [Balmaseda M.A., Davey M.K. and Anderson D.L.T.: Decadal and seasonal dependence of ENSO](#)
1708 [prediction skill,J Clim.,8, 2705–2715, 1995.](#)

1709 [Barnston A. G., et al.: Skill of real-time seasonal ENSO model predictions during 2002-2011,Bull.](#)
1710 [Amer. Meteor. Soc.,93, 631-651, 2012.](#)

1711 [Belkin M. and P. Niyogi: Laplacian eigenmaps for dimensionality reduction and data](#)
1712 [representation,Neural Comput.,15,1373-1391, 2003.](#)

1713 [Bjerknes J.: Atmospheric teleconnections from the equatorial Pacific,Mon. Wea. Rev.,97,163-172, 1969.](#)

1714 [Burnham, K. P.; Anderson, D. R: Model Selection and Multimodel Inference \(2nd ed.\),](#)
1715 [Springer-Verlag, 2002.](#)

1716 [Cao H. X.: Self-memorization Equation in Atmospheric Motion,Science in China \(Series B\),36\(7\),](#)
1717 [845-855, 1993.](#)

1718 [Chen D., S. E. Zebiak, A. J. Busalacchi and M. A. Cane: An Improved Procedure for El Niño](#)
1719 [Forecasting: Implications for Predictability,Science, 269, 1699-1702, 1995.](#)

1720 [Chen G., Shao B. M. Han Y., et al.: Modality of semiannual to multidecadal oscillations in global sea](#)
1721 [surface temperature variability. Journal of Geophysical Research, 115, 1-14, 2010.](#)

1722 [Chen X. D., Xia J., Xu Q.: Differential Hydrological Grey Model\(DHGM\) with self-memory function](#)
1723 [and its application to flood forecasting,Sci China Tech Sci.,52,1039–1049, 2009.](#)

1724 [Clarke A. J. and S. Van Gorder: Improving El Niño prediction using a space-time integration of](#)
1725 [Indo-Pacific winds and equatorial Pacific upper ocean heat content, Geophys. Res. Lett.,30,1399.](#)
1726 [doi:10.1029/2002GL016673, 2003.](#)

1727 [Delecluse P., Davey M., Kitamura Y., Philander S., Suarez M., Bengtsson L.: TOGA review paper:](#)
1728 [coupled general circulation modeling of the tropical Pacific,J Geophys Res,103,14357–14373, 1998.](#)

带格式的: 字体颜色: 自动设置

1729 [Davey M., Huddleston M., Sperber K.R., et al.: A study of coupled model climatology and variability](#)
1730 [in tropical ocean regions,Clim. Dyn.,18,403–420, 2002.](#)

1731 [Dommenges and Latif: A Cautionary Note on the Interpretation of EOFs, Journal of](#)
1732 [Climate,15\(2\),216–225, 2002.](#)

1733 [Drosowsky W.: Statistical prediction of ENSO \(Niño 3\) using sub-surface temperature data,Geophys.](#)
1734 [Res.Lett., 33 , L03710. doi:10.1029/2005GL024866, 2006.](#)

1735 [Everitt B.S., Skrondal A.: Cambridge Dictionary of Statistics, Cambridge University Press, 2010.](#)

1736 [Feng G. L., Cao H. X., Gao X. Q., et al.: Prediction of precipitation during summer monsoon with](#)
1737 [self-memorial model,Adv Atmos Sci.,18 ,701–709, 2001.](#)

1738 [Fraedrich K.: Estimating weather and climate predictability on attractors,J .A tmos.Sci.,44,7 22-728,](#)
1739 [1987.](#)

1740 [Glantz MH, Katz RW, Nicholls N \(eds\): Teleconnections linking worldwide climate anomalies,](#)
1741 [74pp,Cambridge University Press, Cambrige, UK, 1991.](#)

1742 [Golbraikh A. and Tropsha A.: Beware of q 2 ! Journal of Molecular Graphics and Modelling, 20 ,](#)
1743 [269–276, 2002.](#)

1744 [Golbraikh A.,Shen M., Xiao Z. Y., Xiao Y. D., Lee Kuo-Hsiung, Tropsha A.: Rational selection of](#)
1745 [training and test sets for the development of validated QSAR models. Journal of Computer-Aided](#)
1746 [Molecular Design, 17\(2\), 241-253, 2003.](#)

1747 [Gu X. Q.: A spectral model based on atmospheric self memorization principle,Chinese Science](#)
1748 [Bulletin,43\(20\),1692-1702 , 1998.](#)

1749 [Hong M., Zhang R., Wu G. X., et al.: A Nonlinear Dynamic System Reconstruction of the Subtropical](#)
1750 [High Characteristic Index based on Genetic Algorithm. Chinese Journal of Atmospheric](#)
1751 [Sciences,31\(2\):346-352, 2007.](#)

1752 [Hong M., Zhang R.andMa C. C.et al.: A Non-Linear Dynamical–Statistical Model for Reconstruction](#)
1753 [of the Air–Sea Element Fields in the Tropical Pacific Ocean,Atmosphere–Ocean, doi:](#)
1754 [10.1080/07055900.2014.908765, 2014.](#)

1755 [Hong M., Zhang R., et al.: Reconstruction and forecast experiments of a statistical-dynamical model of](#)
1756 [the Western Pacific subtropical high and Eastern Asian summer monsoon factors, Weather and](#)
1757 [Forecasting, 30:206-216 , 2015](#)

1758 [Hong M., Zhang R., et al.: Catastrophe and Mechanism Analyses of Multiple Equilibria in the Western](#)

带格式的: 字体颜色: 自动设置

1759 [Pacific Subtropical High System Based on Objective Fitting of Spatial Basis Functions. Monthly](#)
1760 [Weather Review, 144, 997-1015, 2016.](#)

1761 [Hong M., Zhang R., et al.: Bifurcations and catastrophes in a nonlinear dynamical model of the western](#)
1762 [Pacific subtropical high ridge line index and its evolution mechanism, Theor. Appl. Climatol., 129,](#)
1763 [363-384, 2017.](#)

1764 [Hu, T.S., K.C. Lam, and S.T. Ng: River flow time series prediction with a range-dependent neural](#)
1765 [network,Hydrol. Sci. J., 46, 729–745, 2001.](#)

1766 [Hu Y. J., Zhong Z., Zhu Y. M. et al.: A statistical forecast model using the time-scale decomposition](#)
1767 [technique to predict rainfall during flood period over the middle and lower reaches of the Yangtze](#)
1768 [River Valley. Theoretical and Applied Climatology, doi: 10.1007/s00704-017-2094-9,2017.](#)

1769 [Huang, J., Y. Yi, S. Wang, et al.: An analogue-dynamical long-range numerical weather prediction](#)
1770 [system incorporating historical evolution,Quart J Roy Meteor Soc, 119\(511\),547-565, 1993.](#)

1771 [Islam M.N. Sivakumar B.: Characterization and prediction of runoff dynamics:a nonlinear dynamical](#)
1772 [view. Advances in Water Resources, 25, 179-190, 2002.](#)

1773 [James A. Carton and Benjamin S. Giese: A Reanalysis of Ocean Climate Using Simple Ocean Data](#)
1774 [Assimilation \(SODA\),Monthly Weather Review,136\(8\),2999-3011 , 2008.](#)

1775 [Jin E. K., James L. K., Wang B., et al.: Current status of ENSO prediction skill in coupled](#)
1776 [ocean-atmosphere models,Climate Dyn,31, 647-664, 2008.](#)

1777 [Johnson S.D., Battistis D.S. and Sarachik E. S.: Empirically Derived Markov Models and Prediction of](#)
1778 [Tropical Pacific Sea Surface Temperature Anomalies, Journal of Climate,13,3-17, 2000.](#)

1779 [Kalnay E., Kanamitsu M. and Kistler R.: The NCEP/NCAR 40-year reanalysis project, Bull. Amer.](#)
1780 [Meteor. Soc.,77,437-470 , 1996.](#)

1781 [Kathrin Böttner, Jennifer Salau, and Joachim Krieter: Temporal correlation coefficient for directed](#)
1782 [networks. Springerplus, 5\(1\): 1198-1203, 2016.](#)

1783 [Kim Ji-Won ,Soon-Il An,Sang-Yoon Jun,Hey-Jin Park,Sang-Wook Yeh.: ENSO and East Asian winter](#)
1784 [monsoon relationship modulation associated with the anomalous northwest Pacific anticyclone,](#)
1785 [Climate Dynamics, 49\(4\), 1157–1179, 2017.](#)

1786 [L'Heureux Michelle L., Collins Dan C., Hu Zeng-Zhen. Linear trends in sea surface temperature of the](#)
1787 [tropical Pacific Ocean and implications for the El Niño-Southern Oscillation, Climate Dynamics, 40,](#)
1788 [1223–1236, 2013.](#)

1789 [Liebmann B. and C.A. Smith: Description of a Complete \(Interpolated\) Outgoing Longwave Radiation](#)

1790 [Dataset, Bulletin of the American Meteorological Society, 77, 1275-1277, 1996.](#)

1791 [Luo, J.-J., S. Masson, S. Behera, S. Shingu, and T. Yamagata: Seasonal climate predictability in a](#)

1792 [coupled OAGCM using a different approach for ensemble forecasts, J. Climate, 18, 4474-4497, 2005.](#)

1793 [Mehcho C.R., Robertson A.W., Barth N., et al.: The seasonal cycle over the tropical Pacific in coupled](#)

1794 [atmosphere-ocean general circulation models, Mon Weather Rev, 123, 2825-2838, 1995.](#)

1795 [Molteni F., et al.: ECMWF seasonal forecast system 3, CLIVAR Exch, 43, 7-9, 2007.](#)

1796 [Moore A. M., Zavala-Garay J. and Tang Y., et al.: Optimal forcing patterns for coupled models of](#)

1797 [ENSO, J Climate, 19, 4683-4699, 2006.](#)

1798 [Neelin J.D., Latif M. and Allaart M.A.F.: Tropical air-sea interaction in general circulation](#)

1799 [models, Clim Dyn., 7, 73-104, 1992.](#)

1800 [Nicosia V, Tang J, Mascolo C, Musolesi M, Russo G, Latora V: Graph metrics for temporal networks.](#)

1801 [In: Holme P, Saramäki J, editors. Temporal networks. Berlin: Springer, pp. 15-40, 2013.,](#)

1802 [Palmer T. N., Alessandri A. and Andersen U., et al.: Development of a European multi-model](#)

1803 [ensemble system for seasonal to interannual prediction \(DEMETER\), Bull Amer Met Soc., 85, 853-872,](#)

1804 [2004.](#)

1805 [Philander S.G., Pacanowski R.C., N-C Lau et al.: Simulation of ENSO with a global atmospheric GCM](#)

1806 [coupled to a high resolution, tropical Pacific Ocean GCM. J. Climate, 5, 308-329, 1992.](#)

1807 [Qin G. H. and Li Z. H.: Over-fitting of BP NN research and its application, Engineering Journal of](#)

1808 [Wuhan University, 39\(6\), 1671-1679, 2006.](#)

1809 [Rasmusson E.M. and Carpenter T.H.: Variations in tropical seasurface temperature and surface wind](#)

1810 [fields associated with the Southern Oscillation/El Niño, Mon Weather Rev., 10, 354-384, 1982.](#)

1811 [Rayner NA, Parker DE, Horton EB, Folland CK, Alexander LV, Rowell DP, Kent EC, Kaplan A:](#)

1812 [Global analyses of sea surface temperature, sea ice, and night marine air temperature since the late](#)

1813 [nineteenth century. J Geophys Res 108\(D14\):4407. doi:10.1029/2002JD002670, 2003.](#)

1814 [Reynolds, R. W., N. A. Rayner, T. M. Smith, D. C. Stokes, and W. Wang: An improved in situ and](#)

1815 [satellite SST analysis for climate, J. Climate, 15, 1609-1625, 2002.](#)

1816 [Saha S., Nadiga C. and Thiaw J., et al.: The NCEP climate forecast system, Journal of](#)

1817 [Climate, 19, 3483-3517, 2006.](#)

1818 [Saji N. H., Goswami B. N., Vinayachandran P. N., et al.: A dipole mode in the tropical Indian](#)

带格式的: 字体颜色: 自动设置

带格式的: 字体颜色: 自动设置

1819 [Ocean.Nature, 401\(6751 \),360-363, 1999.](#)

1820 [Smith T.M.: Improved extended reconstruction of SST\(1854-1997\). J. Climate, 17, 2466-2477, 2004.](#)

1821 [Takens, F.: Detecting strange attractors in fluid turbulence,Lecture Notes in](#)

1822 [Mathematics,898\(2\),361-381 , 1981.](#)

1823 [Sivakumar B, Berndtsson R, Persson M.: Monthly Runoff Prediction Using Phase -space](#)

1824 [Reconstruction. Hydrological Sciences Journal, 46\(3\), 377 -388, 2001.](#)

1825 [Sivakumar B., Jayawardena A.W., Fernando T.M.K.G.: River flow forecasting: use of phase-space](#)

1826 [reconstruction and artificial neural networks approaches. Journal of Hydrology, 265, 225-245, 2002.](#)

1827 [Timmermann A., Voss H. U. and Pasmanter R.: Empirical Dynamical System Modeling of ENSO](#)

1828 [Using Nonlinear Inverse Techniques, Journal of Physical Oceanography, 31,1579-1598 , 2001.](#)

1829 [Tomita, T., and T. Yasunari: Role of the northeast winter monsoon on the biennial oscillation of the](#)

1830 [ENSO/monsoon system,J. Meteor. Soc. Japan, 74,399–413 , 1996.](#)

1831 [Trenberth, E. K., et al.: Progress during TOGA in understanding and modeling global teleconnections](#)

1832 [associated with tropical sea surface temperatures,J. Geophys. Res., 107, C7, 14291-14324,1998.](#)

1833 [Wang B., Wu R., Lukas R.: Roles of western North Pacific wind variation in thermocline adjustment](#)

1834 [and ENSO phase transition,J Meteor Soc Japan,77,1-16,1999a.](#)

1835 [Wang B., Wu R., Li T.: Atmosphere-warm ocean interaction and its impacts on Asian-Australian](#)

1836 [monsoon variation. J. Climate, 16, 1195-1211, 2003.](#)

1837 [Wang B., Lee J. Y., Shukla J., et al.: Advance and prospectus of seasonal prediction: assessment of](#)

1838 [the APCC / CliPAS 14-Model Ensemble Retrospective Seasonal Prediction\(1980—2004\),Climate](#)

1839 [Dyn.,33\(1\),93-117 , 2009a.](#)

1840 [Wang C., Weisberg R. H. and Virmani J. I.: Western Pacific interannual variability associated with the](#)

1841 [El Niño-Southern Oscillation,J Geophy Res.,104,5131-5149, 1999b.](#)

1842 [Wang, L., W. Chen, and R. H. Huang: Interdecadal modulation of PDO on the impact of ENSO on the](#)

1843 [east Asian winter monsoon, Geophys. Res. Lett., 35, L20702, doi:10.1029/2008GL035287, 2008.](#)

1844 [Wang, W. C., K. W. Chau, C. T. Cheng, and L. Qiu: A comparison of performance of several artificial](#)

1845 [intelligence methods for forecasting monthly discharge time series. J. Hydrol., 374, 294–306,](#)

1846 [doi:10.1016/j.jhydrol.2009.06.019,2009b.](#)

1847 [Wang L.: Intelligent Optimization Algorithms and Its Application, pp. 23-24, Tsinghua University](#)

1848 [Press, Chendu, 2001.](#)

1849 [Webster P. J., Moore A. M., Loschnigg J. P., et al.: Coupled ocean-atmosphere dynamics in the Indian](#)
1850 [Ocean during 1997- 98, Nature, 401\(6751 \),356-360, 1999.](#)

1851 [Weinberger K. O. and L. Saul: Unsupervised learning of image manifolds by semidefinite](#)
1852 [programming,Int. J. Comput. Vision.,70, 77-90, 2006.](#)

1853 [Xu B.C., Wang Z.S., Wu J.P. and Zhou E.M.: Interaction between sea surface temperature \(SST\) of](#)
1854 [information regions and southern oscillation index \(SOI\) in Tropical Pacific Ocean. *Marine Science*](#)
1855 [Bulletin, 12\(5\),211-25,1993.](#)

1856 [Yang, S., K. M. Lau, and K. M. Kim: Variations of the East Asian jet stream and](#)
1857 [Asian-Pacific-American winter climate anomalies, J. Climate, 15,306–325 , 2002.](#)

1858 [Yang Se-Hwan and Lu Riyu: Predictability of the East Asian winter monsoon indices by the coupled](#)
1859 [models of ENSEMBLES, Advances in Atmospheric Sciences, 31\(6\), 1279–1292, 2014](#)

1860 [Yim SY, Wang B, Kwon M: Interdecadal change of the controlling mechanisms for East Asian early](#)
1861 [summer rainfall variation around the mid-1990s.ClimDyn., 42,1325–1333, 2013.](#)

1862 [Yim, S.-Y., B. Wang, W. Xing, M.-M.Lu: Prediction of Meiyu rainfall in Taiwan by multi-lead](#)
1863 [physicalempiricalmodels.Clim. Dyn., 44 \(11-12\), 3033-3042, doi:10.1007/s00382-014-2340-0, 2015.](#)

1864 [Yoon, J., and S. W. Yeh: Influence of the Pacific Decadal Oscillation on the relationship between El](#)
1865 [Niño and the northeast Asian summer monsoon, J. Climate,23, 4525–4537, 2010.](#)

1866 [Yu H., J. Huang, and J. Chou: Improvement of Medium-Range Forecasts Using the](#)
1867 [Analogue-Dynamical Method.Mon. Wea. Rev., 142, 1570–1587, doi:](#)
1868 [http://dx.doi.org/10.1175/MWR-D-13-00250.1, 2014a.](#)

1869 [Yu H., J. Huang, W. Li, and G. Feng: Development of the analogue-dynamical method for error](#)
1870 [correction of numerical forecasts,J. Meteor. Res., 28\(5\), 934–947, doi: 10.1007/s13351-014-4077-4 ,](#)
1871 [2014b.](#)

1872 [Zhang R. and Hong M., et al.: Non-linear Dynamic Model Retrieval of Subtropical High Based on](#)
1873 [Empirical Orthogonal Function and Genetic Algorithm,Applied Mathematics and](#)
1874 [Mechanics,27\(12\),1645-1654, 2006.](#)

1875 [Zhang R. and Hong M..et al.: Retrieval of the non-linear dynamic forecast model of El Nino/La Nina](#)
1876 [index based on the genetic algorithm optimization. Chinese Journal of Geophysics,51\(5\),1354-1362,](#)
1877 [2008.](#)

1878 [Zhang R. H., Zhou G. Q. and Chao J. P.: ENSO Dynamics and Its Prediction,Chinese Journal of](#)

带格式的: 字体颜色: 自动设置

带格式的: 字体颜色: 自动设置

1879 [Atmospheric Sciences,27\(4\) ,674-688, 2003a.](#)

1880 [Zhang, R.H., S. E. Zebiak, R. Kleeman, and N.Keenlyside: A new intermediate coupled model for El](#)

1881 [Niño simulation and prediction. Geophys. Res.Lett., 30, doi:10.1029/2003GL018010, 2003b.](#)

1882 [Zhang, R. H., A. Sumi, and M. Kimoto: Impact of El Niño on the East Asian monsoon: A diagnostic](#)

1883 [study of the '86/87 and '91/92 events.J. Meteor. Soc. Japan, 74, 49–62, 1996.](#)

1884 [Zhang Y. L., Yu Y. Q., Duan W. S.: The spring prediction barrier of ENSO in retrospective prediction](#)

1885 [experiments as shown by the four coupled ocean-atmosphere models. Acta Meteorologica Sinica, 70\(3\),](#)

1886 [506-519, 2012.](#)

1887 [Zhao J. H., Liu X. Y. and Jiang H. Y., et al.: Characteristics of Sea Surface Height in Tropical Pacific](#)

1888 [and its relationship with ENSO events.Meteorological and Environmental Sciences, 35\(2\),33-39, 2012.](#)

1889 [Zhou, L.-T., and R. G. Wu: Respective impacts of the East Asian winter monsoon and ENSO on winter](#)

1890 [rainfall in China.J. Geophys. Res.,115, doi: 10.1029/2009JD012502, 2010.](#)

带格式的: 字体颜色: 自动设置

1892 **REFERENCES**

1893 ~~Ashok K, Guan Z, Yamagata T : Impact of the Indian Ocean Dipole on the decadal relationship~~

1894 ~~between the Indian mon soon rainfall and ENSO, Geophys Res Let,28(23), 4499-4502, 2001.~~

1895 ~~Balmaseda M.A., Davey M.K. and Anderson D.L.T.: Decadal and seasonal dependence of ENSO~~

1896 ~~prediction skill,J Clim.,8, 2705-2715, 1995.~~

1897 ~~Barber R.T. and Chavez F.P.: Biological consequences of El Niño,Science,222,1203-1210, 1983.~~

1898 ~~Barnston A. G., et al.: Skill of real time seasonal ENSO model predictions during 2002-2011,Bull.~~

1899 ~~Amer. Meteor. Soc.,93, 631-651, 2012.~~

1900 ~~Belkin M. and P. Niyogi: Laplacian eigenmaps for dimensionality reduction and data~~

1901 ~~representation,Netural Comput.,15,1373-1391, 2003.~~

1902 ~~Bjerknes J.: Atmsopheric teleconnections from the equatorial Pacific,Mon. Wea. Rev.,97,163-172, 1969.~~

1903 ~~Cao H. X.: Self-memorization Equation in Atmospheric Motion,Science in China (Series B),36(7),~~

1904 ~~845-855, 1993.~~

1905 ~~Chen D., S. E. Zebiak, A. J. Busalacchi and M. A. Cane: An Improved Procedure for El Niño~~

1906 ~~Forecasting: Implications for Predictability,Science, 269, 1699-1702, 1995.~~

1907 ~~Chen X. D., Xia J., Xu Q.: Differential Hydrological Grey Model(DHGM) with self memory function~~

1908 ~~and its application to flood forecasting,Sci China Tech Sci.,52,1039-1049, 2009.~~

1909 [Chou J.: The problem of utilizing past data in numerical weather forecasting, *Sci. China*, 6, 635-644,](#)
1910 [1974 \(in Chinese\).](#)

1911 [Clarke A. J. and S. Van Gorder: Improving El Niño prediction using a space-time integration of](#)
1912 [Indo-Pacific winds and equatorial Pacific upper-ocean heat content, *Geophys. Res. Lett.*, 30, 1399.](#)
1913 [doi:10.1029/2002GL016673, 2003.](#)

1914 [Delecluse P., Davey M., Kitamura Y., Philander S., Suarez M., Bengtsson L.: TOGA review paper:](#)
1915 [coupled general circulation modeling of the tropical Pacific, *J Geophys Res*, 103, 14357-14373, 1998.](#)

1916 [Davey M., Huddleston M., Sperber K.R., et al.: A study of coupled model climatology and variability](#)
1917 [in tropical ocean regions, *Clim. Dyn.*, 18, 403-420, 2002.](#)

1918 [Dommenges and Latif: A Cautionary Note on the Interpretation of EOFs, *Journal of*](#)
1919 [Climate](#), 15(2), 216-225, 2002.

1920 [Drosowsky W.: Statistical prediction of ENSO \(Niño 3\) using sub-surface temperature data, *Geophys.*](#)
1921 [Res. Lett.](#), 33, L03710. doi:10.1029/2005GL024866, 2006.

1922 [Feng G. L., Cao H. X., Gao X. Q., et al.: Prediction of precipitation during summer monsoon with](#)
1923 [self-memorial model, *Adv Atmos Sci.*, 18, 701-709, 2001.](#)

1924 [Fraedrich K.: Estimating weather and climate predictability on attractors, *J Atmos. Sci.*, 44, 722-728,](#)
1925 [1987.](#)

1926 [Glantz MH, Katz RW, Nicholls N \(eds\): Teleconnections linking worldwide climate anomalies,](#)
1927 [74pp, Cambridge University Press, Cambridge, UK, 1991.](#)

1928 [Gu X. Q.: A spectral model based on atmospheric self-memorization principle, *Chinese Science*](#)
1929 [Bulletin](#), 43(20), 1692-1702, 1998.

1930 [Hong M., Zhang R. and Ma C. C. et al.: A Non-Linear Dynamical-Statistical Model for Reconstruction](#)
1931 [of the Air-Sea Element Fields in the Tropical Pacific Ocean, *Atmosphere-Ocean*, doi:](#)
1932 [10.1080/07055900.2014.908765, 2014.](#)

1933 [Hu, T.S., K.C. Lam, and S.T. Ng: River flow time-series prediction with a range-dependent neural](#)
1934 [network, *Hydrol. Sci. J.*, 46, 729-745, 2001.](#)

1935 [Huang J., Y. Yi, S. Wang, et al.: An analogue dynamical long-range numerical weather prediction](#)
1936 [system incorporating historical evolution, *Quart J Roy Meteor Soc.*, 119\(511\), 547-565, 1993.](#)

1937 [Huang J. P. and Yi Y. H.: A Non-linear Dynamic System Reconstructing of Actual data, *Science in*](#)
1938 [China](#), 3(3), 331-336, 1991.

1939 [James A. Carton and Benjamin S. Giese: A Reanalysis of Ocean Climate Using Simple Ocean Data](#)

1940 [Assimilation \(SODA\), Monthly Weather Review, 136\(8\), 2999-3011, 2008.](#)

1941 [Jin E. K., James L. K., Wang B., et al.: Current status of ENSO prediction skill in coupled](#)

1942 [ocean-atmosphere models, Climate Dyn, 31, 647-664, 2008.](#)

1943 [Johnson S.D., Battisti D.S. and Sarachik E. S.: Empirically Derived Markov Models and Prediction of](#)

1944 [Tropical Pacific Sea Surface Temperature Anomalies, Journal of Climate, 13, 3-17, 2000.](#)

1945 [Kalnay E., Kanamitsu M. and Kistler R.: The NCEP/NCAR 40 year reanalysis project, Bull. Amer.](#)

1946 [Meteor. Soc., 77, 437-470, 1996.](#)

1947 [Liao D., Zhou Y.H. and Liao X.H.: Modulation of the SSTA Decadal Variation on ENSO Events and](#)

1948 [Relationships of SSTA with LOD, SOI, etc., Acta Astronomica Sinica, 48\(1\), 36-47, 2007.](#)

1949 [Liebmann B. and C.A. Smith: Description of a Complete \(Interpolated\) Outgoing Longwave Radiation](#)

1950 [Dataset, Bulletin of the American Meteorological Society, 77, 1275-1277, 1996.](#)

1951 [Li L. P., Wang P. X., He J. H. and Wang D. X.: Analysis of interdecadal and interannual](#)

1952 [Characteristics of the Tropical western Pacific Warm Pool heat status, Journal of Tropical](#)

1953 [Meteorology, 20\(5\), 472-482, 2004.](#)

1954 [Luo, J.J., S. Masson, S. Behera, S. Shingu, and T. Yamagata: Seasonal climate predictability in a](#)

1955 [coupled OAGCM using a different approach for ensemble forecasts, J. Climate, 18, 4474-4497, 2005.](#)

1956 [Mehoso C.R., Robertson A.W., Barth N., et al.: The seasonal cycle over the tropical Pacific in coupled](#)

1957 [atmosphere-ocean general circulation models, Mon Weather Rev, 123, 2825-2838, 1995.](#)

1958 [Molteni F., et al.: ECMWF seasonal forecast system 3, CLIVAR Exch, 43, 7-9, 2007.](#)

1959 [Moore A. M., Zavala Garay J. and Tang Y., et al.: Optimal forcing patterns for coupled models of](#)

1960 [ENSO, J Climate, 19, 4683-4699, 2006.](#)

1961 [Neelin J.D., Latif M. and Allaart M.A.F.: Tropical air-sea interaction in general circulation](#)

1962 [models, Clim Dyn., 7, 73-104, 1992.](#)

1963 [Palmer T. N., Alessandri A. and Andersen U., et al.: Development of a European multi-model](#)

1964 [ensemble system for seasonal to interannual prediction \(DEMETER\), Bull Amer Met Soc., 85, 853-872,](#)

1965 [2004.](#)

1966 [Panofsky H.A., Brier G.W.: Some applications of statistics to meteorology, Pennsylvania State](#)

1967 [University Press, Pennsylvania, 1968.](#)

1968 [Rasmusson E.M. and Carpenter T.H.: Variations in tropical seasurface temperature and surface wind](#)

1969 [fields associated with the Southern Oscillation/El Niño, Mon Weather Rev.,10, 354-384, 1982.](#)

1970 [Reynolds, R. W., N. A. Rayner, T. M. Smith, D. C. Stokes, and W. Wang: An improved in-situ and](#)

1971 [satellite SST analysis for climate, J. Climate,15,1609-1625, 2002.](#)

1972 [Saha S., Nadiga C. and Thiaw J., et al.: The NCEP climate forecast system, Journal of](#)

1973 [Climate,19,3483-3517, 2006.](#)

1974 [Saji N. H., Goswami B. N., Vinayachandran P. N., et al.: A dipole mode in the tropical Indian](#)

1975 [Ocean, Nature, 401\(6751\),360-363, 1999.](#)

1976 [Takens, F.: Detecting strange attractors in fluid turbulence, Lecture Notes in](#)

1977 [Mathematics,898\(2\),361-381, 1981.](#)

1978 [Tetko, I. V., Livingstone, D. J., Luik, A. I.: Neural network studies. I. Comparison of Overfitting and](#)

1979 [Overtraining, J. Chem. Inf. Comput. Sci.,35 \(5\), 826-833, 1995.](#)

1980 [Timmermann A., Voss H. U. and Pasmanter R.: Empirical Dynamical System Modeling of ENSO](#)

1981 [Using Nonlinear Inverse Techniques, Journal of Physical Oceanography, 31,1579-1598, 2001.](#)

1982 [Tomita, T., and T. Yasunari: Role of the northeast winter monsoon on the biennial oscillation of the](#)

1983 [ENSO/monsoon system, J. Meteor. Soc. Japan, 74,399-413, 1996.](#)

1984 [Trenberth, E. K., et al.: Progress during TOGA in understanding and modeling global teleconnections](#)

1985 [associated with tropical sea surface temperatures, J. Geophys. Res., 107, C7, 14291-14324, 1998.](#)

1986 [Wang B., Wu R., Lukas R.: Roles of western North Pacific wind variation in thermocline adjustment](#)

1987 [and ENSO phase transition, J. Meteor. Soc. Japan, 77,1-16, 1999a.](#)

1988 [Wang B., Lee J. Y., Shukla J., et al.: Advance and prospectus of seasonal prediction: assessment of](#)

1989 [the APCC / CliPAS-14 Model Ensemble Retrospective Seasonal Prediction \(1980-2004\), Climate](#)

1990 [Dyn.,33\(1\),93-117, 2009.](#)

1991 [Wang C., Weisberg R. H. and Virmani J. L.: Western Pacific interannual variability associated with the](#)

1992 [El Niño-Southern Oscillation, J. Geophys. Res.,104,5131-5149, 1999b.](#)

1993 [Wang, L., W. Chen, and R. H. Huang: Interdecadal modulation of PDO on the impact of ENSO on the](#)

1994 [east Asian winter monsoon, Geophys. Res. Lett., 35, L20702, doi:10.1029/2008GL035287, 2008.](#)

1995 [Wang L.: Intelligent Optimization Algorithms and Its Application, pp. 23-24, Tsinghua University](#)

1996 [Press, Chendu, 2001.](#)

1997 [Wang W., Su J. Y., Hou B. W. et al.: Dynamic prediction of building subsidence deformation with](#)

1998 [data-based mechanistic self-memory model, Chinese Science Bulletin, 57\(26\),3430-3435, 2012.](#)

1999 Webster P. J., Moore A. M., Loschnigg J. P., et al.: Coupled ocean atmosphere dynamics in the Indian Ocean during 1997–98, *Nature*, 401(6751), 356–360, 1999.

2000

2001 Weinberger K. Q. and L. Saul: Unsupervised learning of image manifolds by semidefinite programming, *Int. J. Comput. Vision.*, 70, 77–90, 2006.

2002

2003 Xu J. J. and Wang D. X.: Diagnosis of interannual and interdecadal variation in SST over Indian Pacific Ocean and numerical simulation of their effect on Asian summer monsoon, *Acta Oceanologica Sinica*, 22(3), 34–43, 2000.

2004

2005

2006 Yang, S., K. M. Lau, and K. M. Kim: Variations of the East Asian jet stream and Asian-Pacific American winter climate anomalies, *J. Climate*, 15, 306–325, 2002.

2007

2008 Yim SY, Wang B, Kwon M: Interdecadal change of the controlling mechanisms for East Asian early summer rainfall variation around the mid-1990s. *Clim Dyn.*, 42, 1325–1333, 2013.

2009

2010 Yim, S. Y., B. Wang, W. Xing, M. M. Lu: Prediction of Meiyu rainfall in Taiwan by multi-lead physical empirical models. *Clim. Dyn.*, 44 (11–12), 3033–3042, doi:10.1007/s00382-014-2340-0, 2015.

2011

2012 Yoon, J., and S. W. Yeh: Influence of the Pacific Decadal Oscillation on the relationship between El Niño and the northeast Asian summer monsoon, *J. Climate*, 23, 4525–4537, 2010.

2013

2014 Yu H., J. Huang, and J. Chou: Improvement of Medium-Range Forecasts Using the Analogue Dynamical Method, *Mon. Wea. Rev.*, 142, 1570–1587, doi: <http://dx.doi.org/10.1175/MWR-D-13-00250.1>, 2014a.

2015

2016

2017 Yu H., J. Huang, W. Li, and G. Feng: Development of the analogue dynamical method for error correction of numerical forecasts, *J. Meteor. Res.*, 28(5), 934–947, doi: 10.1007/s13351-014-4077-4, 2014b.

2018

2019

2020 Zhang R. and Hong M., et al.: Non-linear Dynamic Model Retrieval of Subtropical High Based on Empirical Orthogonal Function and Genetic Algorithm, *Applied Mathematics and Mechanics*, 27(12), 1645–1654, 2006.

2021

2022

2023 Zhang R. and Hong M., et al.: Retrieval of the non-linear dynamic forecast model of El Niño/La Niña index based on the genetic algorithm optimization. *Chinese Journal of Geophysics*, 51(5), 1354–1362, 2008.

2024

2025

2026 Zhang R. H., Zhou G. Q. and Chao J. P.: ENSO Dynamics and Its Prediction, *Chinese Journal of Atmospheric Sciences*, 27(4), 674–688, 2003.

2027

2028 Zhang, R. H., A. Sumi, and M. Kimoto: Impact of El Niño on the East Asian monsoon: A diagnostic

域代码已更改

2029 [study of the '86/87 and '91/92 events, J. Meteor. Soc. Japan, 74, 49–62, 1996.](#)

2030 [Zhao J. H., Liu X. Y. and Jiang H. Y., et al.: Characteristics of Sea Surface Height in Tropical Pacific](#)

2031 [and its relationship with ENSO events, Meteorological and Environmental Sciences, 35\(2\), 33–39, 2012.](#)

2032 [Zhou, L. T., and R. G. Wu: Respective impacts of the East Asian winter monsoon and ENSO on winter](#)

2033 [rainfall in China, J. Geophys. Res., 115, doi: 10.1029/2009JD012502, 2010.](#)

2034

2035

2036

2037

2038

2039

2040

2041

2042

2043

2044

2045

2046

2047 **List of Figures:**

2048 [Fig.1\(a, c\) First and second modes of the EOF deconstruction of the SSTA field, and \(b, d\) the](#)

2049 [corresponding PC time series.](#)

2050 ~~The time series (a) and the spatial mode (b) of the first mode; the time series(c) and the spatial mode~~

2051 ~~(d) of the second mode of the SSTA filed~~

2052 **Fig. 2** Forecast results of the first time coefficient series (a) and the second time coefficient series (b) of

2053 the SSTA field by the original model

2054 **Fig. 3.** The cross-validated retroactive hindcast results of the first time coefficient series (a) and the

2055 second time coefficient series (b) of the SSTA field by the original model

2056 **Fig. 4.** Long-term step-by-step forecast results of the first time coefficient series (a) and the second

2057 time coefficient series (b) of the SSTA field by the improved model

2058 **Fig. 5.** The cross-validated retroactive hindcast results of the first time coefficient series (a) and the

2059 second time coefficient series (b) of the SSTA field by the improved model

2060 **Fig. 6.** The forecast SSTA field (a) and the actual SSTA field (b) of an El Niño event (Dec.1997)

2061 **Fig. 7.** The forecast SSTA field (a) and the actual SSTA field (b) of a La Niña event (Dec.1999)

2062 **Fig. 8.** The forecast SSTA field (a) and the actual SSTA field (b) of neutral event (Nov.2002)

2063 **Fig. 9.** The improved dynamical-statistical model prediction of the ENSO index

2064 ~~Fig.10. The cumulative correlation coefficients (a) and cumulative mean absolute percentage error (b)~~

2065 ~~changing with time of different lead times~~

2066 **Fig. 10.** Temporal correlation between model forecasts and observations for all seasons combined, as

2067 a function of lead time. Each line highlights one model.
 2068 **Fig.1211.** RMSE in standardized units, as a function of lead time for all seasons combined. Each line
 2069 highlights one model.

2070
 2071
 2072
 2073
 2074
 2075
 2076
 2077

2078 **Table captions:**

2079 **Table 1.** The correlation analysis between the front two time series T_1, T_2 and nine impact factors

带格式的: 字体: 加粗
 带格式的: 缩进: 首行缩进: 0 字符, 行距: 单倍行距

2080 **Table 1.** Forecast results of models of different variables

2081 **Table2.**The CC and MAPE of long-term fitting test when the retrospective order p is different

带格式的: 行距: 单倍行距

2082 **Table 2.** The correlation coefficient (CC) and Mean absolute percentage error (MAPE) of long term
 2083 fitting test when the retrospective order p is different

2084 **Table3.** The forecast results of T_1 and T_2 in different examples within 6 and 12 months

2085 **Table. 4.** The TC and the MAPE between model forecasts and observations within 12 months for
 2086 Nov.–Jan., Dec.–Feb., and Jan.–Mar. as lead time of winter, for Feb.–Apr., Mar.–May and Apr.–June as
 2087 lead time of spring, for May–July, June–August and July–Sep. as lead time of summer and for
 2088 August–Oct., Sep.–Nov. and Oct.–Dec. as lead time of autumn.

带格式的: 行距: 单倍行距

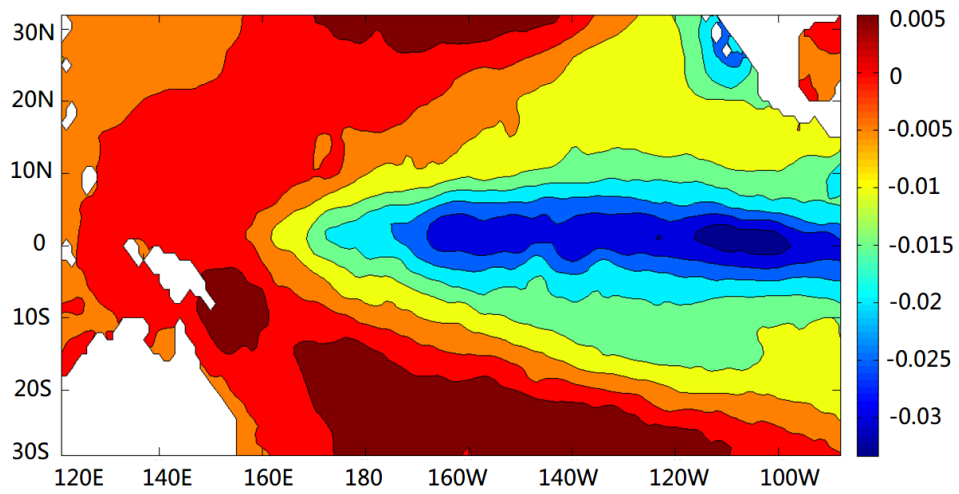
2089 **Table4.** Temporal correlation (CC) and the mean absolute percentage error (MAPE) between model
 2090 forecasts and observations within 12 months for November–January–December–February, and
 2091 January–March as lead time of winter and for May–July, June–August and July–Sep. as lead time of
 2092 summer.

2093 **Table5.** The forecast results of the different data periods **Table 5.** The correlation coefficients among
 2094 four factors

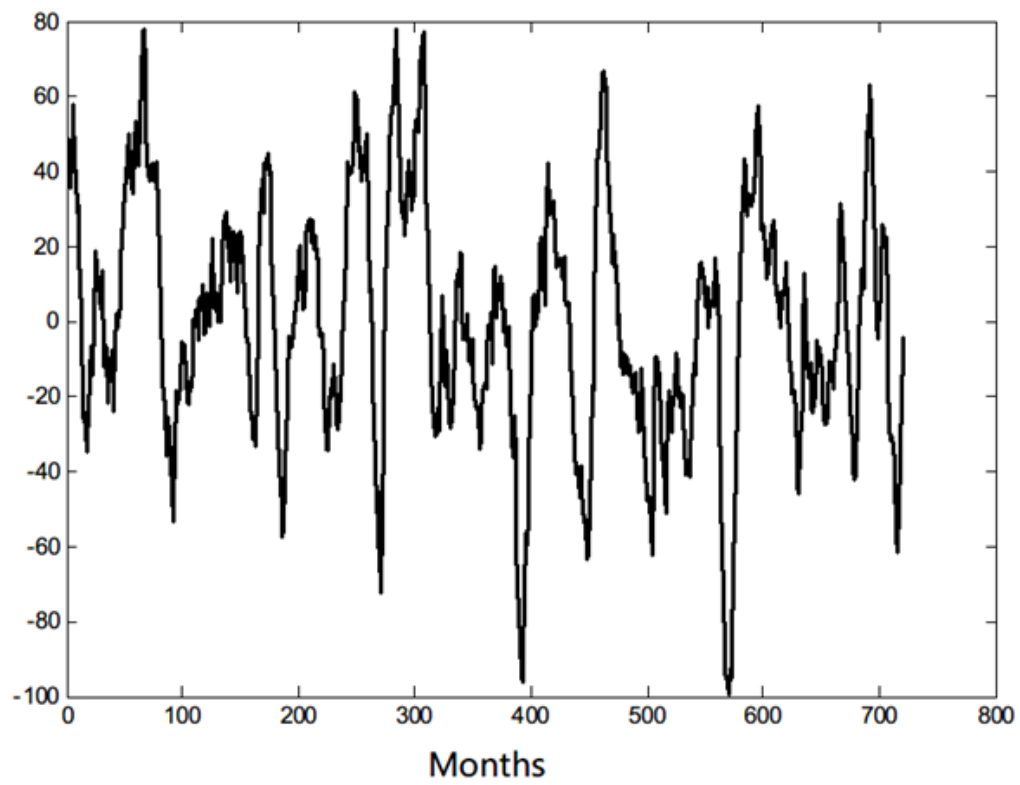
带格式的: 制表位: 3.21 字符, 左对齐 + 8.72 字符, 左对齐 + 13.09 字符, 左对齐 + 17.45 字符, 左对齐 + 21.81 字符, 左对齐 + 26.17 字符, 左对齐 + 30.53 字符, 左对齐 + 34.9 字符, 左对齐 + 39.26 字符, 左对齐 + 43.62 字符, 左对齐 + 47.98 字符, 左对齐 + 52.34 字符, 左对齐 + 56.7 字符, 左对齐 + 61.07 字符, 左对齐 + 65.43 字符, 左对齐 + 69.79 字符, 左对齐

2096 **Figure:**

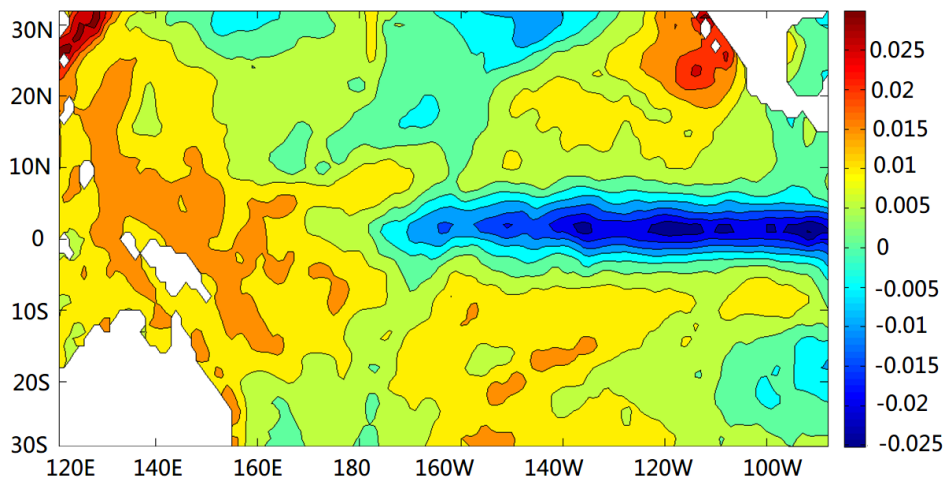
带格式的
 带格式的: 行距: 单倍行距



(a)



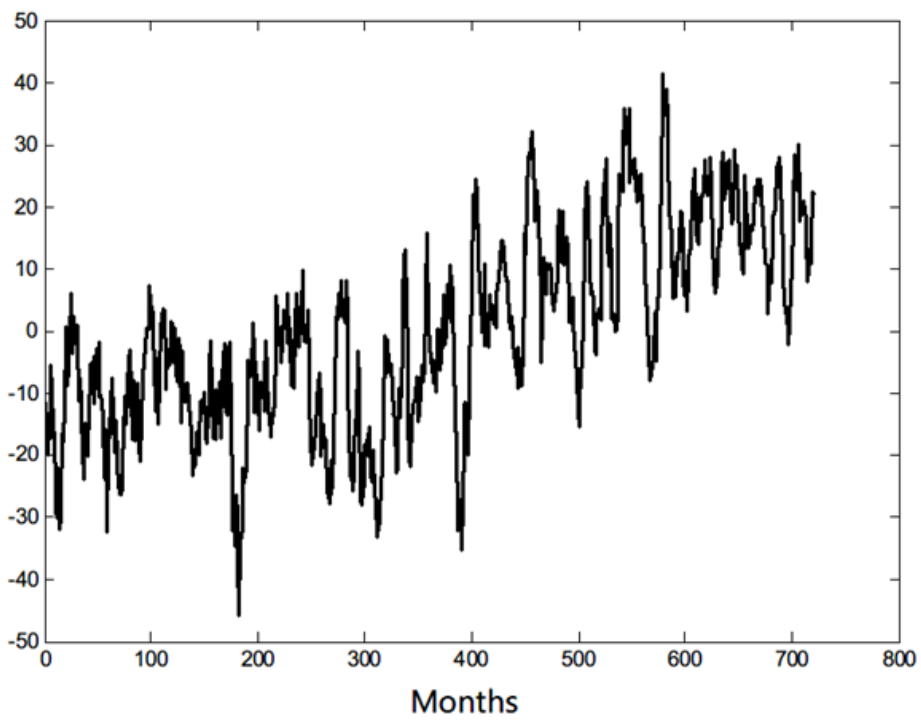
(b)



2101

2102

(c)



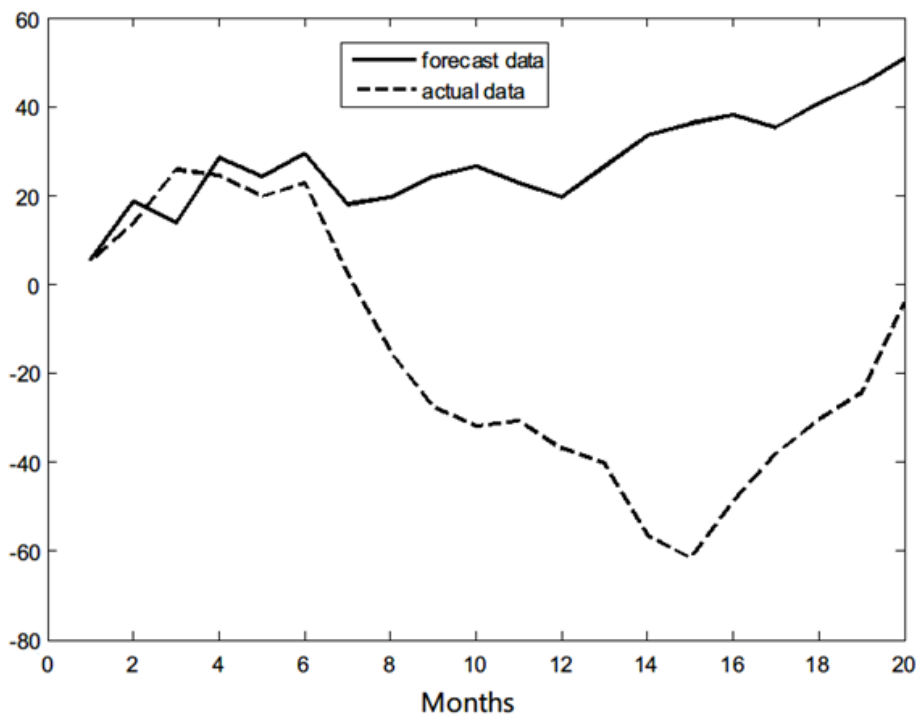
2103

2104

(d)

2105 **Fig. 1** (a, c) First and second modes of the EOF decomposition of the SSTA field, and (b, d) the

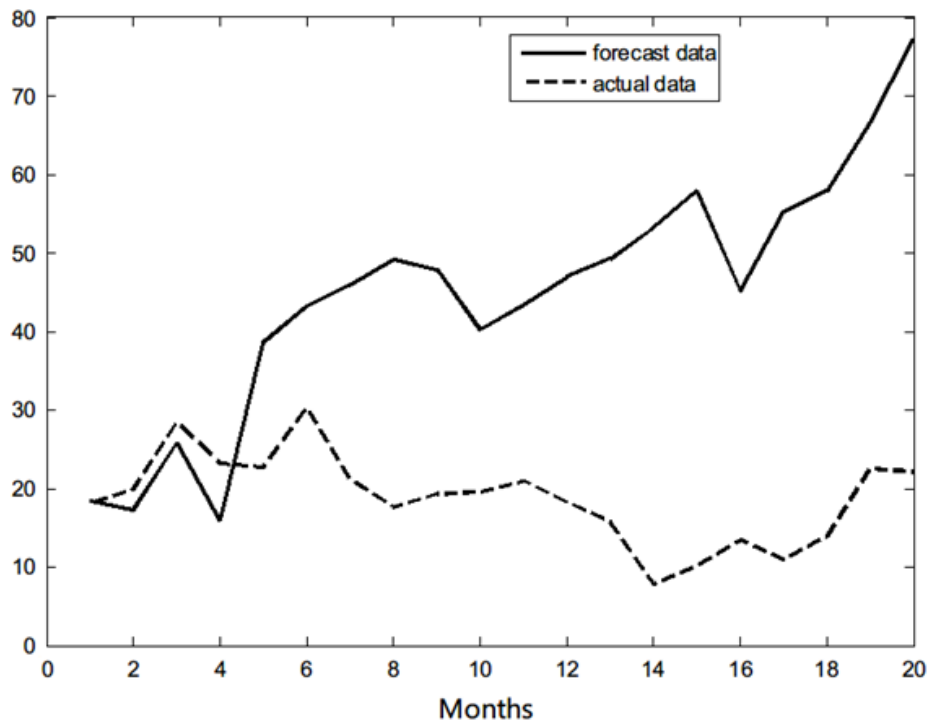
2106 corresponding PC time series.



2107

2108

(a)



2109

2110

(b)

2111 Fig.2 Forecast results of the first time coefficient series T_1 [错误!未找到引用源。](#) (a) and the second

2112 time coefficient series T_2 ~~T_2~~ (b) of the SSTA field by the original model

2113

2114

2115

2116

2117

2118

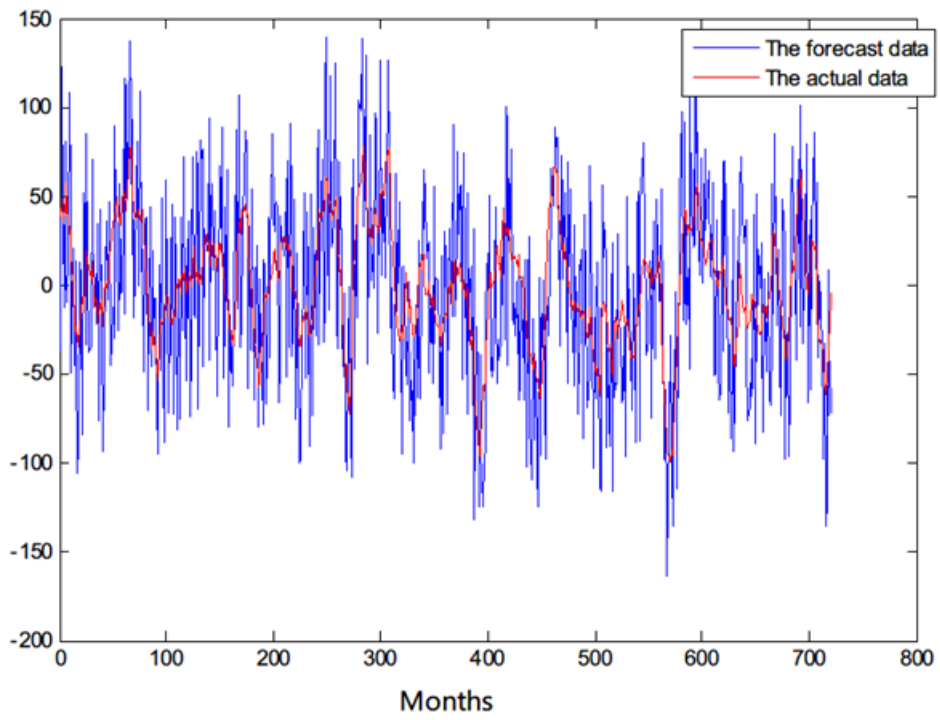
2119

2120

2121

2122

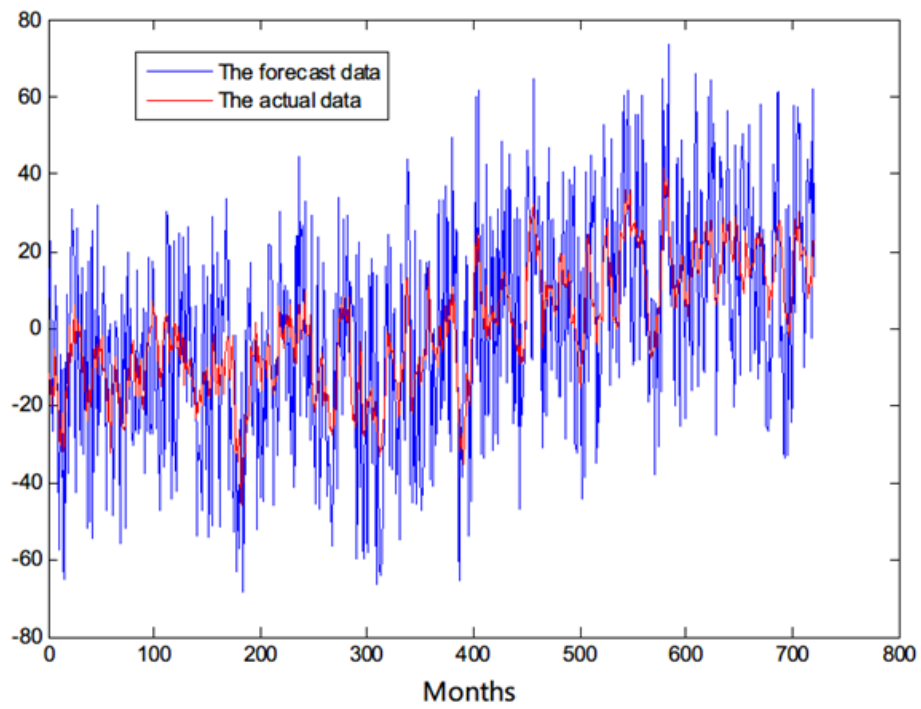
2123



2124

2125

(a)



2126

2127

(b)

2128 Fig.3The cross-validated retroactive hindcast results of the first time coefficient series $\underline{T_1} - \overline{T_1}$ (a)and

2129 the second time coefficient series $\underline{T_2} - \overline{T_2}$ (b)of the SSTA field by the original model

2130

2131

2132

2133

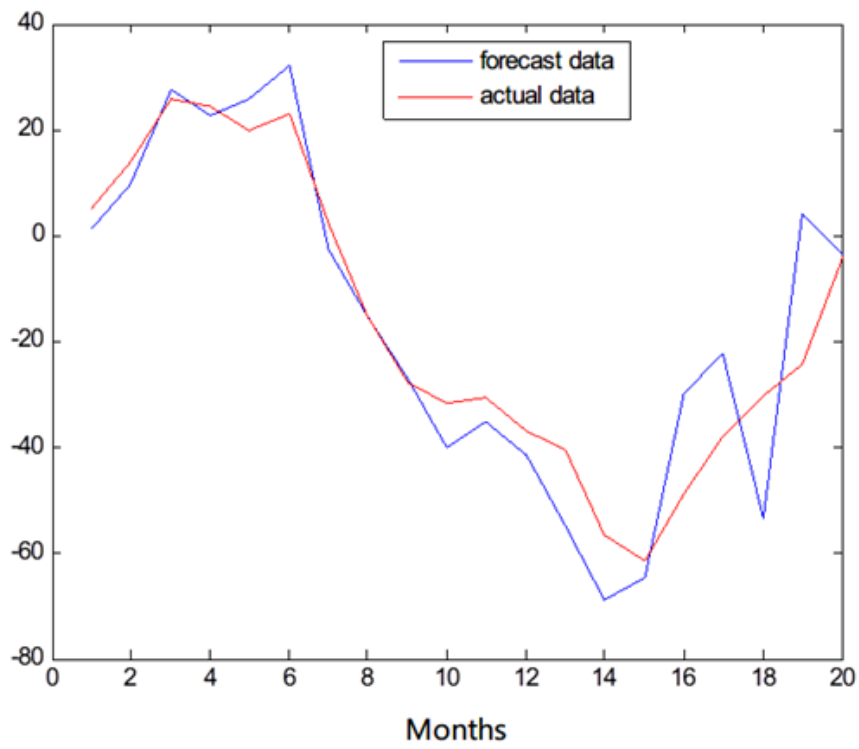
2134

2135

2136

2137

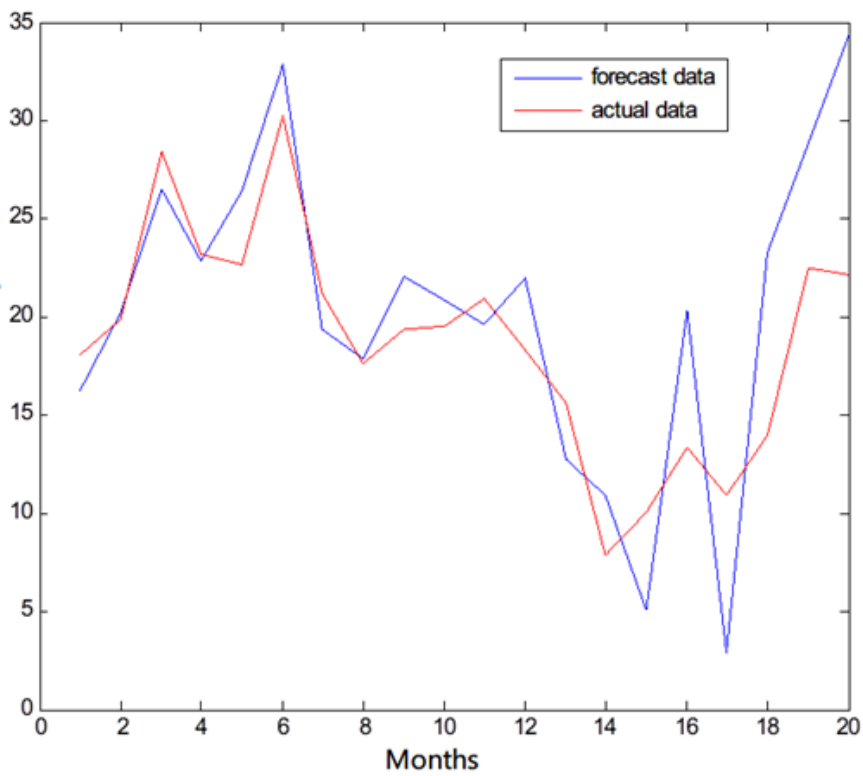
2138



2139

2140

(a)



2141

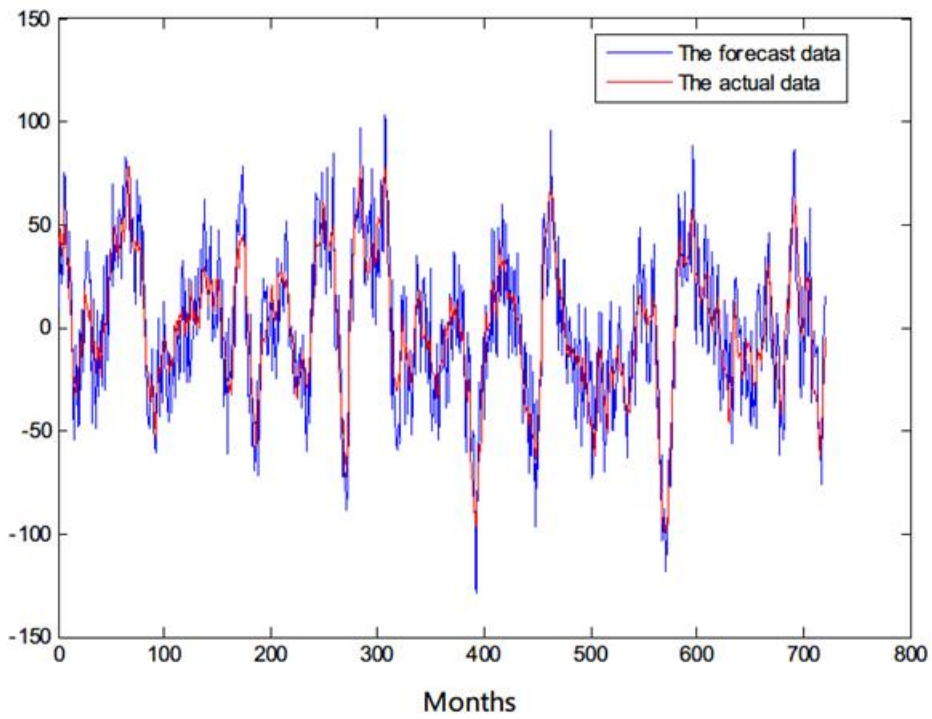
2142

(b)

2143 Fig. 4. Long-term step-by-step forecast results of the first time coefficient series $\underline{T_1 T_1}$ (a) and the

2144 second time coefficient series $\underline{T_2 T_2}$ (b) of the SSTA field by the improved model

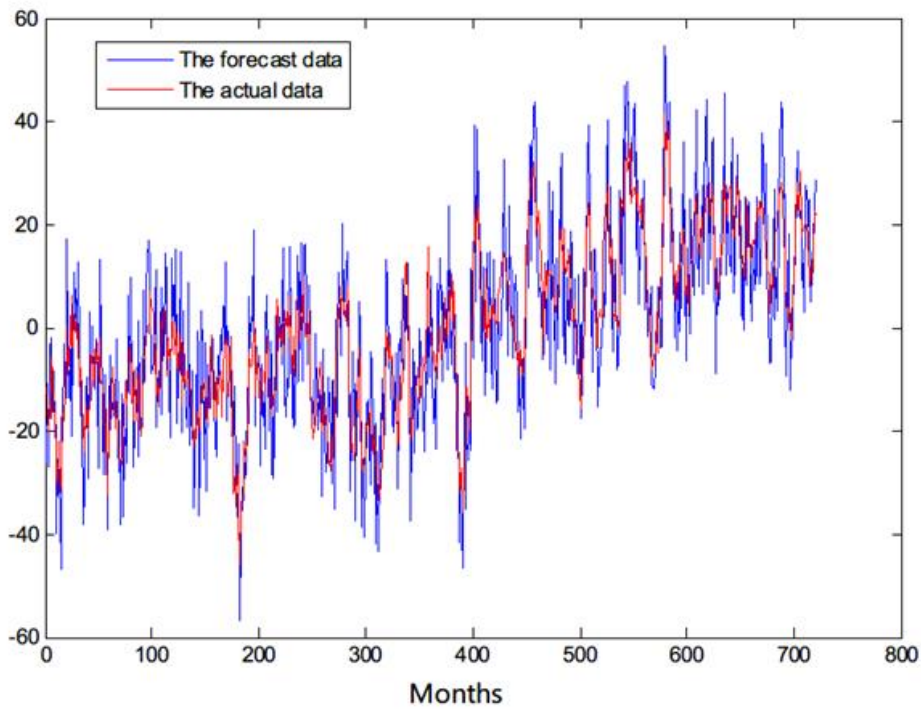
2145



2146

2147

(a)



2148

2149

(b)

2150 | Fig. 5. The cross-validated retroactive hindcast results of the first time coefficient series T_1 (a) and

2151 | the second time coefficient series T_2 (b) of the SSTA field by the improved model

2152

2153

2154

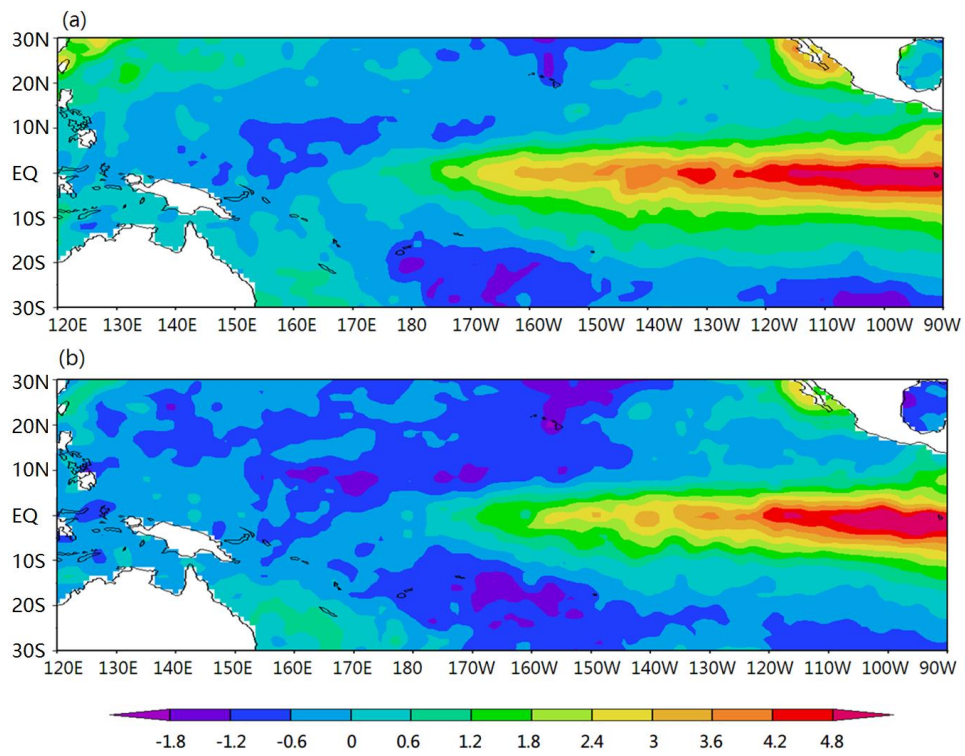
2155

2156

2157

2158

2159



2160

2161 Fig.6. The forecast SSTA field(a) and the actual SSTA field (b)of an El Niño event (Dec.1997)

2162

2163

2164

2165

2166

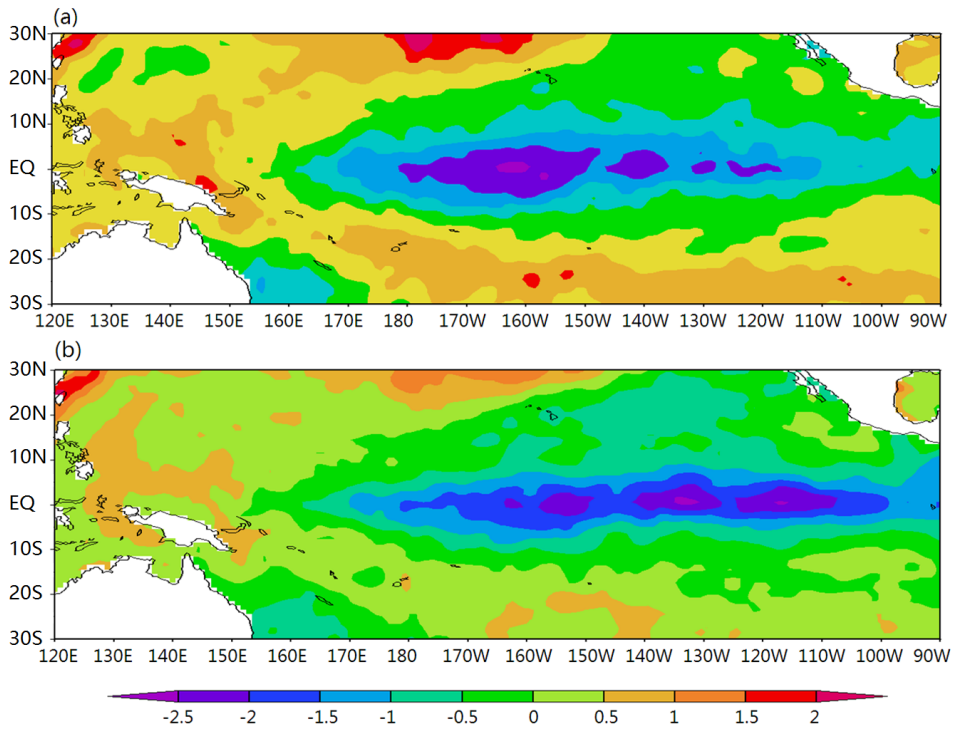
2167

2168

2169

2170

2171



2172

2173 Fig.7. The forecast SSTA field(a) and the actual SSTA field (b)of a La Niña event (Dec.1999)

2174

2175

2176

2177

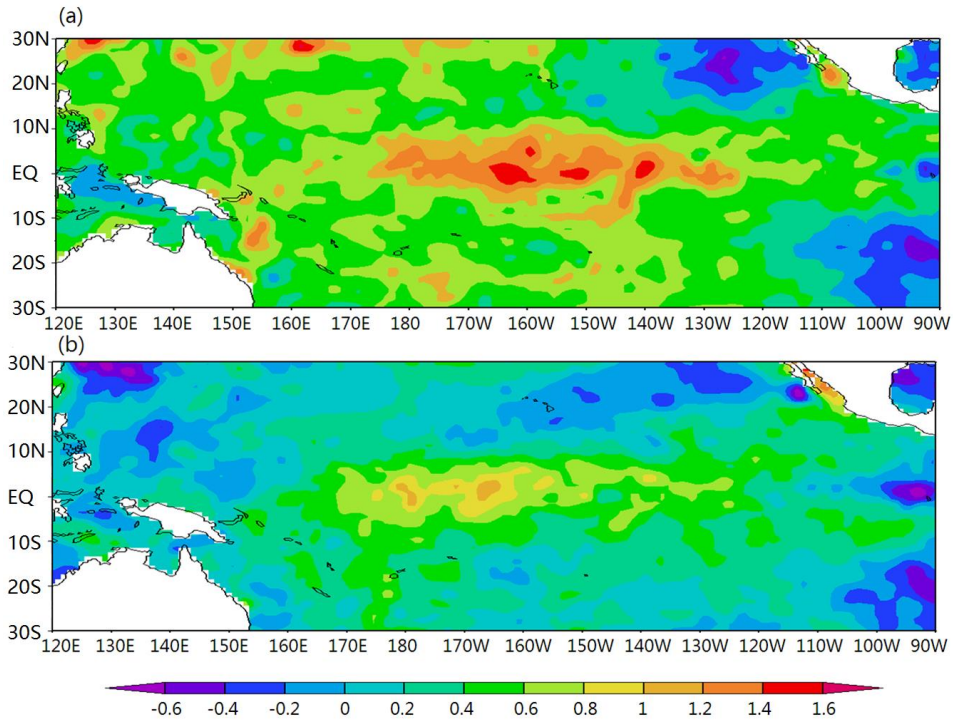
2178

2179

2180

2181

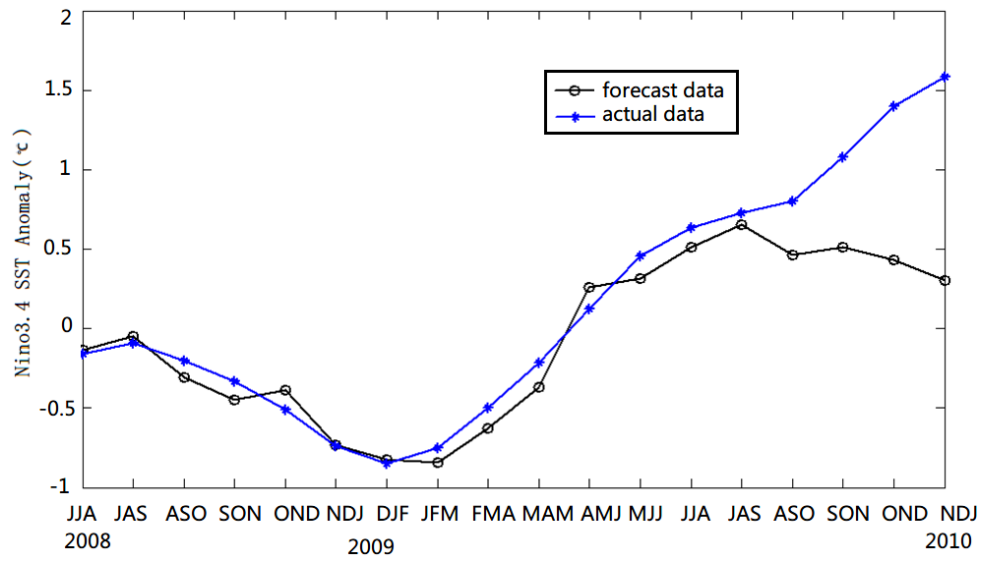
2182



2183

2184 Fig.8. The forecast SSTA field(a) and the actual SSTA field (b)of neutral event (Nov.2002)

2185



2186

2187

Fig.9. The improved dynamical-statistical model prediction of the ENSO index

2188

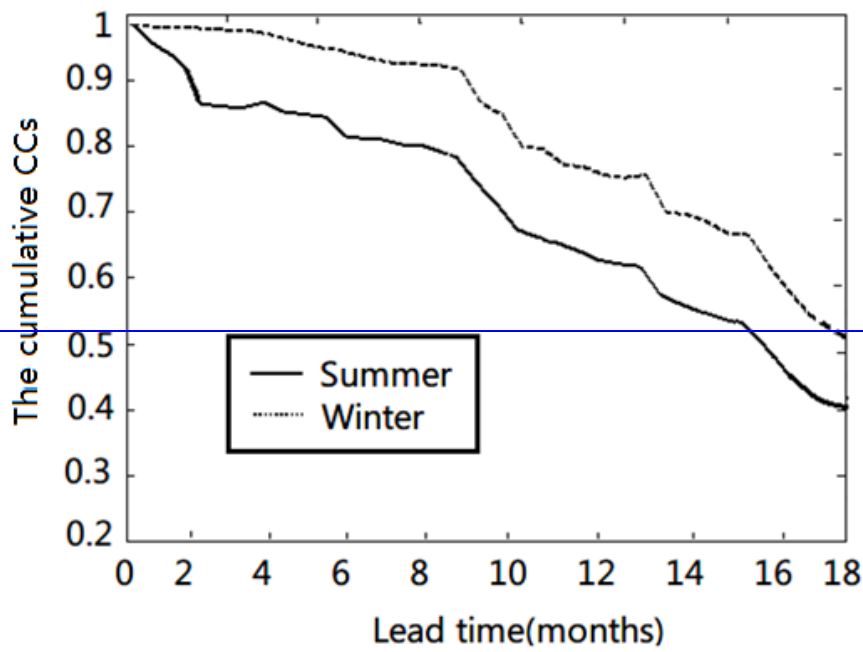
2189

2190

2191

2192

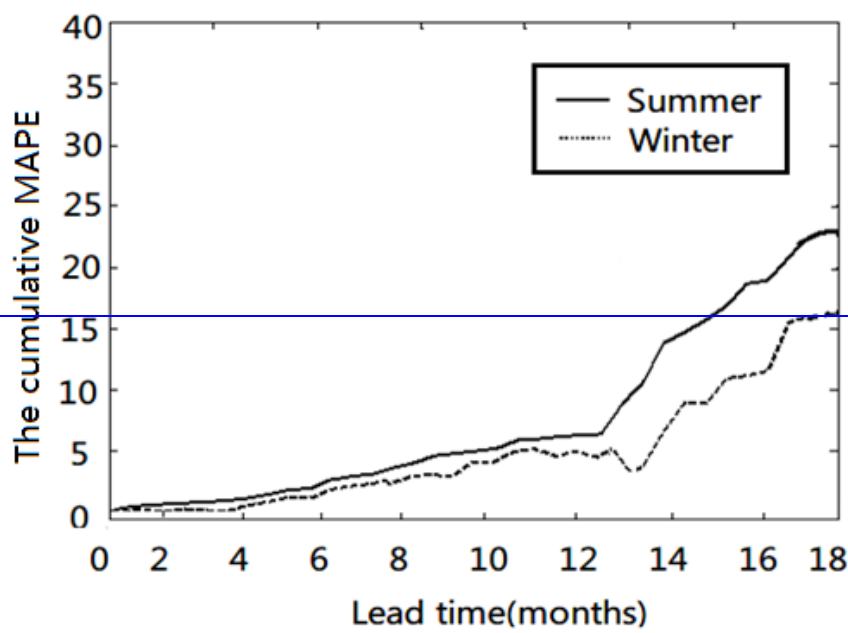
2193



2194

2195

(a)



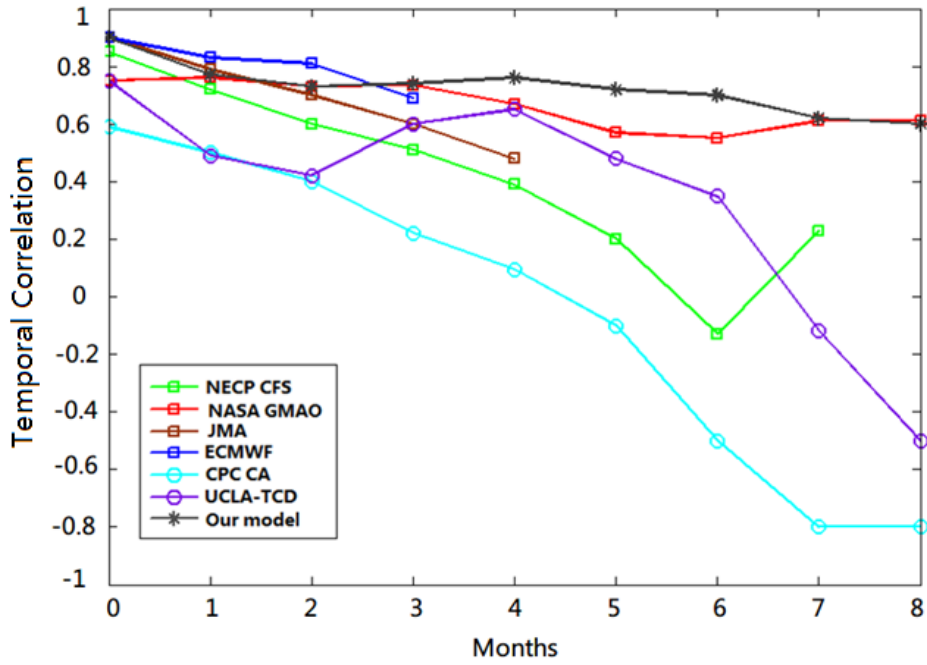
2196

2197

(b)

2198 Fig.10. The cumulative correlation coefficients (CCs) (a) and cumulative mean absolute percentage
 2199 error (MAPE) (b) changing with time of different lead times

2200



2201

2202 | Fig. 4410. Temporal correlation between model forecasts and observations for all seasons combined, as
2203 a function of lead time. Each line highlights one model.

2204

2205

2206

2207

2208

2209

2210

2211

2212

2213

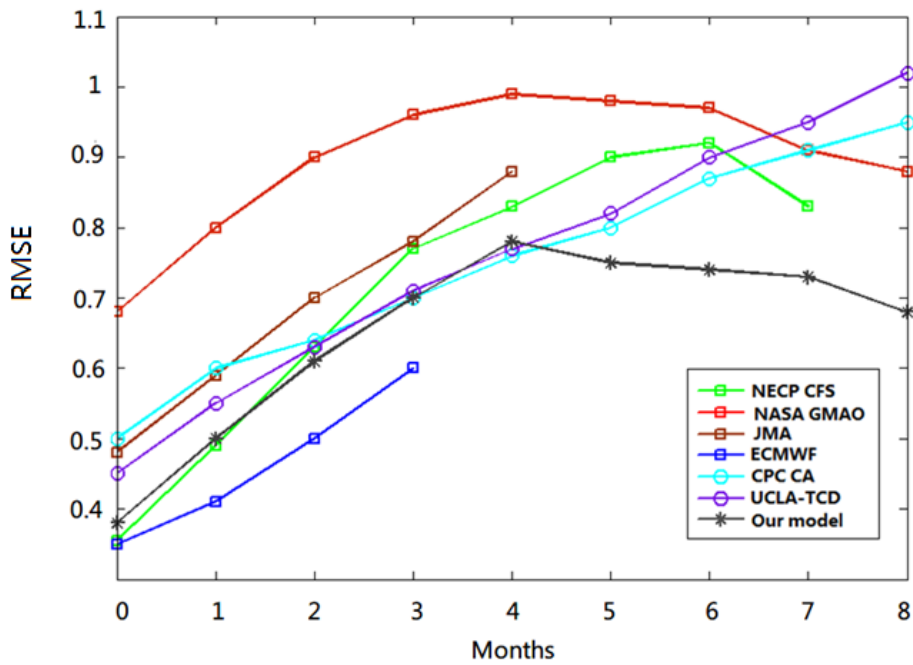
2214

2215

2216

2217

2218



2219

2220 Fig . 4211. RMSE in standardized units, as a function of lead time for all seasons combined. Each line

2221 highlights one model.

2222

2223

2224

2225

2226

2227

2228

2229

2230

2231

2232

2233

2234

2235

2236 **Table:**

2237 Table 1. The correlation analysis between the front two time series T_1, T_2 and nine impact factors

<u>Factors</u>	<u>u_1</u>	<u>u_2</u>	<u>PNA</u>	<u>DMI</u>	<u>SOI</u>	<u>PDOl</u>	<u>EAWMI</u>	<u>OLR</u>	<u>SSH*</u>
<u>T_1</u>	<u>0.3161</u>	<u>0.5684</u>	<u>0.4386</u>	<u>-0.3457</u>	<u>0.7734</u>	<u>0.4081</u>	<u>0.6284</u>	<u>0.3287</u>	<u>0.3363</u>
<u>T_2</u>	<u>0.2118</u>	<u>0.4181</u>	<u>0.2560</u>	<u>-0.2345</u>	<u>0.5232</u>	<u>0.3065</u>	<u>0.4825</u>	<u>0.1816</u>	<u>0.2169</u>

2238

2239 Table 1. The forecast results of the models of different variables

<u>The model</u>	<u>The forecast skill of 60 cross-validated retroactive hindcasts-experiments of the ENSO index for all seasons combined at lead-times of 8 months</u>	
	<u>the temporal correlation</u>	<u>the root mean square error</u>
<u>One variable (T_1)</u>	<u>0.5051</u>	<u>0.8075</u>
<u>Two variables (T_1, T_2)</u>	<u>0.5613</u>	<u>0.7679</u>
<u>Three variables (T_1, T_2, SOI)</u>	<u>0.6027</u>	<u>0.7275</u>
<u>Four variables ($T_1, T_2, SOI, EAWMI$)</u>	<u>0.6344</u>	<u>0.6728</u>
<u>Five variables ($T_1, T_2, SOI, EAWMI, u_1$)</u>	<u>0.5923</u>	<u>0.7344</u>
<u>Six variables ($T_1, T_2, SOI, EAWMI, u_1, PNA$)</u>	<u>0.5528</u>	<u>0.7806</u>

2240

2241

2242

2243

2244

2245

2246

2247

2248

2249

2250

2251

2252

2253

2254

带格式的: 字体: Times New Roman, 字体颜色: 自动设置

带格式的: 字体: Times New Roman, 字体颜色: 自动设置

带格式的: 字体: Times New Roman, 字体颜色: 自动设置

带格式的: 字体: Times New Roman, 字体颜色: 自动设置

带格式的: 字体: Times New Roman, 字体颜色: 自动设置

带格式的: 字体: Times New Roman, 10 磅, 字体颜色: 自动设置

带格式的: 字体: Times New Roman, 10 磅, 字体颜色: 自动设置

带格式的: 字体: Times New Roman, 10 磅, 字体颜色: 自动设置

带格式的: 字体: Times New Roman, 10 磅, 字体颜色: 自动设置

带格式的: 字体: Times New Roman, 10 磅, 字体颜色: 自动设置

带格式的: 字体: Times New Roman, 10 磅, 字体颜色: 自动设置

带格式的: 字体: Times New Roman, 10 磅, 字体颜色: 自动设置

带格式的: 字体: Times New Roman, 10 磅, 字体颜色: 自动设置

带格式的: 字体: Times New Roman, 10 磅, 字体颜色: 自动设置

带格式的: 字体: Times New Roman, 10 磅, 字体颜色: 自动设置

带格式的: 字体: Times New Roman, 10 磅, 字体颜色: 自动设置

带格式的: 字体: Times New Roman, 10 磅, 字体颜色: 自动设置

带格式的: 字体: Times New Roman, 10 磅, 字体颜色: 自动设置

带格式的: 字体: Times New Roman, 10 磅, 字体颜色: 自动设置

带格式的: 字体: Times New Roman, 10 磅, 字体颜色: 自动设置

带格式的: 字体: Times New Roman, 10 磅, 字体颜色: 自动设置

带格式的: 字体: Times New Roman, 10 磅, 字体颜色: 自动设置

带格式的: 字体: Times New Roman, 10 磅, 字体颜色: 自动设置

带格式的: 字体: Times New Roman, 10 磅, 字体颜色: 自动设置

带格式的: 字体: Times New Roman, 10 磅, 字体颜色: 自动设置

带格式的: 字体: Times New Roman, 10 磅, 字体颜色: 自动设置

带格式的: 字体: Times New Roman, 10 磅, 字体颜色: 自动设置

带格式的: 字体: Times New Roman, 10 磅, 字体颜色: 自动设置

带格式的: 字体: Times New Roman, 10 磅, 字体颜色: 自动设置

带格式的: 字体: Times New Roman, 10 磅, 字体颜色: 自动设置

带格式的: 字体: Times New Roman, 10 磅, 字体颜色: 自动设置

带格式的: 字体: Times New Roman, 10 磅, 字体颜色: 自动设置

带格式的: 字体: Times New Roman, 10 磅, 字体颜色: 自动设置

带格式的: 字体: Times New Roman, 10 磅, 字体颜色: 自动设置

带格式的: 字体: Times New Roman, 10 磅, 字体颜色: 自动设置

2255
 2256
 2257
 2258
 2259
 2260
 2261
 2262
 2263
 2264
 2265
 2266
 2267
 2268
 2269
 2270
 2271
 2272

2273 **Table 2.** The correlation coefficient (CC) and Mean absolute percentage error (MAPE) of long-term
 2274 fitting test when the retrospective order p is different

p		4	5	6	7	8	9	10
The forecast results of long-term fitting test	CC	0.75	0.73	0.81	0.74	0.70	0.72	0.68
	MAPE	18.42%	19.36%	14.56%	20.39%	25.31%	24.18%	27.33%
p		11	12	13	14	15	16	
The forecast results of long-term fitting test	CC	0.68	0.70	0.65	0.62	0.60	0.62	
	MAPE	28.10%	26.58%	30.91%	33.14%	34.97%	33.56%	

2275
 2276
 2277
 2278
 2279

2280

2281

2282

2283

2284

2285

2286

2287

2288

2289

2290

Table3. The forecast results of T_1 and T_2 in different examples within 6 and 12 months

Forecast events	The results within 6-months		The results within 12-months	
	CC	MAPE	CC	MAPE
The average of 18 El Niño examples of T_1	0.824	8.45%	0.719	12.67%
The average of 22 La Niña examples of T_1	0.846	7.68%	0.740	11.28%
The average of 20 Neutral examples of T_1	0.885	6.23%	0.789	9.85%
The average of total 60 examples of T_1	0.850	7.41%	0.748	10.95%
The average of 18 El Niño examples of T_2	0.811	8.79%	0.703	13.28%
The average of 22 La Niña examples of T_2	0.833	7.35%	0.731	11.96%
The average of 20 Neutral examples of T_2	0.896	6.68%	0.795	10.08%

The average of total 60 examples of T_2	0.842	7.64%	0.740	11.71%
---	-------	-------	-------	--------

2291
2292
2293
2294
2295
2296
2297
2298
2299
2300
2301

2302 [Table 4. The TC and the MAPE between model forecasts and observations within 12 months for](#)
 2303 [Nov.–Jan., Dec.–Feb., and Jan.–Mar. as lead time of winter, for Feb.–Apr., Mar.–May and Apr.–June as](#)
 2304 [lead time of spring, for May–July, June–August and July–Sep. as lead time of summer and for](#)
 2305 [August–Oct., Sep.–Nov. and Oct.–Dec. as lead time of autumn.](#)

Forecast events	Lead time of all seasons combined		Lead time of summer (MJJ-JJA-JAS)		Lead time of autumn (ASO-SON-OND)		Lead time of winter (NDJ-DJF-JFM)		Lead time of spring (FMA-MAM-AMJ)	
	ETC	MAPE	ETC	MAPE	ETC	MAPE	ETC	MAPE	ETC	MAPE
The average of 18 El Niño examples	0.60 4	9.70%	0.56 9	10.33%	0.632	8.85%	0.67 7	8.02%	0.538	11.6%
The average of 22 La Niña examples	0.62 5	8.97%	0.58 1	9.82%	0.645	8.41%	0.69 5	7.83%	0.579	9.82%

带格式的

带格式的: 字体: Times New Roman, 10 磅

- 带格式的
- 带格式的
- 带格式的
- 带格式的
- 带格式的

The average of 20 Neutral examples	0.79 8	5.96%	0.75 2	6.86%	0.831	5.31%	0.84 4	4.60%	0.765	7.07%
The average of total 60 examples	0.71 2	7.62%	0.63 3	8.51%	0.786	6.88%	0.77 6	6.52%	0.653	8.03%

2306
2307
2308
2309
2310
2311

Table 4. Temporal correlation(CC) and the mean absolute percentage error (MAPE) between model forecasts and observations within 12 months for Nov-Jan, Dec-Feb, and Jan-Mar as lead time of winter and for May-July, June-August and July-Sep. as lead time of summer.

带格式的: 字体: 10 磅

Forecast events	Lead time of all-seasons-combined		Lead time of summer (MJJ-JJA-JAS)		Lead time of winter (NDJ-DJF-JFM)	
	CC	MAPE	CC	MAPE	CC	MAPE
The average of 18 El Niño examples	0.604	9.70%	0.569	10.33%	0.677	8.02%
The average of 22 La Niña examples	0.625	8.97%	0.581	9.82%	0.695	7.83%
The average of 20 Neutral examples	0.798	5.96%	0.752	6.86%	0.844	4.60%
The average of total 60 examples	0.712	7.62%	0.633	8.51%	0.776	6.52%

2312
2313
2314
2315
2316
2317
2318

τ_1		0.419	0.401	0.337
τ_2	0.419		0.424	0.356
SOI	0.401	0.424		0.408
EAWMI	0.337	0.356	0.408	

带格式表格

2326

2327